NOVEL PARAMETRIC APPROACH TO CHARACTERIZE CRUMB RUBBER MODIFIED ASPHALT BINDER PERFORMANCE BASED ON PARALLEL PLATE DYNAMIC SHEAR RHEOMETRY

By

Anas Ahmad Jamrah

A DISSERTATION

Submitted to
Michigan State University
in partial fulfilment of the requirements
for the degree of

Civil Engineering – Doctor of Philosophy

2018

ABSTRACT

NOVEL PARAMETRIC APPROACH TO CHARACTERIZE CRUMB RUBBER MODIFIED ASPHALT BINDER PERFORMANCE BASED ON PARALLEL PLATE DYNAMIC SHEAR RHEOMETRY

By

Anas Ahmad Jamrah

One of the major recycling markets of waste tires generated in the United States is represented by Ground Tire Rubber (GTR). Crumb Rubber (CR) is the terminology used for GTR materials reduced to a particle size ranging from 4.75 mm to less than 0.075 mm and is a commonly used additive for asphalt modification. While environmentally friendly and presents a major sustainable alternative to other engineering materials; the use of CR additives in asphalt did not develop as a solution to an environmental problem. CR is used to improve asphalt binder properties, and in turn to improve pavement performance in the field. However, the adoption of CR Modified (CRM) materials in the field has been limited. This is partially due to challenges and limitations on characterizing the engineering behavior of CRM binders relating to pavement performance, as compared to standard Styrene-Butadiene-Styrene (SBS) polymer modifiers. This research is an effort to address some of these challenges. The major contributions of this work are outlined below:

- Identify a feasible Dynamic Shear Rheometer (DSR) testing geometry for characterizing CRM binder rheology, through establishing a link to asphalt mixture mechanical properties.
- Evaluate the interaction mechanisms between CR and asphalt binders and the influence of CR swelling on CRM binder performance.
- Propose practical QC/QA test methods for identifying for estimating the engineering properties of swollen CR in asphalt binder and its' relationship to performance.

Due to the presence of swollen CR particles as suspensions in asphalt binder, a major challenge for adopting CRM binders is that they cannot be specified using standard rheological characterization methods. This is especially true at high concentrations and/or large CR particle sizes. The first contribution of this dissertation addresses this challenge by identifying a suitable and efficient DSR geometry for CRM binder characterization through a comparative analysis for binder rheology and mixture properties covering a wide range of CR concentrations and sizes. The second contribution addresses the nature of interaction between CR and asphalt binder at elevated temperatures. The changes in base asphalt rheology due to the absorption/diffusion of the light asphalt binder fractions (aromatic oils) into CR were used to identify the influence of interaction conditions on binder stiffening and softening effects of CR.

Common CRM binder testing continues to rely on empirical tests that indicate modification, but do not address material behavior relating to pavement performance. The third contribution of this dissertation provides new QC/QA test methods that can be used during construction. Alternative parameters derived from rheological characteristics of CRM binders were evaluated as indicators of CR pre-treatment and fatigue and rutting characteristics. These parameters can be obtained and applied to QC screening of CRM binders without the need for micromechanical modeling or advanced testing/characterization techniques.

This dissertation presents a comprehensive comparative analysis evaluating performance characteristics in CRM binders as influenced by different material variables including a wide range of base asphalt binder Performance Grades and CR sizes. The conclusions drawn herein provide a better understanding of CR modification techniques relative to performance-based specifications on asphalt binders and will encourage the overall adoption of CRM materials in paving applications.

TO MY FAMILY…

ACKNOWLEDGEMENTS

First and foremost, I would like to thank my advisor, Dr. M. Emin Kutay for his support and guidance throughout my years of graduate studies at Michigan State University. Dr. Kutay has been a great mentor to me, and I am very lucky to have had him as my advisor.

I would also like to thank the members of my Ph.D. advisory committee. The discussions I've had with Dr. Andre Lee, Dr. Karim Chatti, and Dr. Neeraj Buch and the feedback they've given me was very important to complete this work. Special thanks are also due to Dr. Gilbert Baladi for his support throughout the years. The efforts by Ms. Margaret Connor, Ms. Laura Post, and Ms. Laura Taylor with the administrative process are also appreciated.

I am also very grateful to the many friends I have met at Marathon Petroleum Company. I want to thank every one of you, especially the Asphalt Technology Group. Special thanks are due to my supervisor Brian Wilt for his support.

Finally, I would like to thank my beautiful family. If it wasn't for my wife Sarah and her never-ending support, this dissertation would have never been completed. Sarah, your contribution to this work has been very vital. Without you and Farah, this wouldn't have happened. I owe this to YOU. My deepest gratitude goes to my father and my mother. Their support, both financial and emotional has been very critical for my academic and professional success. I have always wanted to be like my father, and I think that Dr. Jamrah was the main motivator that led me down this path. Special thanks to both of you from Dr. Jamrah Jr. Knowing that you are proud of me is the best feeling in the world. The Three Musketeers, my brothers, Ayman, Ameen, and Ashraf; thank you for everything that you do for me.

TABLE OF CONTENTS

LIST OF TABLES

LIST OF FIGURES

CHAPTER 1. INTRODUCTION

There are approximately 250 million waste tires generated annually in the United States (Rubber Manufacturers Association 2016). In 2015, a total of 280 million tires were generated. Of these, 220 million were automobile tires and 60 million were truck tires. Around 37 million tires were reused, leaving the remaining 243 million tires to be managed (Rubber Manufacturers Association 2016). The two major tire recycling markets in the United States are represented by Tire-Derived Fuel (TDF) and Ground Tire Rubber (GTR). In 2015, a total of 117 million of the waste tires generated were disposed of as TDF amounting to 47% of the recycling market. Similarly, 62 million of the waste tires generated were consumed in GTR applications, representing 26% of the recycling market. Common TDF markets include cement kilns, pulp and paper mills, and electric utility boilers. GTR in varying sizes is used in sports surfaces, molds, playgrounds, automotive industry, asphalt industry, and approximately 1% of GTR was exported in 2015 (Rubber Manufacturers Association 2016). Figure 1 shows historical market trends for waste tire use in the United States between 1990 and 2015. Crumb Rubber (CR) is the terminology used for GTR materials reduced to a particle size ranging from 4.75 mm to less than 0.075 mm (No. 4 to No. 200 sieve). CR materials used as additives for asphalt modification typically range in size from 1.20 mm to 0.15 mm (No. 16 to No. 100 sieve) and represented 15% of the GTR market in 2015 (Rubber Manufacturers Association 2016). This study is aimed at investigating various aspects of the usage of fine GTR materials as asphalt modifiers and will be referred to as Crumb Rubber or CR in this dissertation.

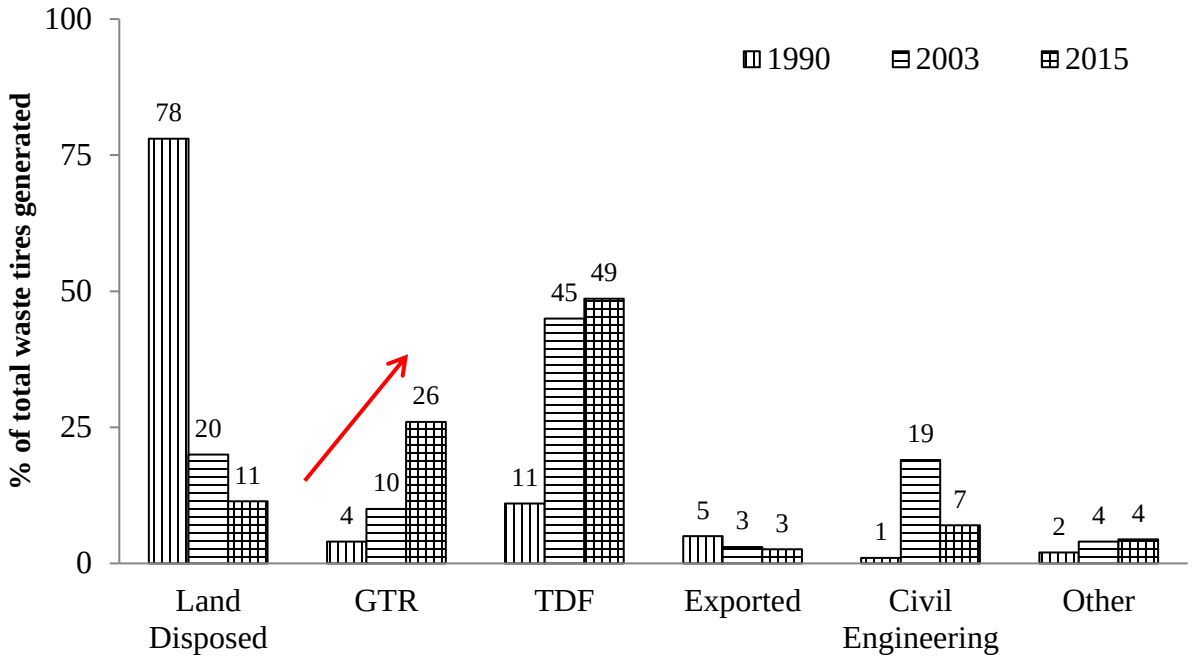

Figure 1: U.S. waste tire market trends (Rubber Manufacturers Association 2016).

While environmentally friendly and presents a major sustainable alternative for the engineering material market; the use of CR additives in asphalt did not develop as a solution to an environmental problem. In the early 1940s, CR was introduced in asphalt pavements in an experiment aimed at utilizing the flexible properties of rubber to build longer lasting pavements. Engineers and chemists worked on improving the elastic properties of asphalt binder by blending it with natural and synthetic rubbers. Waste tires, which are compounds of natural and synthetic rubbers, were studied as part of that effort (Heitzman 1992).

CR has been traditionally incorporated into asphalt paving mixtures using two major methods; the wet process, and the dry process. In the wet process, CR is used as an asphalt binder modifier, while the dry process incorporates granulated CR into the mixture as a fine aggregate replacement. The dry process can only be applied in Hot Mix Asphalt (HMA) paving mixtures, while the wet process can be used in other applications such as surface treatments and crack

sealants. It should be noted that there are several other technologies that cannot be classified as wet or dry technology. These include:

- Crumb Rubber Terminal Blend (CRTB): Somewhat similar to wet method but the CR particles are blended with asphalt binder at asphalt terminal (Kutay and Ozturk (2012)).
- Pre-swollen Crumb Rubber (PSCR): Similar to dry technology except that the crumb rubber particles are pre-soaked and swollen using an oily compound or asphalt binder (Jamrah and Kutay 2015).
- Devulcanized Rubber (DVR): In this technology, the crumb rubber is blended with and saturated with different polymeric additives and forced through a mill and pelletized, in order to make the rubber soluble in asphalt binder. The DVR pellets are blended with asphalt binder in asphalt terminal using high shear mill.
- Polymer coated rubber (PCR): In this technology, crumb rubber particles are pre-coated with polymers and used as either wet or dry technology.

The dry process typically utilizes 1 to 3% CR by total weight of aggregates in the asphalt mixture, where CR is used as a fine aggregate replacement. The rubber particles are blended with aggregates before the asphalt binder is added (Chesner et al. 1988). This process can be applied in open graded, gap graded, and dense graded mixtures (to some extent). This technology was first developed in Sweden in the 1960s and was patented and marketed for use in the United States under the name *PlusRide*. This technology utilizes CR in the size range of between 2.0 and 4.2 mm. The target mixture air void level is typically 2.0 to 4.0%, and the volumetric asphalt binder content is between 7.5 and 9.0% (Caltrans 2009). The generic dry process technology was developed between the 1980s and 1990s in the United States to produce dense graded HMA mixtures. This technology requires a more detailed mix design as it utilizes both coarse, and fine

CR to match aggregate gradations. In the dry process, no interaction between CR and asphalt binder is expected to take place at the interface between aggregates coated with asphalt binder and the rubber particles. By limiting the reaction time with asphalt binder and specifying coarse granulated CR, the rubber particles can maintain their shape and rigidity. Therefore, CR particles are expected to act as elastic inclusions in the voids between the aggregates. However, this assumption is often criticized by pavement engineers.

The wet process was first developed by Charles McDonald in the 1960s. In this technology, 15 to 25% CR is used to modify asphalt binder at elevated temperatures and produce a viscous fluid through asphalt-rubber interaction. According to ASTM D-8 (2009) asphalt rubber is "*a blend of asphalt cement, reclaimed tire rubber, and certain additives in which the rubber component is at least 15 percent by weight of the total blend and has reacted in the hot asphalt binder sufficiently to cause swelling of the rubber particles*". In addition, asphalt rubber physical characteristics must conform to specification requirements of ASTM Standard D 6114 (2009). The "wet process" includes any method that uses CR as asphalt binder modifier before the asphalt is added to aggregate. The main mechanism of interaction in this technology is the diffusion of light asphalt components (aromatic oils and resins) into the CR material at high temperatures, causing them to swell into the polymer chains (Attia and Abdelrahman 2009). Several extender oils and additives can be added to the asphalt rubber to promote the interaction between CR particles and asphalt binder, as well as to improve the low temperature properties of the modified material (Hicks et al. 1999). This interaction depends on a number of factors including blending temperature, blending time duration, blending speed (shear rate), CR type, size, and surface area, as well as asphalt binder source. These variables need to be monitored during the production

process, as CR Modified (CRM) binder properties are extremely dependent on the variability of these factors.

Wet process binders can be used in several types of paving applications. These include spray applications for surface treatments or interlayers, and HMA. Superior performance of CRM asphalt binders and mixtures has been reported by numerous researchers (Carlson and Zhu 1999, Hicks et al. 1999, and Way 1999). CR stiffens the conventional base binders at relatively high temperatures and increases elasticity (recoverable deformation). This improves permanent deformation (rutting) characteristics. Fatigue resistances of asphalt mixtures are also improved, partially due to the softening effects at intermediate and low temperatures. Low temperature properties are typically not affected (Caltrans 2009). In addition, CRM binders are reported to reduce reflective cracking, improve aging resistance, and have better chip retention in hot mix pavements (Way and Vilamoura 2000, Sousa 2005, Bertollo 2004, and Kaloush et al. 2003). Lower maintenance cost (Jung et al. 2002) and lower noise generation (Leung et al. 2006) are also some of the benefits of using wet process CRM binders.

Despite the environmental benefits and improved pavement performance, the adoption of CR materials as asphalt binder modifiers has been limited. This is partially due to challenges and limitations on the applicability and handling of this technology to field paving applications, as compared to standard Styrene-Butadiene-Styrene (SBS) polymer modifiers. One of the major challenges for adopting CRM binders is the fact that they cannot be specified using the Superpave Performance Grading (PG) system (with the exception of the devulcanized rubber modified binder). The physical characteristics of CRM binders have been and continue to be specified in most adopting states by the viscosity increase, and penetration tests (Heitzman 1992, Epps 1994). These tests are highly variable, and do not provide sufficient relationships to field performance.

Fundamental engineering properties of these materials need to be measured for a better understanding of the modification effects on field performance. A second limitation is the lack of a sound Quality Control (QC) process for screening CRM binders during construction. In addition, a comprehensive understanding of the interactions between asphalt binder and CR, and the chemical characteristics of the modified material has not been well established. To address some of the challenges facing practitioners in implementing and adopting CR as an asphalt modifier; the main objectives of this research are listed below:

- Identify a feasible Dynamic Shear Rheometer (DSR) testing geometry for characterizing CRM binder rheology, through establishing a viable link to asphalt mixture mechanical properties.
- Evaluate the interaction mechanisms between CR and asphalt binders and the influence of CR swelling on CRM binder performance.
- Propose practical QC/QA test methods for identifying levels CR pre-treatment, as well as for estimating the engineering properties of swollen CR in asphalt binder and its' relationship to performance.

Chapter 3 of this dissertation includes the results of a testing program aimed at quantifying the feasibility of using different DSR test geometries to characterize the rheology of CRM binders incorporating a varying range of CR sizes and concentrations. The relationship between CRM binder rheology and asphalt mixture properties will then be used to identify the DSR geometry capable of producing the most accurate representations of mix performance. The DSR test geometry identified in Chapter 3 is then used in the study presented in Chapter 4 to evaluate the mechanisms of interaction between asphalt binders and CR at different elevated temperatures.

Both the interaction effects, as well as CRM binder performance were evaluated in that particular DSR geometry.

Due to the relatively high cost of the wet process, and inconsistent performance of the dry process; pre-treated CR was introduced by the industry and is an emerging technology. CR pre-treatment is done by mixing CR particles with low viscosity petroleum-based products or aromatic oils compatible with the lighter asphalt fractions to enhance the compatibility of CR with the modified binder matrix and block the penetration of asphalt liquid into CR. This modifier is incorporated into the asphalt mixture in a manner similar to that of the dry process. The study presented in Chapter 5 utilizes the rheological interaction mechanisms identified in Chapter 4 to quantify the extent of CR pre-treatment. This will be of high value to practitioners to identify sufficiently pre-treated CR materials in the laboratory before being incorporated in CRM HMA mixtures as more products are being introduced in the market.

CRM binder testing and characterization continues to rely on empirical tests that indicate modification, but do not address fundamental engineering behavior relating to pavement performance. Chapter 6 provides alternative parameters derived from rheological characteristics of CRM binders evaluated as indicators of overall binder performance and provided strong correlations to CRM binder fatigue and rutting characteristics. These parameters can be obtained and applied to QC screening of CRM binders without the need for micromechanical modeling or advanced testing/characterization techniques.

This dissertation presents a comprehensive comparative analysis evaluating performance characteristics in CRM binders as influenced by different material variables including a wide range of base asphalt binder Performance Grades and CR sizes. The conclusions drawn herein provide a

better understanding of CR modification techniques and can be used in performance-based specifications on asphalt binders.

CHAPTER 2. RELEVANT LITERATURE REVIEW

There are two main types of rubber; natural, and synthetic. Raw natural rubber is composed of long straight chain isoprene hydrocarbon (polyisoprene). Natural rubber is sticky in nature and easily deforms at high temperatures and is brittle at low temperatures. Due to the chemical nature of natural rubber, the long polymer chains can move independently, relative to each other; which can cause inelastic deformations. Therefore, vulcanization of natural rubber is necessary to transform it into a strong and elastic material. Vulcanization can be done in two different processes; mould cured (hot) and pre-cure (cold) processes. Mould cured vulcanization is used for the majority of rubber products including tires. Pre-cured vulcanization is used for production of thin and soft products such as surgical gloves. Synthetic rubber is made from petroleum products and other minerals and is produced in two stages; production of monomers – small unit molecules – and polymerization. Examples of synthetic rubber include Styrene-Butadiene Rubber (SBR), and Silicon rubbers (Rahman 2004).

Tires are composites of natural and synthetic rubber, carbon black, metal and textiles, in addition to the additives used in the compounding and vulcanization processes. Natural rubber provides the elastic properties, and synthetic rubber improves thermal stability. The proportion of natural to synthetic rubber in tires varies depending on the size and application of the tire. In general, the more rugged the intended use of a tire is, the greater the ratio of natural to synthetic rubber is. In general, the ratio of natural to synthetic rubber is 1:2 in automobile tires, and 2:1 in heavy truck tires (Chesner et al. 1988). Carbon black enhances the rigidity in tire treads to improve traction, helps control abrasion to reduce aquaplaning, improves the flexibility of tire sidewalls, and reduces the heat buildup. Crumb rubber is typically composed of both automobile and heavy

truck tires. A comparison of the components in these two types of tires is presented below in Table 1 (Shulman 2000).

2.1 CR Production Methods

The life span of a tire is approximately five to seven years during which a tire can be retreated. Once a tire reaches its end of life, it is collected for landfilling and recovery. Such tires are defined as waste tires. Typical waste automobile tire weighs 9 kilograms, and typical waste truck tire weighs 18 kilograms. Approximately 60 to 70% of waste tires is recoverable rubber (Chesner et al. 1988).

Table 1: Automobile and heavy truck tire composition (Shulman 2000).

Material	Automobile vehicles (%)	Heavy trucks (%)
Rubber/ elastomers	48	45
Carbon black	22	22
Metal	15	25
Zinc oxide	1	2
Textile	5	-
Sulphur	1	1
Additives	8	5

Waste tires can be recycled as whole tires, slit tires, and shredded or chipped tires. Slit tires are produced by cutting a tire into two halves. The size of tire shreds produced in the primary shredding process varies between 300 to 460 mm long and 100 to 230 mm wide. Tire chips range between 76 mm and 13 mm. Reducing the size of tire shreds produces CR materials suitable for use in asphalt modification (Chesner et al. 1988). CR products used in the asphalt industry are

highly controlled materials. The production process is carefully planned to produce clean and highly consistent materials. The specific gravity of CR products for use in asphalt modification varies from 1.10 to 1.20 depending on the production method. CR must be free from any fabric wires or any other contaminants in accordance to ASTM D6114 (2009).

2.1.1 Ambient Production Process

The ambient process is a method of mechanically grinding waste tires at ambient temperature. Rotating steel blades and drums are used in this process to shred the waste tires. Ambient grinding can be done either by using a granulator, or a crackermill. Granulators reduce the rubber size by means of a cutting and shearing action. Adjustable screens within the machine control the end product size. The crackermill process is the most commonly used ambient production method and utilizes low speed machines in which the rubber is passed through multiple mills to produce various particle sizes as the steel and fibers are removed from the tire. Products of both these processes are normally irregularly shaped and rough in texture and have a cut surface shape with sizes ranging from 9.5 mm to 0.4 mm (3/8 in. to No. 40 sieve) (Rahman 2004).

2.1.2 Cryogenic Production Process

The cryogenic process consists of freezing waste tires in liquid nitrogen, or a similar material, between -87 and -198°C surpassing the Glass Transition (T_g) temperature of all tire rubber polymers until it becomes brittle. Table 2 shows typical glass transition temperatures of tire rubber polymers (Pampulim 2013). A hammer mill is then used to shatter the frozen rubber into smooth particles with relatively lower surface areas compared to rubber produced from ambient grinding.

Table 2: Glass Transition points of tire rubber polymers (Pampulim 2013).

Tire rubber polymer	T_g (°C)
Natural rubber	-58
Polyisoprene rubber	-58
SBR rubber (various grades)	-52 to -48
Polybutadiene rubber	-73
Butyl rubber	-58

2.1.3 Effect of CR Processing Method on Surface Morphology

Several researchers (Memon 2011 and Thodesen 2008) have examined the effect of CR production methods on its' surface morphology. The ambient and cryogenic methods produce rubber particles with different shapes and textures. The morphology of the rubber particles produced from ambient grinding exhibits high pore density, therefore a high surface area. This is caused by the intensive grinding action in the ambient process. On the other hand, the morphology of cryogenic rubber particles exhibits a low pore density and surface area with relatively smooth surfaces. This is due to the instantaneous hammer mill impact on the frozen rubber material (Memon 2011). It is documented in the literature that CR particles with higher surface areas and rough texture show enhanced reaction with asphalt binder when compared with CR with smoother surfaces (Roberts et al. 1989). Therefore, CR produced from ambient grinding is typically used in the wet process modification of asphalt binder, whereas cryogenic CR is favored for use in the dry process in the asphalt industry.

2.2 Interaction Mechanisms of CR and Asphalt Binder

The nature of interaction between asphalt binder and CR has not been fully understood. When the two materials interact, asphalt components are absorbed by the rubber particles causing them to swell. This interaction was first thought of as a non-chemical reaction where the rubber swells in the oily phase of the asphalt at high temperatures to form a gel-like material. Rubber swelling results in less free space between the swollen particles, and therefore results in a viscosity increase in the modified binder (Heitzman 1992). Other studies claimed that this viscosity increase cannot be solely explained by the presence of swollen rubber particles (Bahia and Davis 1994). This reaction consists of two simultaneous processes; partial digestion, and absorption. The partial digestion of CR into asphalt is explained in the literature as depolymerization or devulcanization, and both are chemical reactions that cause a reduction in the molecular weight of the rubber particles by breaking their chemical bonds. Devulcanization breaks the bonds that are formed in the vulcanization process during tire production. The absorption of aromatic oils from the asphalt binder into the polymer chains at high temperatures (160° to 220° C) causes the rubber to swell and soften. Rubber reacts with asphalt binder in a time-temperature dependent manner. Once the rubber is swollen, continued exposure to high temperatures will replace the swelling phenomena by disintegration of the rubber into the asphalt by depolymerization. The asphalt rubber binder should be homogeneous with the rubber after being devulcanized, but not depolymerized. Depolymerization causes a release of rubber components back into liquid phase causing a decrease in viscosity. Figure 2 (adapted from Abdelrahman and Carpenter 1999) shows a schematic progression of this interaction at elevated temperatures where CR is unswollen at t1, swollen at t2, and then begins to depolymerize with extended mixing times at t3.

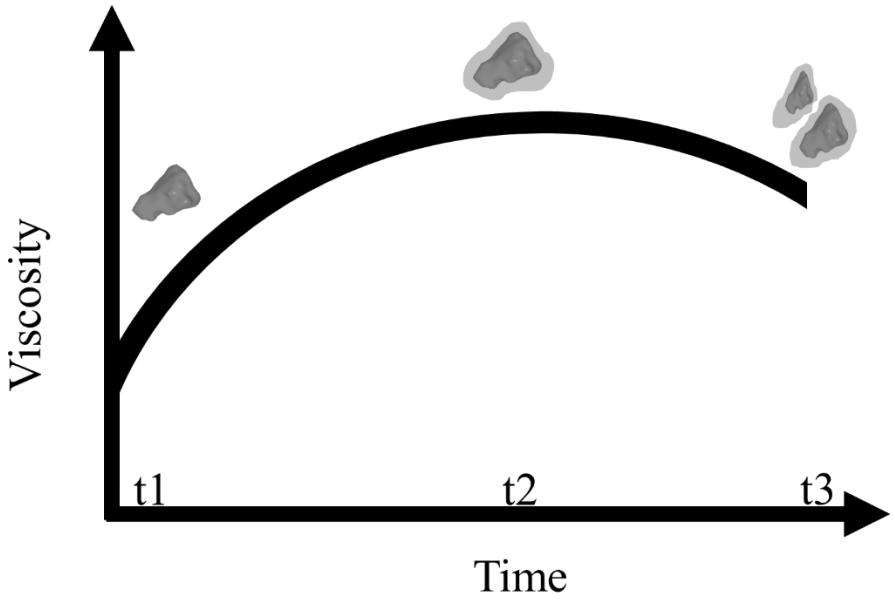

Figure 2: Illustration of the theory of interaction between CR and asphalt binder at elevated temperatures

This interaction is material specific and depends on several factors and conditions. Production variables need to be monitored during the modification/production process of CRM binders to ensure a modified product that meets the anticipated improvements in the base material. The following is a discussion on the effect of each variable to provide a better understanding of the modification process, and the role of each variable.

2.2.1 Interaction Conditions

The final properties of CRM binders are highly dependent on the blending temperature. Low blending temperatures (120° C or less) do not provide conditions severe enough to break up the chemically cross-linked rubber network in CR materials. Differences in rheological behavior in blends processed at low temperatures are only caused by the presence of swollen CR particles. Higher processing temperatures (160° to 200° C) are vital for producing materials with improved properties (Navarro et al. 2004). It is believed that not only rubber absorbs the light aromatic oils

in asphalt, but also releases some of the carbon black and antioxidant components found in CR. The physical interaction process caused by controlling the blending temperature is also emphasized in the literature. The first effect is on the rate of swelling of CR particles. As the temperature increases, the rate of swelling increases. The second effect is on the extent of swelling. As the temperature increases, the extent of swelling decreases (Green and Tolonen 1977). An optimum blending temperature must be selected prior to producing CRM binders.

Blending time can be separated into two main phases, a short-term phase that last 30 to 40 minutes (varies with temperature), and a long-term phase that lasts for a few hours. Most of the changes and modification occur in the first phase, while the properties stabilize in the second. In general, longer reaction times lead to an increase in viscosity, related to the increase in rubber mass caused by absorption of the light asphalt components. However, prolonged reaction (up to 24 hours) causes reduction in viscosity and elastic response, indicating a level of undesirable rubber degradation. Rubber degradation occurs more rapidly at higher temperatures. If the binder is exposed to high temperatures (>210°C) for enough time, depolymerization continues up to full destruction of the polymer network (Abdelrahman and Carpenter 1999).

The use of high shear mixing (3000 to 8000 RPM) in producing CRM asphalt blends allows the interaction process to progress with greater speed. In addition, high shear serves in breaking the particle-particle bonds which leads to better dispersion of CR particles in the polymer matrix, and therefore improved storage stability (Shenoy 1999). However, the influence of blending shear stress is not as significant as blending temperatures (Navarro et al. 2004).

2.2.2 Base Binder Properties

The composition of base binder used in producing CRM binders is a key factor influencing the final rheological properties of the end product (Abdelrahman and Carpenter 1999). In fact,

base binder properties have a greater impact on the rutting susceptibility and viscosity of the modified binder than those of the CR used in the modification (Thodesen 2008). Aromatic fractions of the base binder are the major cause of rubber swelling through the diffusion and absorption phenomena. Therefore, binders with high levels of oily fractions or aromatics are necessary for optimized rubber swelling and viscosity of the final blend.

2.2.3 Rubber Properties

As mentioned earlier, CR can be produced from either truck or automobile tires. The major differences in modified binders utilizing CR from different sources is primarily in viscosity and softening point. Truck tire sourced CRM binders show less of a viscosity increase when compared to CR obtained from automobile tires. This can be explained partially by the fact that truck tires contain a higher content of natural rubber (Table 1), which may lead to the dissolution of tire rubber, rather than swelling in asphalt binders. In addition, and as previously mentioned; CR grinding methods also influence the rate of reaction and viscosity of CRM binders.

CR particle size controls the swelling mechanism over time. Fine rubber particles typically swell faster than coarse particles and depolymerize faster. This affects the liquid phase more than the binder matrix (i.e. CR blended with binder). Coarse rubber particles have less effect on the liquid phase. Liquid phase modifications are more stable than binder matrix modifications. Phase separation and storage stability, to some extent, can also be influenced by CR particle size. Fine rubber particles improve the settling properties of CRM binders. Therefore, fine grained rubber particles are typically used in the production of CRM binders (Abdelrahman and Carpenter 1999). However, CR particle size has little influence on settling properties when high processing conditions are used (Glover et al. 2000).

Attia and Abdelrahman (2009) investigated the interaction mechanisms of CRM asphalt blends by controlling the swelling of CR particles through varying the interaction conditions such as time, temperature, shearing speed, CR particle sizes and addition of polymer modifiers. The study confirmed that temperature is the main key in controlling the interaction mechanisms. The study also observed that the particle size has a significant effect on the performance properties. The coarser CR particles yielded higher stiffness and lower phase angle values under the same interaction conditions as opposed to finer CR particles. Literature indicates that the presence of CR particles in asphalt binder leads to a stiffening effect at high temperatures (e.g., 76°C), and softening effect at lower temperatures (e.g., 15°C). This phenomenon can partially be explained through the rule of mixtures (or particulate filled composite) theories, as illustrated schematically in Figure 3.

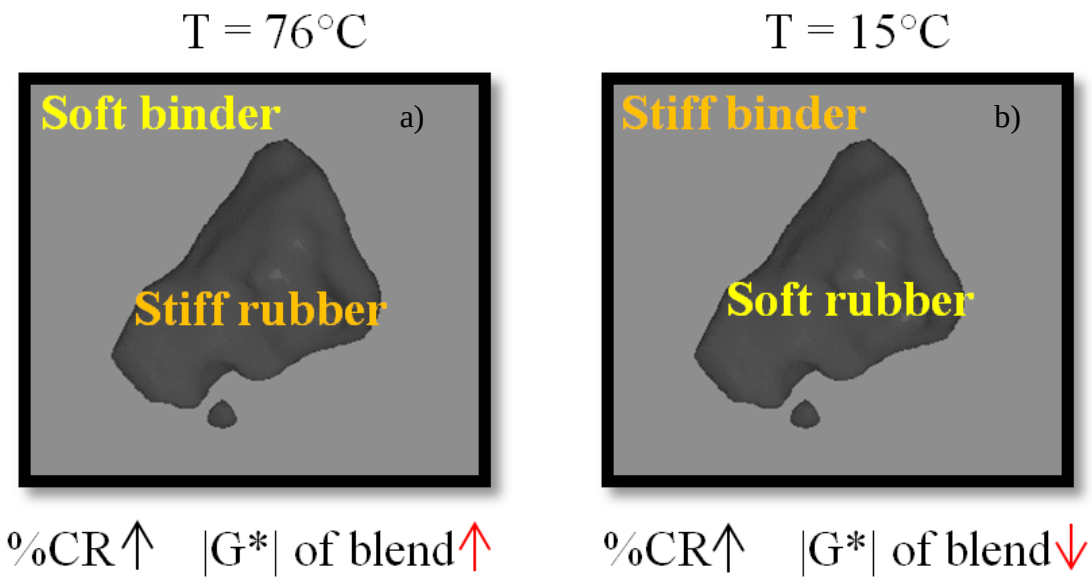

Figure 3: Schematic explanations of (a) stiffening, and (b) softening effects of CRM binder.

When a stiff inclusion is present in a soft medium, the stiffness of the overall blend will be stiffer than the soft medium. At relatively high temperatures (e.g., 76°C), since the binder is softer than the rubber particle, |G*| of the CRM binder is expected to be higher than |G*| of the base binder. Similarly, at low temperatures (e.g., 15°C), the binder becomes stiffer than the rubber

particle, therefore the CRM binder is softer than the base binder. It should be noted that this stiffening and softening effect cannot solely be explained by just the 'presence' of the CR particle in binder. As the rubber particle is mixed with the binder at very high temperatures (e.g., 190°C) and allowed to interact, it absorbs light fractions and swells while releasing some of the anti-oxidants into the asphalt binder. Diffusion as well as chemical interactions also occur during mixing. At the end, the rubber particle becomes a viscoelastic 'rubber-asphalt binder (light fractions)' blend.

2.3 Challenges with PG Grading CRM Binders

As briefly mentioned in Chapter 1, one of the major challenges for specifying CRM binders is the fact that they are mostly suspensions and many States do not allow Superpave Performance Grading (PG) system to be applied to CRM binders since PG system was originally developed for pure viscoelastic fluids (without inclusions). The physical characteristics of CRM binders have been and continue to be specified in most adopting states by empirical tests that are highly variable with no solid link to field performance. Fundamental engineering properties of these materials need to be measured for a better understanding of the modification effects on field performance. The DSR has been used to characterize rheological properties of neat and modified asphalt binders over a wide range of temperatures and frequencies as part of the PG specifications introduced by the Strategic Highway Research Program in 1993. The DSR parallel plate testing geometry with different gap sizes (1.0 and 2.0 mm for low and high test temperatures respectively) have been used for binder testing ever since.

Several researchers suggested the need for modifications on current DSR testing protocols to accommodate rubber particles present in CRM binders. Bahia and Davies (1995) increased the gap height needed for high temperature binder property measurements in the DSR from 1.0 to 2.0

mm to limit the interference of larger rubber particles with the DSR parallel plates. A strain sweep using a 2.0 mm gap height determined that the linear viscoelastic region limits of the asphalt binders investigated were similar to those measured using a 1.0 mm gap height. Tayebali et al. (1997) investigated the applicability of the DSR to CRM binders, and the effect of rubber concentration on the high temperature PG. The research team increased the gap height from 1.0 to 2.0 and from 2.0 to 4.0 mm for high and intermediate PG testing. The overall coefficient of variation reported between test replicates was 6.2% due to the increase in DSR gap height. This variation was inferred to operational errors and sample variance, rather than the interference of rubber particles in the parallel plate setup. In accordance with these findings, Putman et al. (2005) also used a 2.0 mm gap height in the DSR to measure high temperature CRM binder properties.

However, recent studies suggested a need for an alternative testing geometry due to concerns regarding the capability of the parallel plate system to accommodate large (> 30 mesh) rubber particles present in CRM binders (Baumgardner and D'Angelo 2012, Bennert 2013, Alavi 2015, and Hung et al. 2015). For that, an approach commonly used in the food industry (Steffe 1996) utilizing a concentric cylinder that rotates inside a stationary outer cylinder was proposed. The main advantage of this test geometry is the larger gap (~6.2 mm) between the inner and outer cylinder, which helps accommodate the large swollen CR particles.

Baumgardener and D'Angelo (2012) evaluated the capability of the concentric cylinder geometry (a.k.a. cup and bob) to capture the characteristics of neat, polymer modified, and CRM binders and found that this alternative geometry provides similar Superpave $|G^*|/\sin\delta$ parameter to those obtained using the parallel plate geometry. The study also reported similar Multiple Stress Creep and Recovery (MSCR) results obtained from the concentric cylinder to those obtained from the parallel plate setup for neat and polymer modified binders. However, MSCR test results for

CRM binders from the concentric cylinder were not similar to results obtained from the parallel plates. Bennert (2013) found that the Superpave |G*|/sinδ parameter measured using the concentric cylinder geometry was approximately 15% higher than that measured in the parallel plate system (CR sizes included 20, 30, 50 and 60 mesh), while Hung et al. (2015) found no significant differences between the results obtained from the different geometries (one small CR size of 50 mesh was used in modification). In a similar effort, Alavi (2015) compared the rheology of CRM binders with varying rubber sizes and sources and found that the concentric cylinder produced generally about one degree higher continuous PG than that measured by the parallel plates. They used 20% CR content by weight of the asphalt binder. In addition, the study reported slightly higher MSCR recovery and slightly lower MSCR non-recoverable creep compliance in the concentric cylinder, but there was significant scatter in the data because of large percentage of CR (20%). These studies provided very valuable initial indications of how well concentric cylinder measurements compare to those of parallel plates in the DSR. However, these studies are lacking in providing justification or need for this alternative measuring system for the asphalt industry, especially at lower contents of CR used in terminally blend technologies. A comparison between the mechanical properties of asphalt mixtures and their constituting binders is of more value to determine whether the concentric cylinder provides more accurate performance measures. Since CR particles are compressed inside the asphalt mixture in the field, this study hypothesizes that the parallel plate testing geometry may provide more representative properties of CRM binders that can be linked to asphalt mixture characteristics. Artificially increased binder stiffness (or cushioning effects), which are of concern in the parallel plate setup, are more likely to be the actual case exhibited in CRM mixtures in the field. In addition, binder testing in the concentric cylinder setup is extremely time-consuming. Due to the large volume used in this testing geometry (~25 g);

a thirty-minute equilibrium period is needed to reach temperature equilibrium at each test temperature. Characterizing one test replicate (at 5 different temperatures) can consume 4 hours, including testing and equilibrium time. The parallel plate geometry on the other hand requires much shorter testing times. According to AASHTO T315 *"Standard Method of Test for Determining the Rheological Properties of Asphalt Binder Using a Dynamic Shear Rheometer (DSR)"*, a temperature equilibrium time of 15 minutes is recommended at each test temperature. However, a temperature sweep may be conducted on the test material to determine the needed time for temperature equilibrium prior to testing. This equilibrium time can be reduced to as low as three minutes.

CHAPTER 3. EVALUATING CRM BINDER RHEOLOGY IN THE DSR

This component of the dissertation is aimed at investigating and quantifying the feasibility of using the DSR parallel plate test geometry to characterize the rheology of CRM binders. It is hypothesized that that the parallel plate geometry will provide a more viable link to asphalt mixture performance than those characteristics obtained by the recently proposed concentric cylinder system. In addition, parallel plate testing is more time efficient. For this, an experimental approach is presented. CRM binders produced with varying CR sizes and concentrations by means of the wet process were characterized over a range of temperatures and frequencies in both the DSR parallel plate and concentric cylinder geometries. Then, dense graded HMA mixtures were designed using these CRM binders and the performance characteristics were obtained from the dynamic modulus (|E*|) test. The characteristics obtained were used to quantify the relationship between mixture and binder mechanical properties for indications of a suitable DSR test geometry that produces representative material properties relating to mixture performance.

3.1 Materials and Methods

3.1.1 CRM Binders

The asphalt binder used in this study was a neat unmodified PG 58-28. CR was introduced into the asphalt binder at a temperature of 190° C and was allowed to interact for 60 minutes at 1,000 rpm (rotation per minute) shearing speed. To study the effects of particle size on the differences between the two DSR geometries, three different sizes were used in modification. In addition, two dosages of CR were used in the modification (10 and 25% by weight of the asphalt binder) to evaluate the effect of CR concentration on measurements obtained by these two geometries. Table 3 shows CR sizes and modification dosages used in producing the CRM blends.

Table 3: CR modifier sizes and dosages used.

Sieve Size (No.)	Median CR Size (mm)	% By weight of binder	CRM ID
Coarse: No. 16-20	1.00	10	#20-10%
		25	#20-25%
Medium: No. 30*	0.45	10	#30-10%
		25	#30-25%
Fine: No. 40-50	0.35	10	#50-10%
		25	#50-25%

*Includes the entire gradation of a 30x0 mesh crumb rubber material

Figure 4 shows the gradation range of the 30x0 mesh CR material used in blending No. 30 materials shown in Table 3.

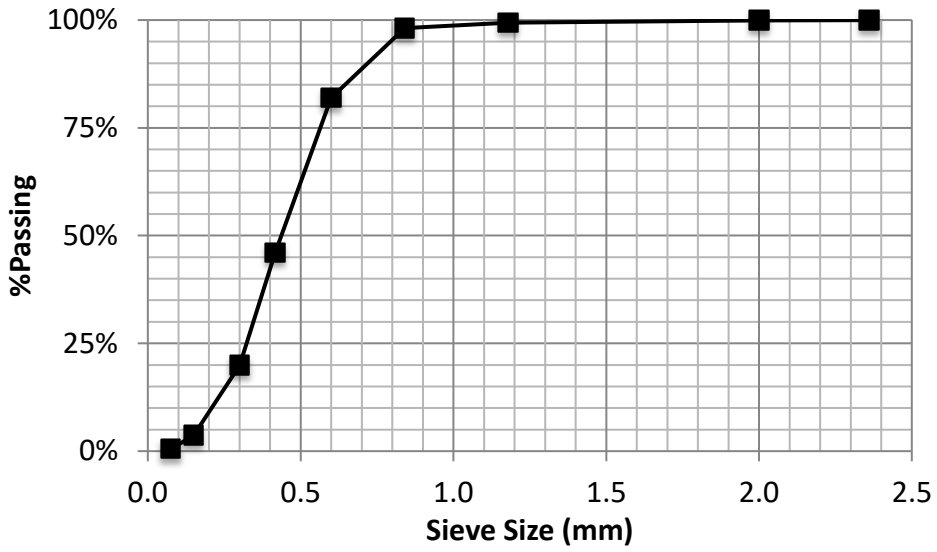

Figure 4: 30x0 mesh CR Gradation.

An Anton Paar MCR 302 Dynamic Shear Rheometer (DSR) was used for both parallel plate (PP), and concentric cylinder (CC) measurements. Strain controlled frequency sweep tests

were conducted on CRM binders and the sampled data included dynamic shear modulus (|G*|) and phase angle (δ). Parallel plate testing (Figure 5) was conducted in accordance with AASHTO T315 at 10% strain level. For measurements using the PP geometry, three test replicates were used to generate the data at 15, 30, 46, 58, 70, and 82°C at a set of varying frequencies ranging from 1.0 to 100.0 rad/sec. For measurements using the CC geometry, same frequency and temperature combinations were used, except the tests at 15°C were not run in CC geometry due to difficulties with testing the large sample size at such a low temperature. A 2.0 mm gap (B in Figure 5) height was used with 8 mm test plates (A in Figure 5) at 30°C. Similarly, a 2.0 mm gap was used (to accommodate CR particles) with 25 mm plates at the remaining temperatures.

CRM binders were also tested in the concentric cylinder setup. Three test replicates were also used to generate the data at the same test temperatures and frequencies used in parallel plate testing. The concentric cylinder geometry used in this analysis consisted of a stationary 14.46 mm inner radius cup, and a rotating cylinder (bob) with 8.33 mm radius; allowing for a 6.2 mm gap between the sides of the cylinder and the walls of the cup (Figure 6). This is one of the main advantages of using this configuration. This increased gap allows accommodation of large CR particles. The second advantage of this geometry is that no sample trimming is required. This geometry is controlled by the surface of the cylinder, and the walls of the cup. Any binder remaining at the bottom of the cup or overflows the cylinder has a negligible effect on shear stress and strain calculations and can be ignored (Baumgardner and D'Angelo 2012). However, the disadvantages of using this geometry include the need for much larger samples (25 g), and therefore long equilibrium times (30 minutes) needed for each test temperature.

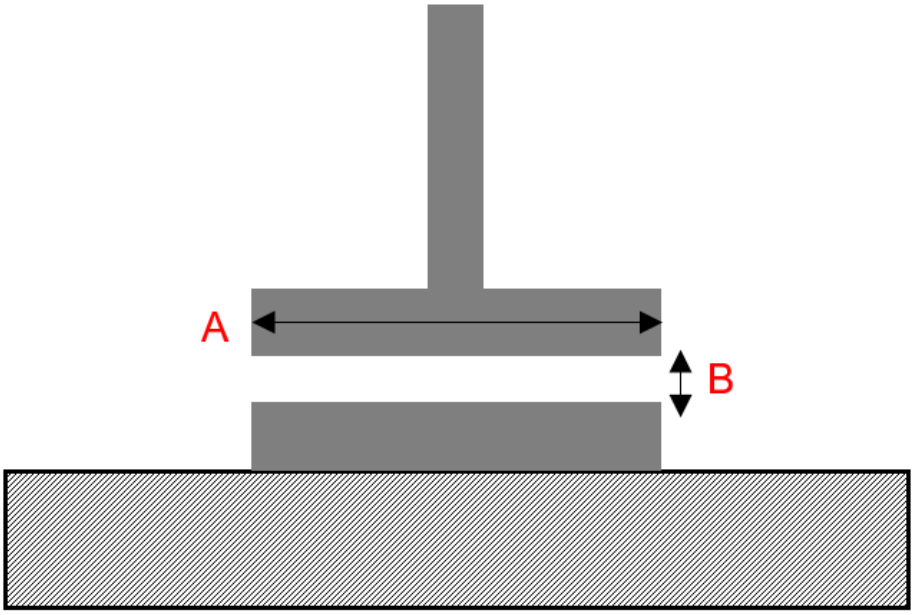

Figure 5: Schematic representation of DSR Parallel Plate geometry.

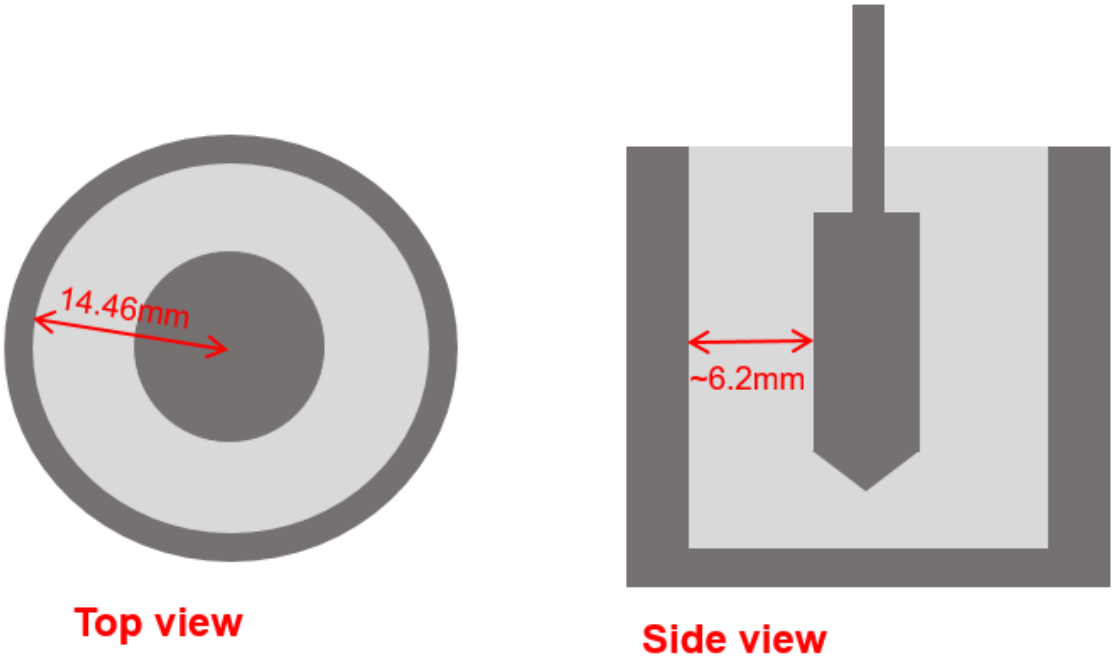

Figure 6: Schematic representation of DSR Concentric Cylinder geometry.

The shear stress (τ) and shear strain (γ) generated from the concentric cylinder geometry are calculated as shown below:

$$\boldsymbol{\tau = \frac{T}{2\pi L r_i^2}} \quad \textit{(1)}$$

$$\boldsymbol{\gamma = \frac{\theta r_e}{(r_e - r_i)}} \quad \textit{(2)}$$

where,

T = torque,

L = length of the bob,

r_i = radius of the cylinder,

r_e = radius of the cup, and

θ = angular rotation of the cylinder.

To combine the effects of frequency and temperature on |G*|, master curves were generated using the values measured at different temperatures and loading frequencies. A |G*| master curve is obtained using the time-temperature superposition (TTS) principle (Kim 2009) by horizontally shifting the measured data for each associated frequency until a good sigmoid fit to the |G*| data of all temperatures is obtained. The resulting frequency is called reduced frequency (f_R), and is defined as follows:

$$\boldsymbol{f_R = f . a_T(T)} \quad \textit{(3)}$$

where f is the frequency of the load and $a_T(T)$ is the shift factor coefficient for a given temperature, T representing the amount of horizontal shift for data measured at a given

temperature. This value is different for each test temperature. Typically, the following sigmoid function is used to describe the |G*| master curve:

$$\boldsymbol{log(|G^*|) = b_1 + \frac{b_2}{1+exp(-b_3-b_4.log(f_R))}} \quad \textit{(4)}$$

where b_1, b_2, b_3, and b_4 are the sigmoid coefficients, and f_R is the reduced frequency defined in Equation 3. After the shifting is completed and the shift factor coefficients are determined, they are plotted against each temperature (T), and a second order polynomial is fitted to the data to obtain the polynomial coefficients a_1 and a_2 in the following equation:

$$\boldsymbol{a_T(T) = 10^{a_1\left(T^2-T_{ref}^2\right)+a_2(T-T_{ref})}} \quad \textit{(5)}$$

where T_{ref} is the reference temperature, usually at a mid-point of test temperature range (i.e. 46 °C in this study).

3.1.2 CRM Mixtures

CRM binders used in the rheological measurements were also used in fabricating asphalt mixtures for performance testing. The Michigan Department of Transportation (MDOT) Superpave mix design guidelines were adopted for this design. This mixture was designed as a MDOT 4E1 mix, indicating its use in the 4th structural pavement layer (top/leveling course), with a design traffic level between 0.30 and 1.0 Equivalent Single Axle Loads (ESALs) (MDOT 2007). This mix design is commonly used in pavement resurfacing applications in the State of Michigan. The design requirements and characteristics for MDOT 4E1 mixtures are shown in Table 4, and the aggregate gradation used is shown in Figure 7, where the Nominal Maximum Aggregate Size (NMAS) was 12.5 mm.

Table 4: MDOT 4E1 Superpave mix design requirements.

Design Parameter	Requirement
Number of Gyrations	$N_{initial}$: 7, N_{design}: 76, N_{max}: 117
Percent of Maximum Specific Gravity (%G_{mm}) at the design number of gyrations, (N_{design}) (See Note)	96.0%
%G_{mm} at the initial number of gyrations, ($N_{initial}$)	90.5%
%G_{mm} at the maximum number of gyrations, (N_{max})	98.0%
VMA* min % at N_{design} (based on aggregate bulk specific gravity, (G_{sb}))	14.0%
VFA** at N_{design}	65-78%
Fines to effective asphalt binder ratio (P_{No200}/P_{be})	0.6-1.2

*VMA: Voids in Mineral Aggregate, **VFA: Voids Filled with Asphalt

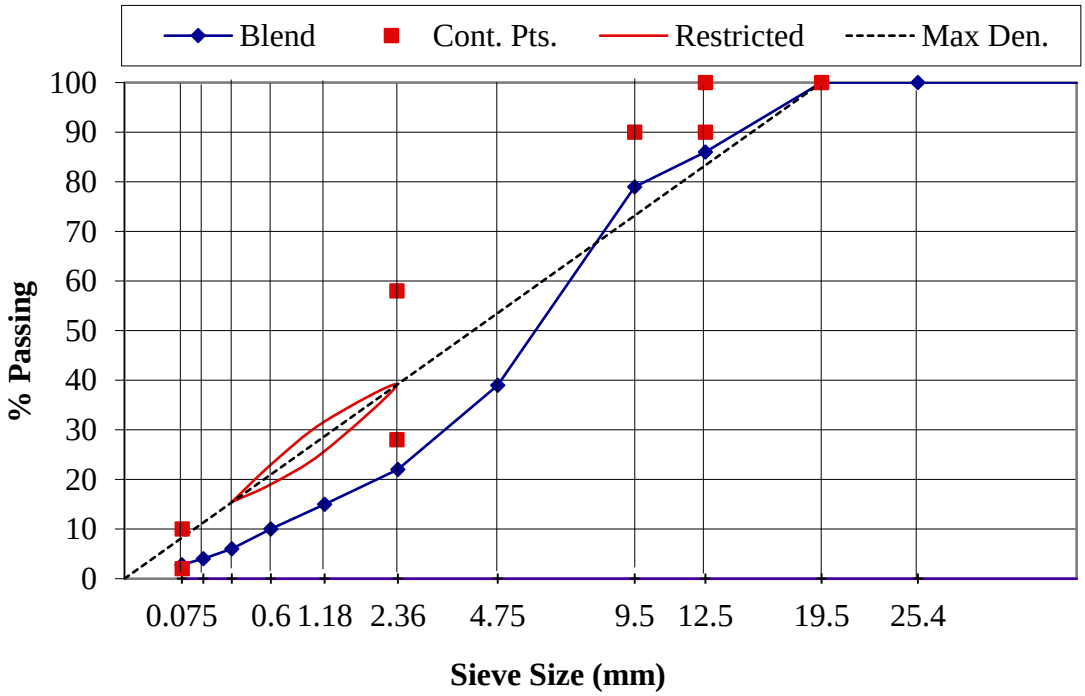

Figure 7: Aggregate gradation utilized in mixture design.

Although mix design volumetrics and aggregate gradation can significantly impact performance characteristics of CRM mixtures, this material is used to establish relationships between CRM mixture and binder performance. The only variable in the mix designs is the CRM binder, and therefore, regardless of the design used in this study; binder rheology tests should be able to capture the most accurate relationships between mixture and binder performance.

Two asphalt mixtures were designed to accommodate the 10 and 25% modifier dosages. Volumetric measurements yielded 7.0% and 6.4% optimum binder contents for 10% and 25% CRM concentrations, respectively. These binder contents were used for asphalt mixtures incorporating different CR sizes, as the measured air void level was within acceptable limits (4.0±0.5%) at the 75 design gyrations.

Cylindrical performance test specimens were compacted to a height of 180 mm and a diameter of 150 mm in accordance with AASHTO PP60 "*Preparation of Cylindrical Performance Test Specimens Using* the *Superpave Gyratory Compactor (SGC)*". The gyratory compacted specimens were then cut and cored to 150 mm high, and 100 mm diameter performance specimens. From rotational viscosity measurements (AASHTO T316), the mixing and compaction temperatures were determined to be 155° and 150° C respectively for binders containing 10% CR by weight of asphalt binder. Increased CR concentrations required a slight increase in mixing and compaction temperatures to 155° and 160° C respectively for 25% CRM binders.

The target air void level for these performance samples was 7±0.5%. Dynamic modulus |E*| tests were conducted in accordance with AASHTO TP 342 "*Determining Dynamic Modulus Mastercurve of Hot Mix Asphalt (HMA)*" at five temperatures (-10, 10, 21, 37, and 54° C), and six frequencies (25.0, 10.0, 5.0, 1.0, 0.5 and 0.1 Hz) for three test replicates.

Similar to binder |G*|, |E*| master curves were developed to combine the effects of frequency and temperature on mixture |E*|. Generating |E*| master curves follows a process identical to the steps described in the previous section for binder |G*| master curves. The only difference is the reference temperature, where 21 °C was used in developing mixture |E*| master curves. It is noted here that reference temperatures used in developing mixture and binder master curves are generally selected at mid-point the range of test temperatures. This temperature does not have to be identical for the mix and binder, as comparisons made in later sections utilize raw measured data, and nor fitted data. Development of |G*| and |E*| master curves is very useful because once the fit factors are determined; binder and mixture moduli can be computed for any temperature and frequency combination.

3.2 Results and Discussion

3.2.1 Comparison of |G| and phase angle mastercurves obtained from Parallel Plate (PP) and Concentric Cylinder (CC) geometries*

Figure 8 through Figure 13 show a comparison of |G*| mastercurves and phase angle measurements for the different CR sizes and concentrations measured using the CC and PP geometries. Based on these plots, the following general conclusions can be drawn for #20 CR:

- At 10% modifier content, the |G*| and phase angle mastercurves are generally quite similar for the two geometries. The curves start to deviate at below 30° C, where 8.0mm plates were used in PP geometry. Variability in log scale was within 4% for |G*| and within 8% for phase angle.
- At 25% CR content, the |G*| mastercurves start to deviate at an earlier reduced frequency, as compared to the 10% CR content. On the other hand, phase angles

measured using the PP geometry were more variable and consistently lower than the phase angles measured using the CC geometry. While phase angle was within 2% for the two geometries, |G*| data varied up to 8%; with generally lower data measured by CC. This phenomenon may be explained by the fact that the large volumetric percentage and large size of the CR particles caused inter-particle interaction (or cushioning); increasing the elasticity of the CR/binder blend. Since the rubber particles are more 'elastic' than the binder, at especially lower temperatures, the CR particles were essentially 'squeezed/compressed' causing the overall |G*| to decrease and the phase angle to decrease.

For #30 CR, the following observations were made:

- At 10% CR content, for the #30 mesh CR that includes a range of different sizes, the PP and CC geometries both produced similar |G*| values. However, some differences were observed at high temperatures. Data variability was up to 21% for |G*| and 8% for phase angle
- At 25% CR content, somewhat surprisingly, the results are similar for both the |G*| and phase angles. Variability in log scale dropped to within 6% for |G*| and within 2% for phase angle in 25% CRM binders as opposed to the higher variability in 10% CRM binders.

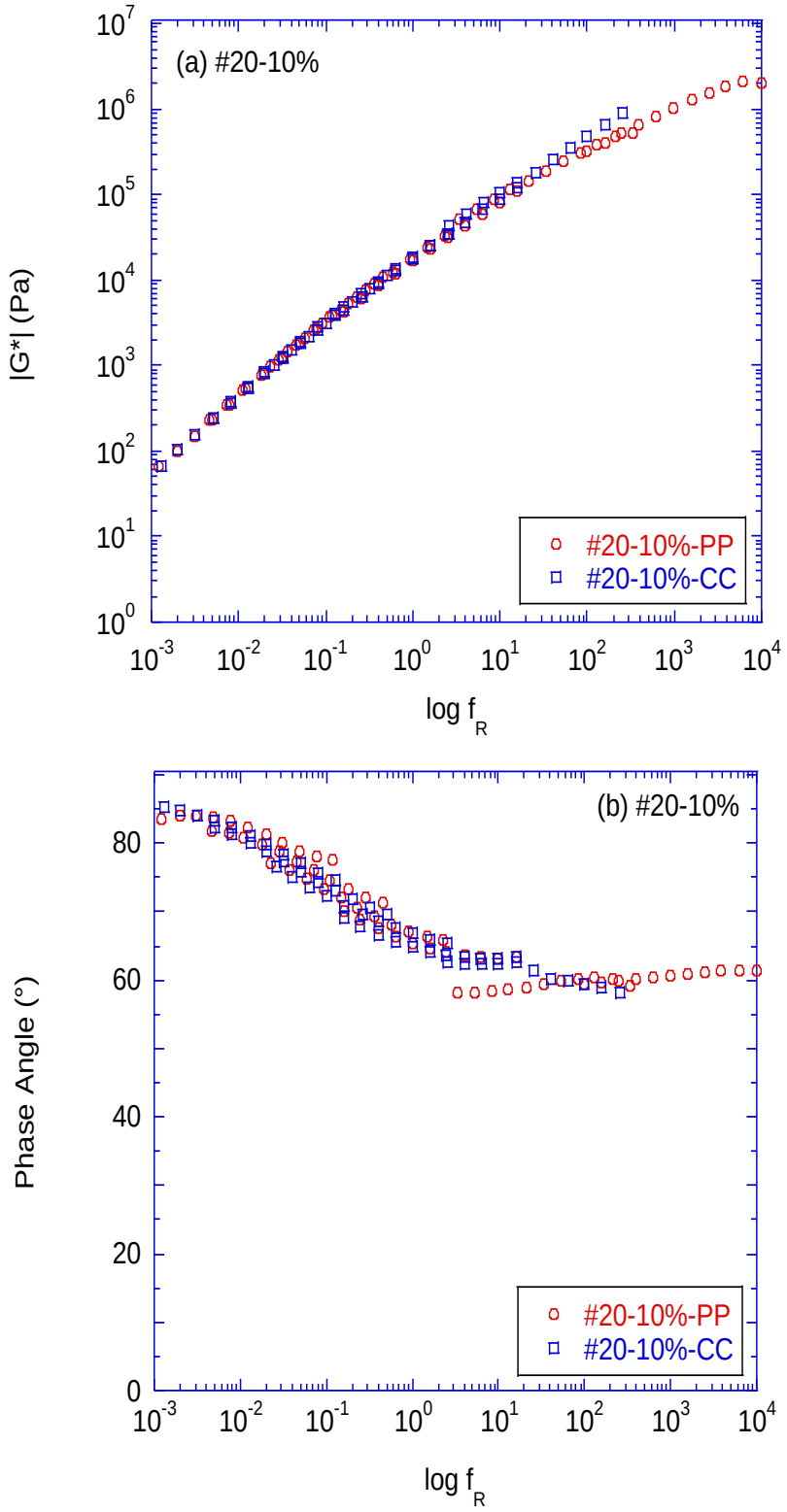

Figure 8: Comparisons of PP and CC obtained (a) |G*| and (b) phase angle for #20-10%.

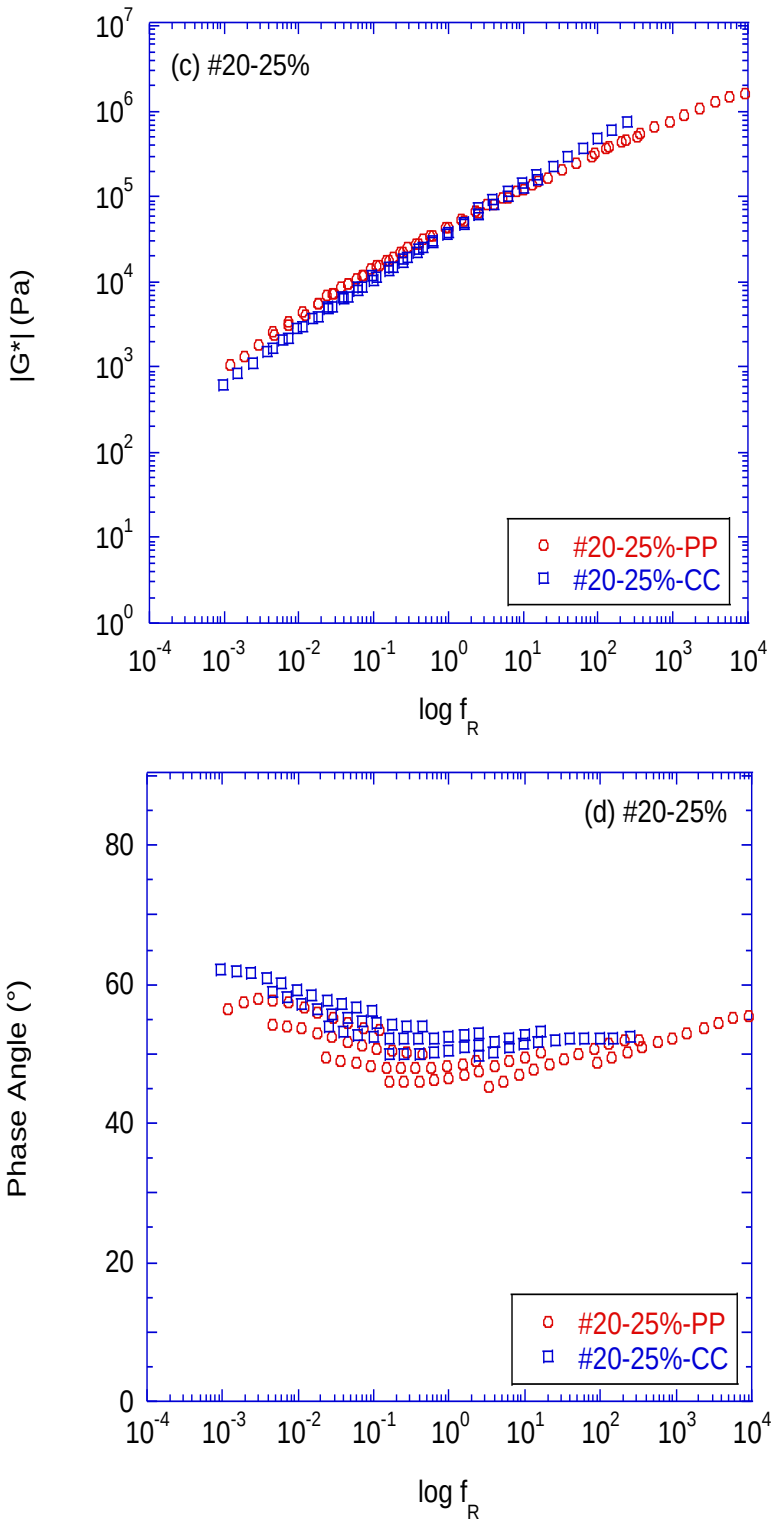

Figure 9: Comparisons of PP and CC obtained (a) |G*| and (b) phase angle for #20-25%.

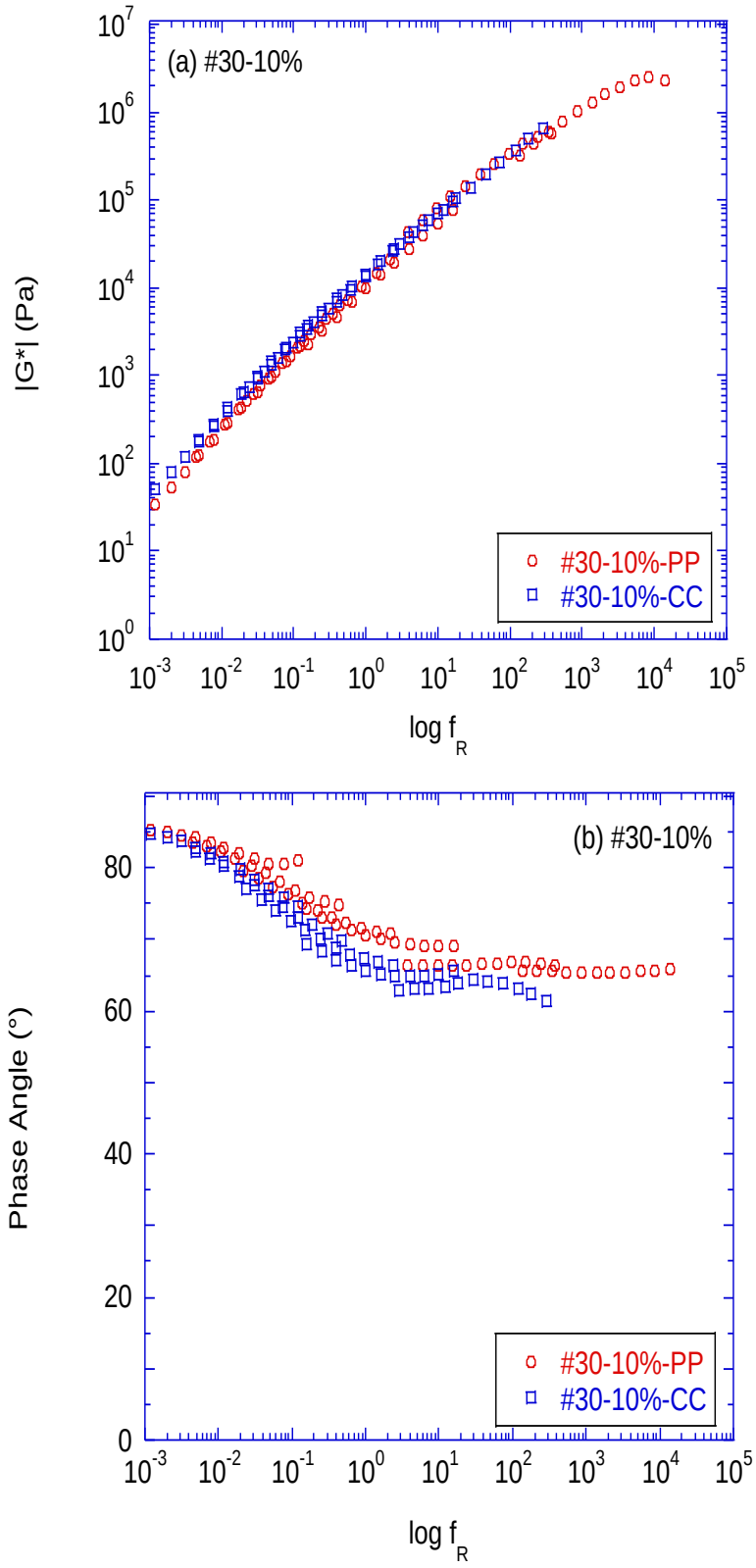

Figure 10: Comparisons of PP and CC obtained (a) |G*| and (b) phase angle for #30-10%.

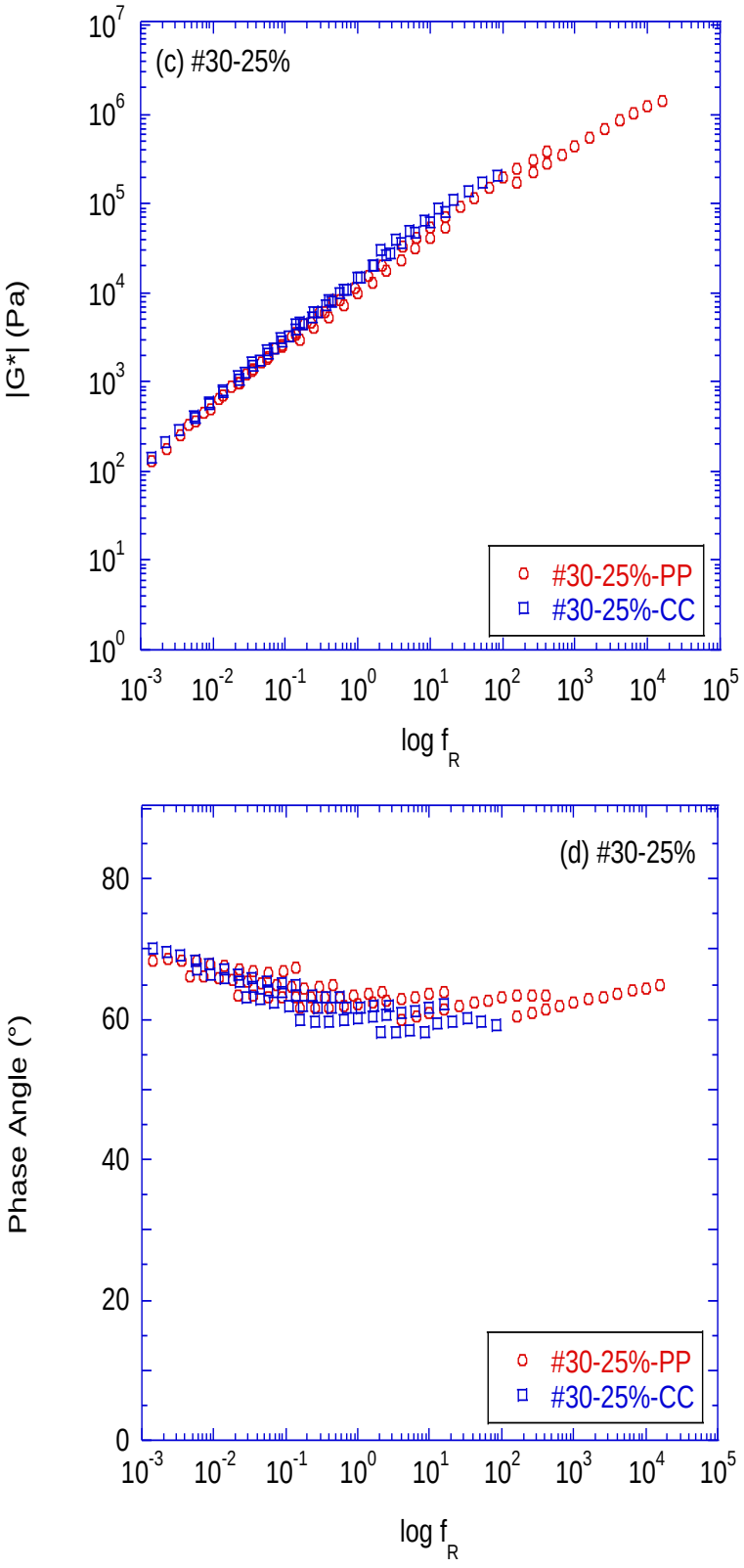

Figure 11: Comparisons of PP and CC obtained (a) |G*| and (b) phase angle for #30-25%.

Similarly, the following observations were made for #50 CR:

- At 10% modifier content, both |G*| and phase angle mastercurves measured using PP and CC geometries are essentially the same. At this CR content and size, it appears 'cushioning' did not occur and the CR particles essentially acted like suspensions in the binder. Therefore, at this size and volumetric percentage, the CR modified binder can be measured by the PP geometry.
- At 25% content, the |G*| mastercurves measured using PP and CC geometries are essentially the same. However, there were differences observed in the phase angles measured by the PP and CC geometries at high temperature/low reduced frequencies. At this time, it is unclear as to why this phenomenon was observed.
- For #50 CR, |G*| and phase angle varied within 4 and 2% respectively at 10% CR, while the variation slightly increased to 8 and 3% for 25% CR.

Furthermore, sigmoid coefficients (Equation 4) and shift factor coefficients (Equation 5) for these binders are provided in Table 5 below for complete interpretation of the master curves generated by the different DSR geometries.

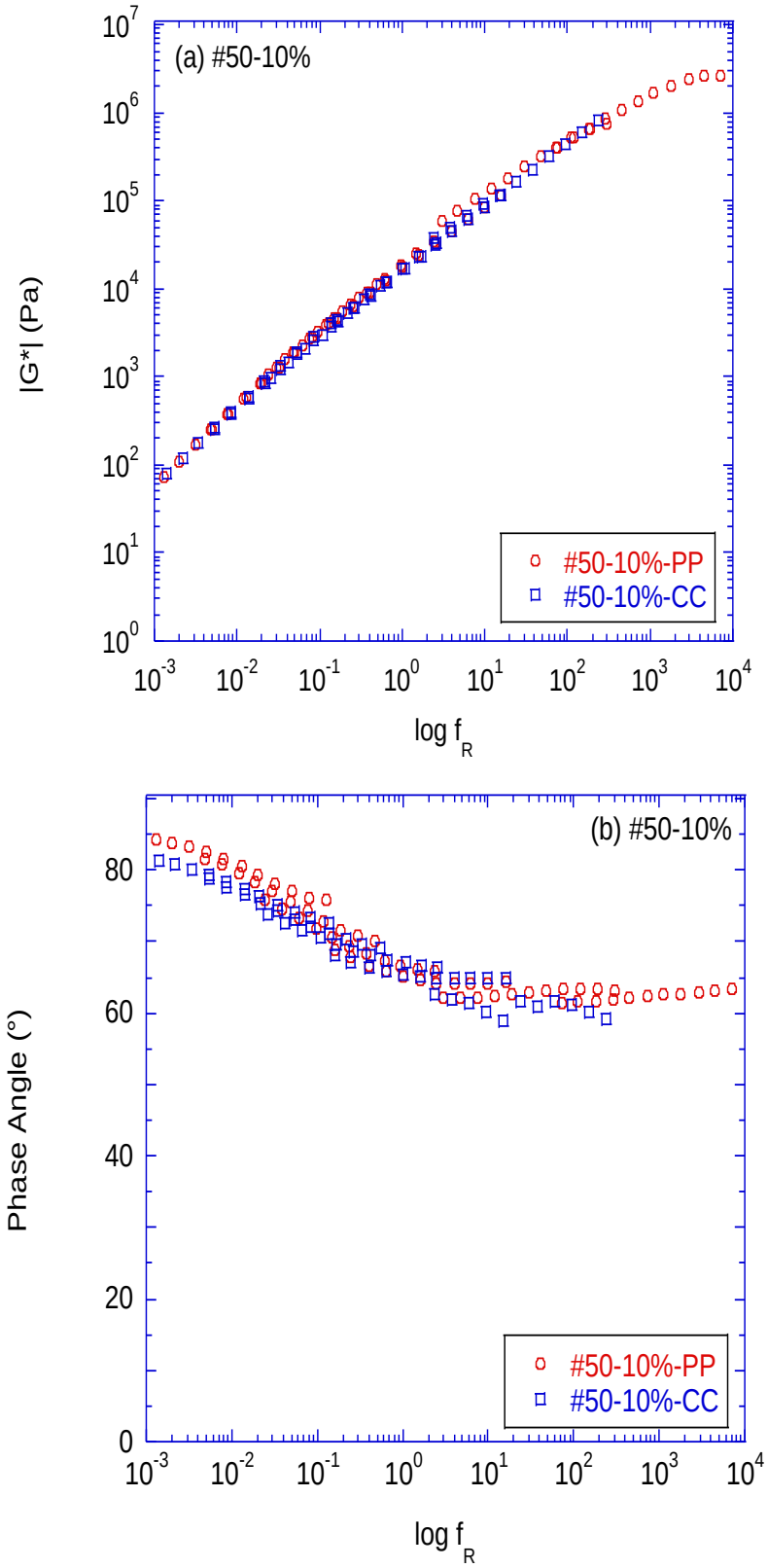

Figure 12: Comparisons of PP and CC obtained (a) |G*| and (b) phase angle for #50-10%.

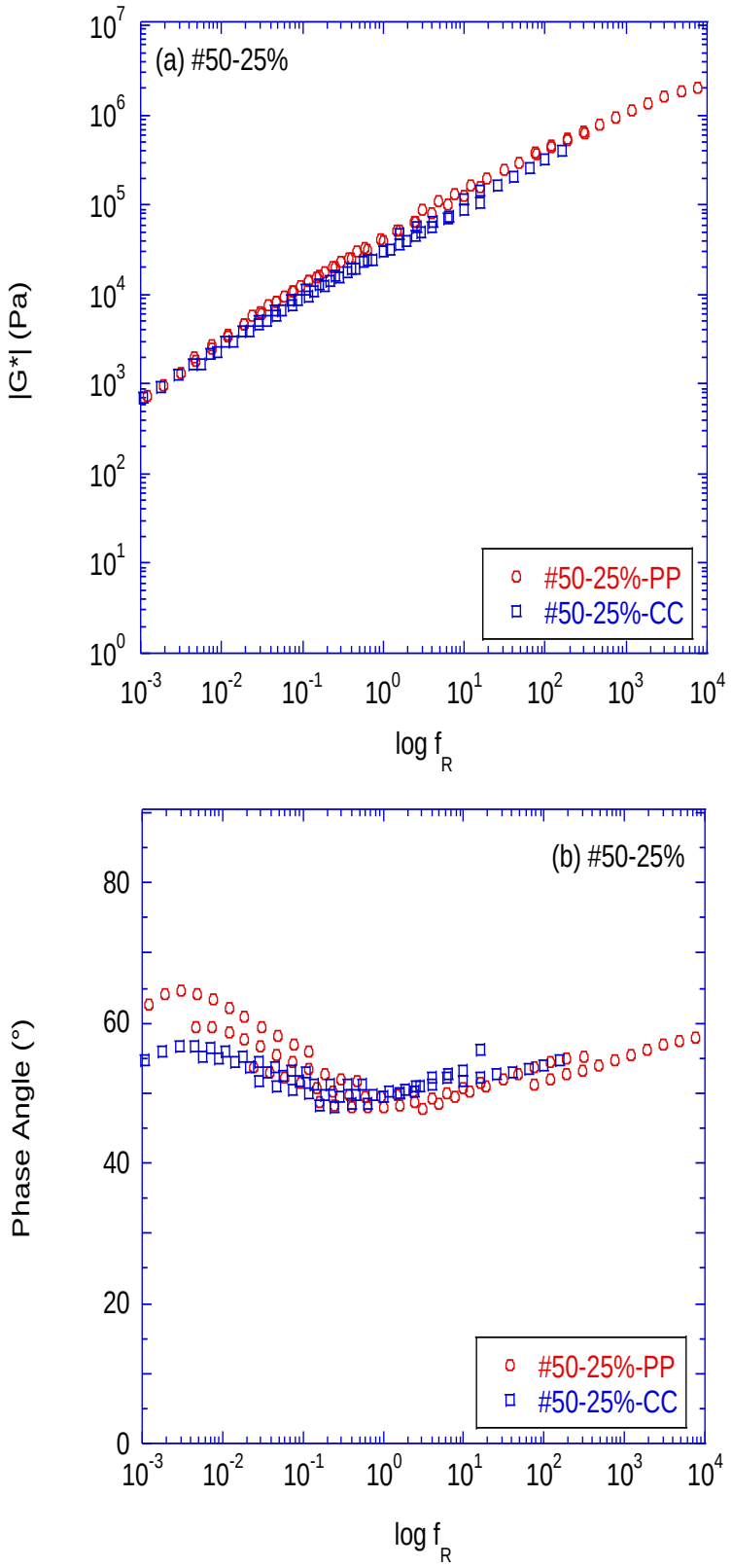

Figure 13: Comparisons of PP and CC obtained (a) |G*| and (b) phase angle for #50-25%.

Table 5: Shift factors and sigmoid coefficients for CRM binder master curves.

Test Geometry	Binder ID	Shift Factors		Sigmoid Coefficients			
		a1	a2	b1	b2	b3	b4
PP	#20-10%	4.70E-04	-1.19E-01	-4.330	11.773	1.005	0.315
	#20-25%	4.41E-04	-1.16E-01	-2.468	10.184	0.840	0.225
	#50-10%	4.08E-04	-1.11E-01	-3.232	11.433	0.664	0.298
	#50-25%	4.12E-04	-1.12E-01	-3.487	11.711	0.821	0.215
	#30-10%	5.35E-04	-1.27E-01	-4.512	12.600	0.766	0.289
	#30-25%	6.05E-04	-1.34E-01	-3.296	10.736	0.802	0.278
CC	#20-10%	3.37E-04	-1.01E-01	-4.230	12.386	0.790	0.285
	#20-25%	2.39E-04	-9.25E-02	-1.542	10.222	0.411	0.230
	#50-10%	3.08E-04	-9.69E-02	-3.048	11.333	0.588	0.290
	#50-25%	6.61E-05	-6.81E-02	-1.350	9.802	0.391	0.227
	#30-10%	3.89E-04	-1.08E-01	-4.810	12.475	0.944	0.293
	#30-25%	2.51E-04	-8.95E-02	-2.372	10.280	0.558	0.276

The variability in test data obtained by PP and CC geometries, as indicated by the Coefficient of Variation (COV) is shown in Table 6. This data was developed based on three test replicates in each DSR geometry and is shown for select test temperature and frequencies. While the COV was generally lower with decreasing test temperatures, CC geometry consistently showed higher variation for most temperature/frequency combinations.

Table 6: Test data variability (COV) for PP and CC DSR geometries.

	Binder ID	1 rad/sec		10 rad/sec		100 rad/sec	
		PP	CC	PP	CC	PP	CC
COV at 30 °C	#20-10%	1.7%	23.1%	1.6%	11.9%	2.8%	9.8%
	#20-25%	7.7%	8.9%	6.4%	7.6%	5.1%	6.9%
	#50-10%	4.9%	1.9%	5.2%	8.3%	2.9%	3.2%
	#50-25%	1.9%	20.8%	1.3%	7.4%	0.8%	2.5%
	#30-10%	5.6%	1.6%	6.4%	7.0%	12.4%	0.6%
	#30-25%	1.2%	1.3%	0.7%	7.3%	0.3%	32.7%
COV at 58 °C	#20-10%	2.9%	11.9%	2.6%	7.4%	2.2%	1.9%
	#20-25%	5.8%	14.8%	6.1%	10.5%	6.8%	6.5%
	#50-10%	2.6%	0.8%	2.7%	0.9%	2.2%	0.4%
	#50-25%	2.5%	7.7%	2.4%	2.1%	2.5%	8.1%
	#30-10%	3.6%	5.2%	2.5%	5.6%	1.0%	5.0%
	#30-25%	3.8%	5.6%	3.2%	4.0%	2.6%	2.9%
COV at 82 °C	#20-10%	4.1%	16.8%	3.7%	14.4%	3.4%	10.3%
	#20-25%	5.1%	19.8%	5.0%	14.5%	5.6%	11.0%
	#50-10%	0.3%	4.5%	0.4%	2.2%	1.2%	0.2%
	#50-25%	3.5%	10.0%	2.8%	7.0%	3.0%	3.8%
	#30-10%	4.5%	0.4%	4.7%	2.7%	4.4%	3.5%
	#30-25%	3.4%	6.8%	2.4%	4.8%	0.6%	3.4%

3.2.2 Correlation between PP and CC Obtained CRM Binder Rheology

As mentioned earlier, three test replicates were used to generate binder rheology data at various frequencies and temperatures for both DSR geometries. Then, linear correlations were made between these measurements for a better understanding of the differences observed between the two testing setups.

As shown in Figure 14, at 10% CR content the #20 CR size produced essentially the same |G*| and phase angle when PP and CC geometries are compared. However, at 25% CR content, the differences between the CC and PP geometries become clear at high at low |G*| values corresponding to low and high temperatures, respectively.

Similar to the findings observed from Figure 10 and Figure 11, Figure 15 shows that #30 CR produced very similar |G*| measurements at both the low and high modifier percentages, with slight differences between the two geometries at high temperatures for 10% CR. In addition, when plotted against each other in a linear scale; the CC geometry consistently measured lower phase angles at 10% CR contents. On the other hand, the two geometries produced more similar phase angles at 25% CR contents.

Figure 16 shows similar comparisons for #50 CR. PP and CC geometries were found to produce very similar |G*| measurements at both the low and high modifier percentages. When plotted against each other in a linear scale; the CC geometry consistently measured lower phase angles at high temperatures for both the low and high CR contents. However, the two geometries produced more similar phase angles at 10% CR contents.

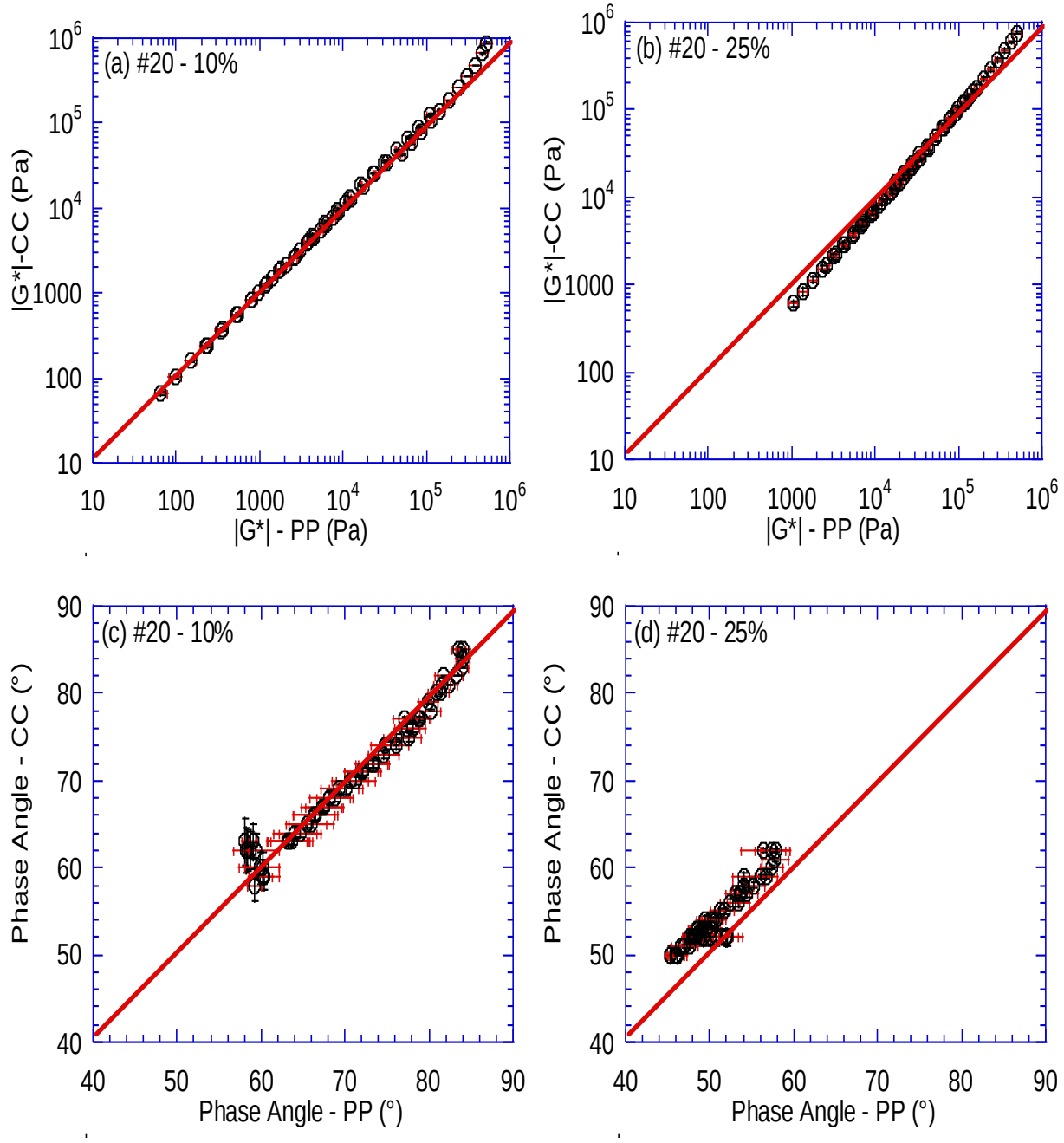

Figure 14: Direct comparison of CC and PP geometries: (a) |G*| of #20-10%, (b) |G*| of #20-25%, (c) phase angle of #20-10% and (d) phase angle of #20-25%.

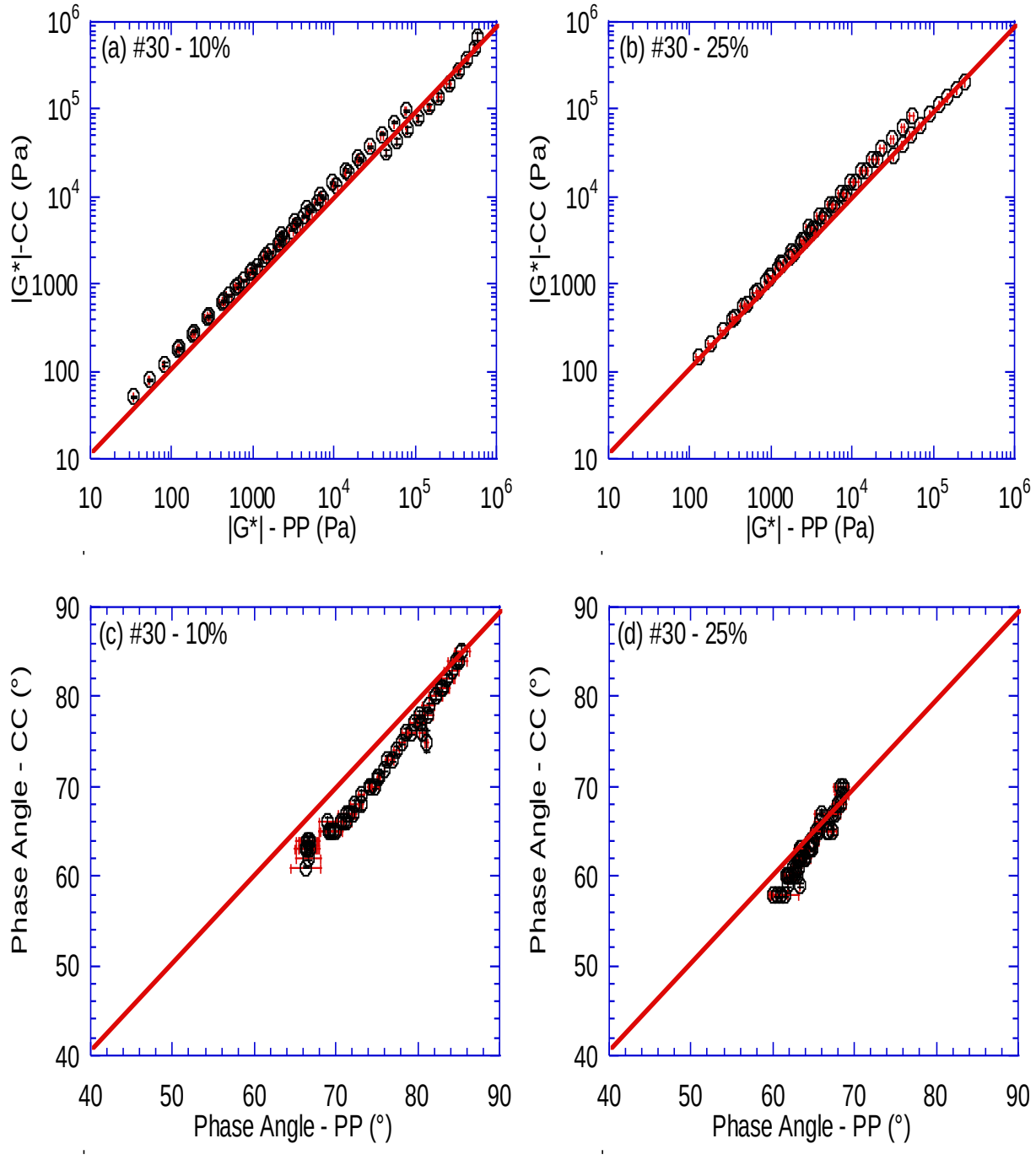

Figure 15: Direct comparison of CC and PP geometries: (a) |G*| of #30-10%, (b) |G*| of #30-25%, (c) phase angle of #30-10% and (d) phase angle of #30-25%.

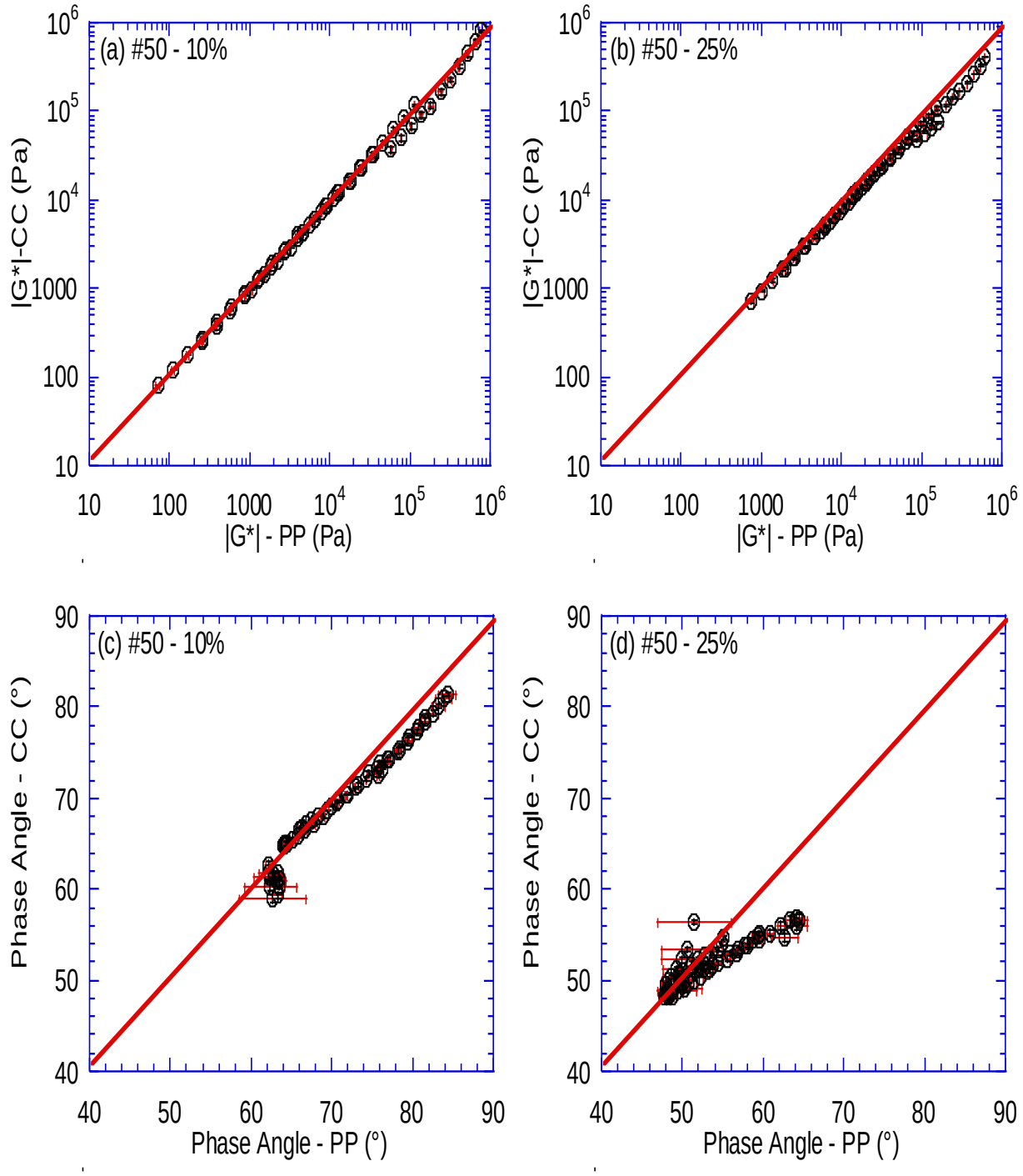

Figure 16: Direct comparison of CC and PP geometries: (a) |G*| of #50-10%, (b) |G*| of #50-25%, (c) phase angle of #50-10% and (d) phase angle of #50-25%.

3.2.3 CRM Mixture Mechanical Properties

HMA mixtures were designed using the CRM binders characterized in this study and tested for their dynamic modulus |E*|. Figure 17 through Figure 19 show |E*| and phase angle master curves for HMAs designed using CRM binders incorporating 10% and 25% CR modifier grouped based on CR size. From these figures, the following conclusions were drawn:

i) For #20 CR, increasing CR content from 10 to 25% caused a stiffening effect on the asphalt mixture at high temperature and low reduced frequency evidenced by a drop in |E*|, with a slight softening effect at low temperatures This is a desirable effect, and is indication of potential improvement on mix performance. In effect, the phase angle was generally lower with increasing CR content, while showing higher phase angle at the extreme low and high reduced frequencies.

ii) For #30 CR containing the entire range of rubber gradation, increasing the binder modifier content from 10 to 25% seemed to improve the high temperature performance, with little to no effect on low temperature properties.

iii) Due to the small- single sized gradation of #50 CR; no difference was observed in mixture |E*| with increased CR content used in binder modification. When incorporated into a mix, #50-10% CR produced essentially the same |E*| mastercurve as that from #50-25% CR. This may be due to the small #50 CR particle sizes that occupied small spaces between the aggregates and aggregate-to-aggregate contact mechanics governed the modulus of the mixture.

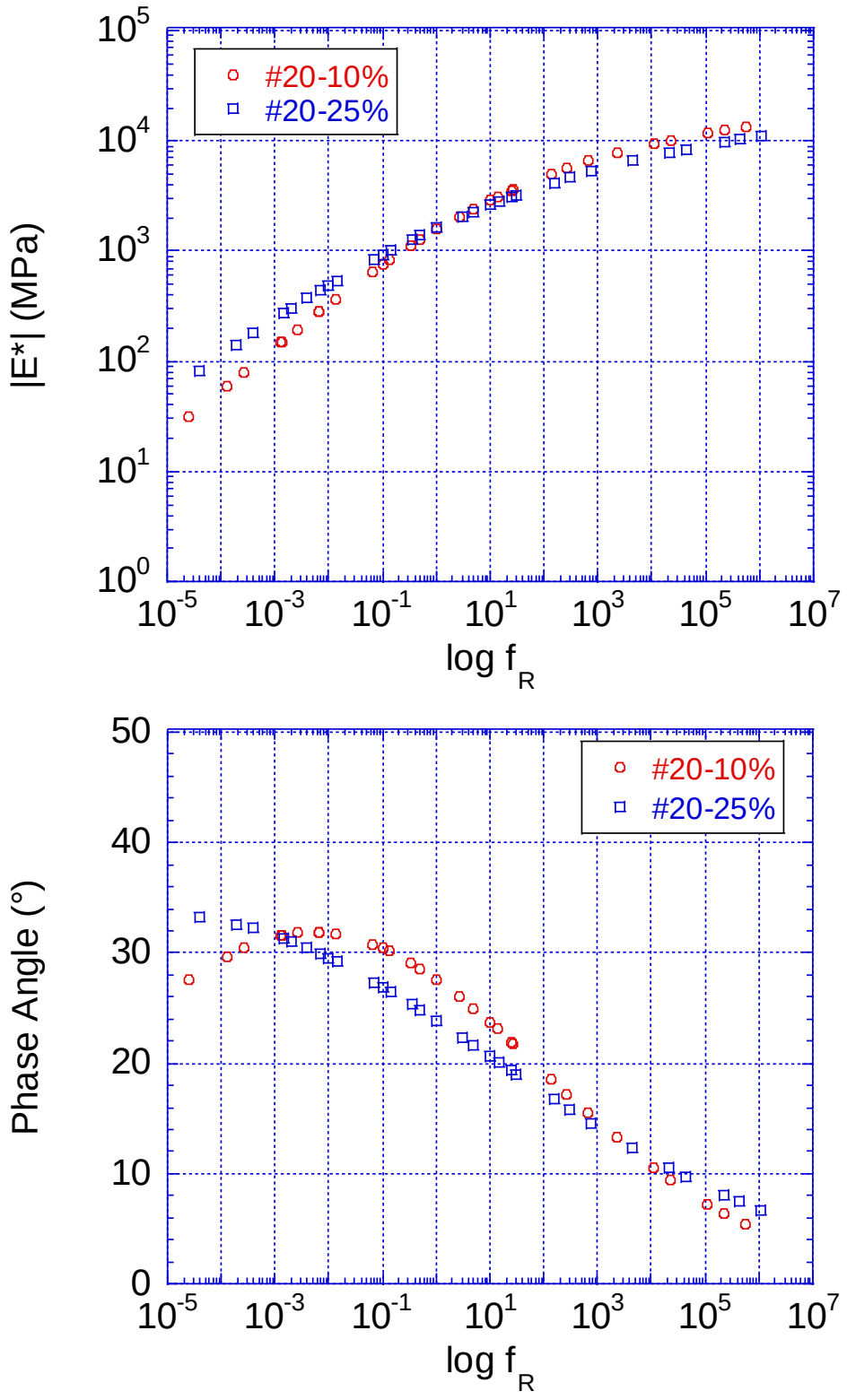

Figure 17: Dynamic modulus |E*| and phase angles mastercurves for #20 CRM mixtures tested in this study.

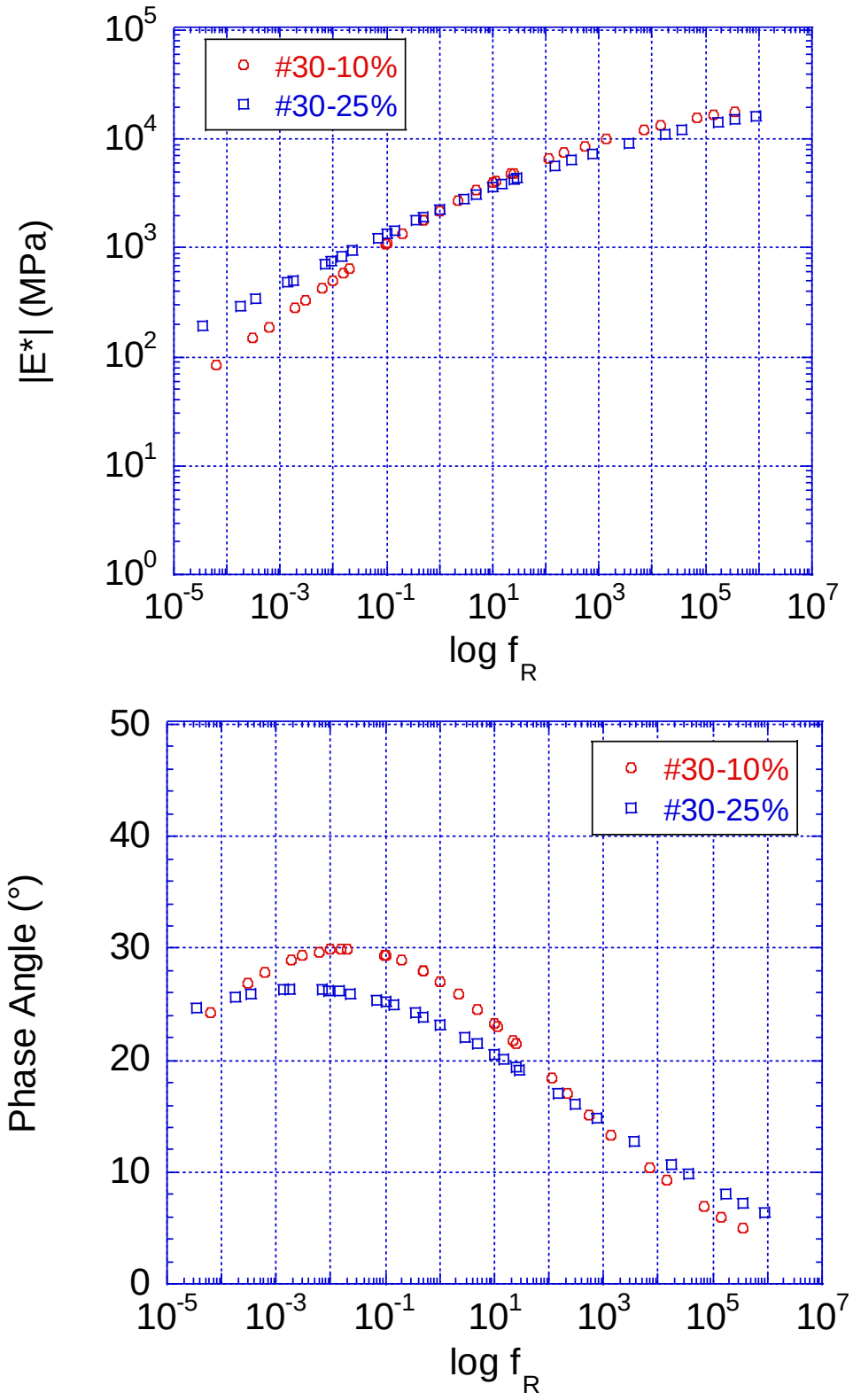

Figure 18: Dynamic modulus |E*| and phase angles mastercurves for #30 CRM mixtures tested in this study.

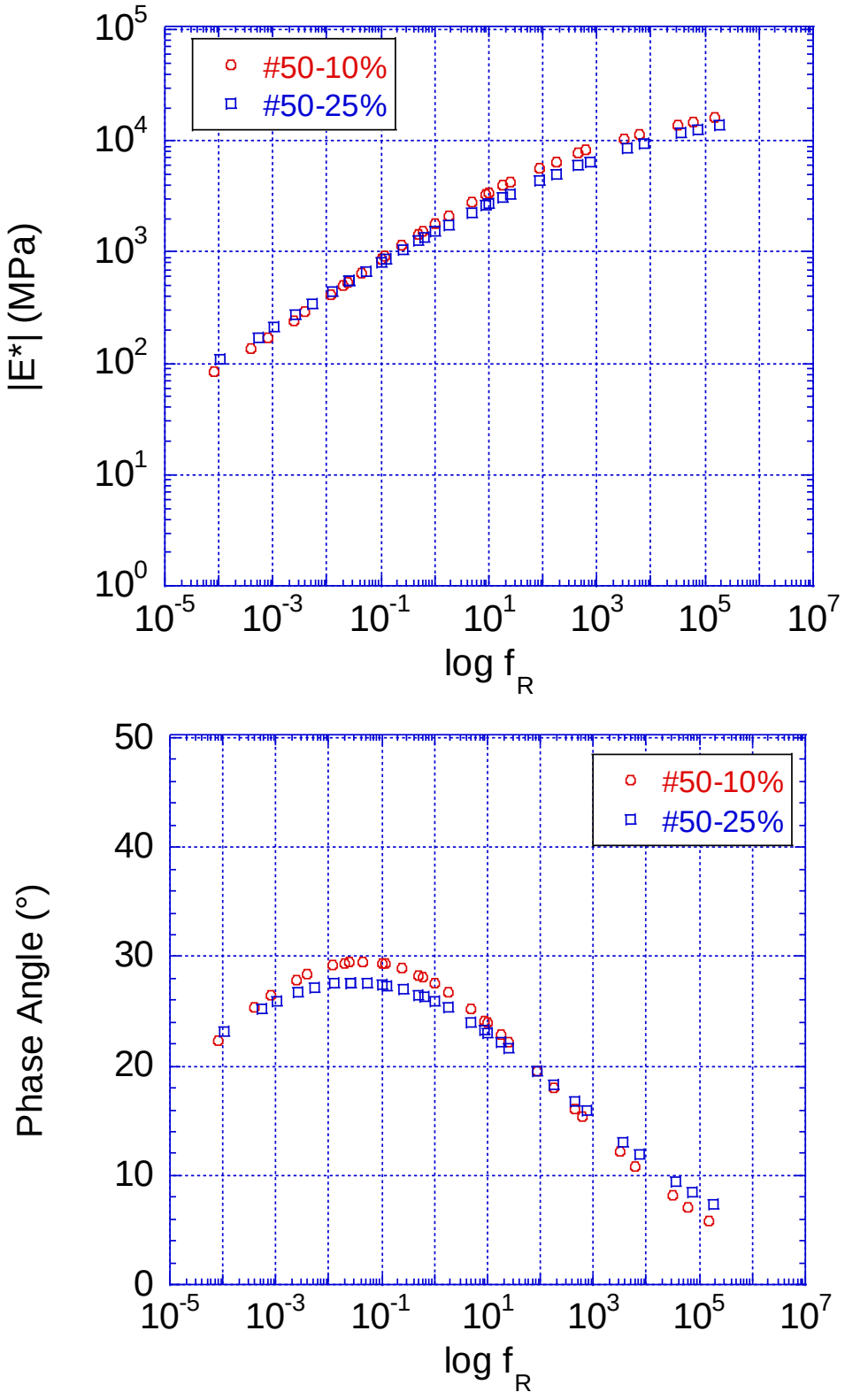

Figure 19: Dynamic modulus |E*| and phase angles mastercurves for #50 CRM mixtures tested in this study.

Sigmoid coefficients (Equation 4) and shift factor coefficients (Equation 5) for these mixtures are provided in Table 7 below for complete interpretation of the master curves.

Table 7: Shift factors and sigmoid coefficients for CRM mixture master curves.

Mixture ID	Shift Factors		Sigmoid Coefficients			
	a1	a2	b1	b2	b3	b4
#20-10%	3.97E-04	-1.33E-01	0.321	4.123	1.039	0.311
#20-25%	5.65E-04	-1.49E-01	-0.747	4.933	1.439	0.288
#50-10%	6.58E-04	-1.54E-01	0.706	3.738	0.792	0.311
#50-25%	4.76E-04	-1.29E-01	0.562	3.945	0.740	0.281
#30-10%	5.70E-04	-1.40E-01	0.238	4.236	1.010	0.338
#30-25%	5.45E-04	-1.34E-01	0.773	3.806	0.736	0.284

3.2.4 Correlation between CRM Mixture |E| and Binder |G*|*

HMA mixture |E*| test results were used to quantify the relationship between mixture and binder mechanical properties. The DSR test geometry capable of producing CRM binder |G*| data with better correlations to mixture performance at different temperatures and frequencies will then be identified as the more suitable geometry for testing CRM binders. Due to the highly correlated CRM binder |G*| data obtained from PP and CC geometries, it was expected that similar correlations to HMA |E*| will be found.

Figure 20 through Figure 22 show the correlation between HMA mixture |E*| and binder |G*| for of the different CRM asphalt binder blends grouped based on CR size and concentration in log-log scale. The data is plotted with binder |G*| in Pa on the y-axis, and mixture |E*| in MPa on the x-axis. Consistent with findings observed in the direct comparisons made between CC and

PP geometries, both geometries seemed to agree well when correlated to mixture |E*|. Although binder |G*| tests were completed at temperatures as high as 82° C; the comparisons below were made between 30 and 58° C only. The reasons behind using the limited set of data are:

1. Unlike the PP geometry, no |G*| tests were completed at 15° C for the CC geometry.
2. To avoid extrapolating mixture |E*| data from sigmoid fit coefficients too far beyond 54° C (highest test temperature).

To further evaluate the differences between these correlations, the same data is shown in linear-linear scale in Figure 23 through Figure 25. A power line is fitted to the data, and the line equation as well as the determination coefficient for each correlation is shown. For 10% CR concentration, mixture |E*| and binder |G*| correlated extremely well for both PP and CC geometries. At this concentration, both geometries seemed to highly correlate with all CR sizes. Similarly, for 25% CR concentration, mixture |E*| and binder |G*| correlated very well for both geometries. Again, this applies to all CR sizes. The largest difference in correlation for 25% CR was observed in the #30 mesh CR. While both were high (100% for PP and 90% for CC), PP geometry correlated much better than CC, as evidenced by the determination coefficient. This makes sense because, at high percentage of CR (i.e., 25%), the CR particles are compressed in between the two parallel plates in PP geometry, just like they are compressed in between the aggregates in a mixture.

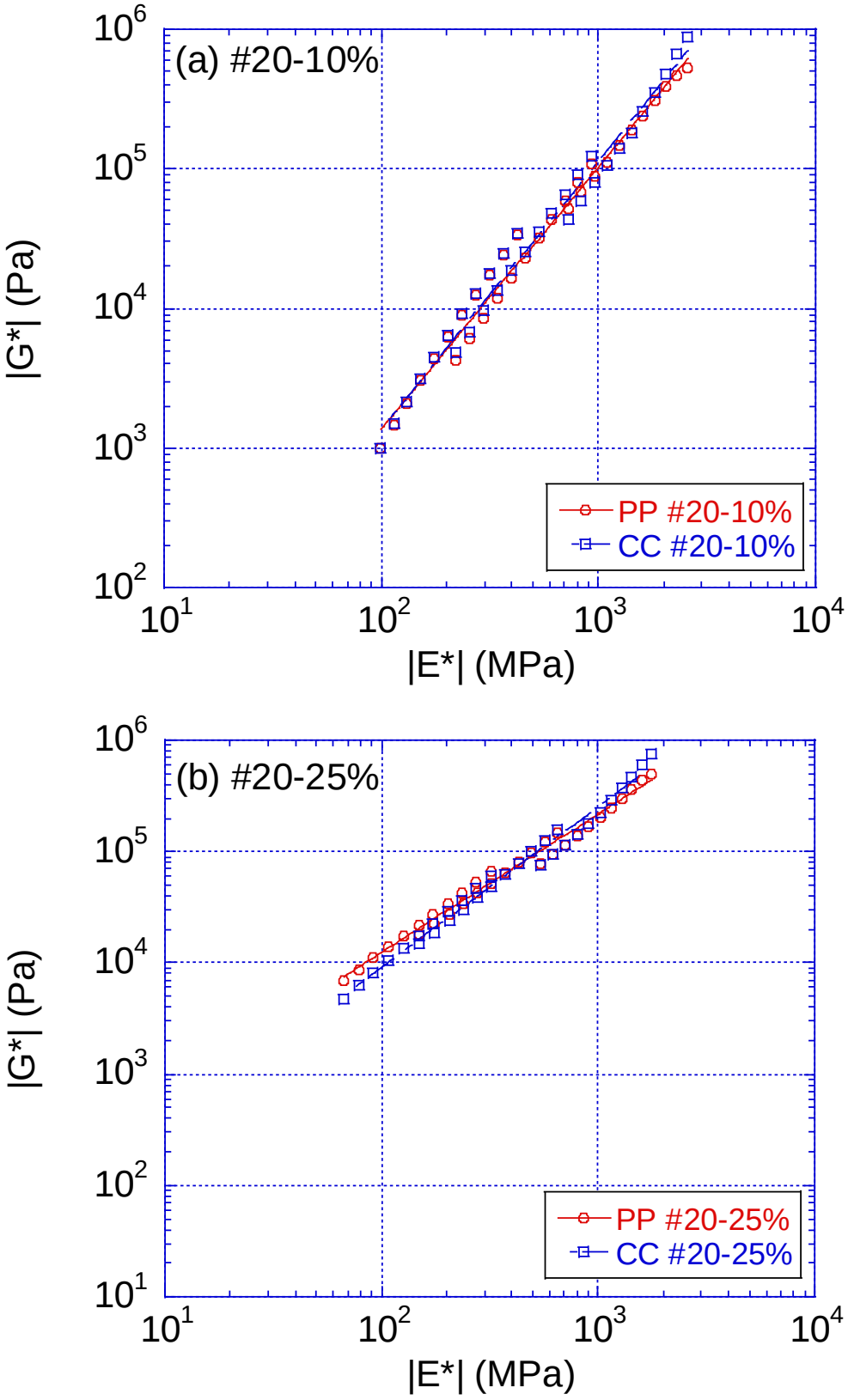

Figure 20: Log-log correlations between |E*| and |G*| for #20 CR (a) 10% and (b) 25%.

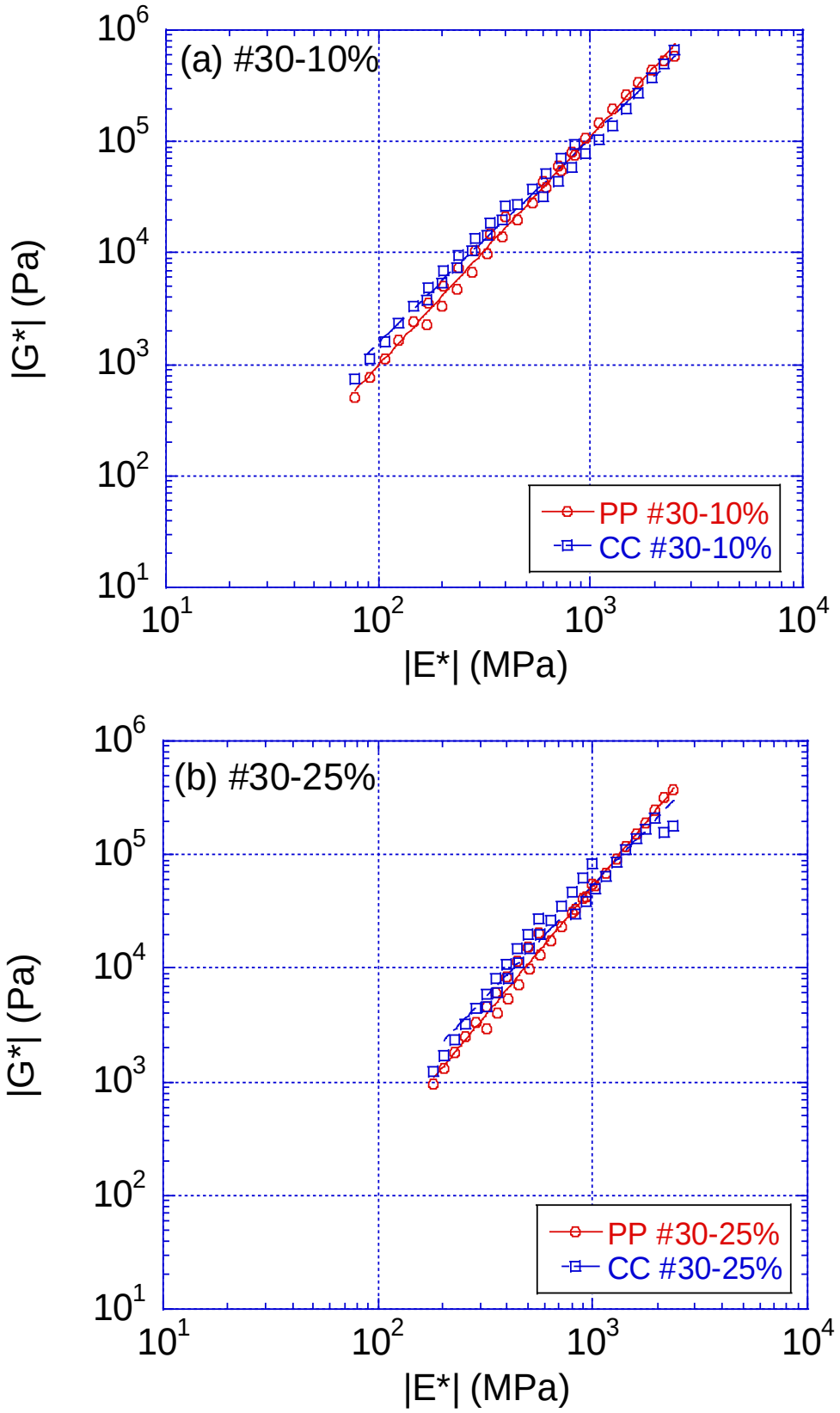

Figure 21: Log-log correlations between |E*| and |G*| for #30 CR (a) 10% and (b) 25%.

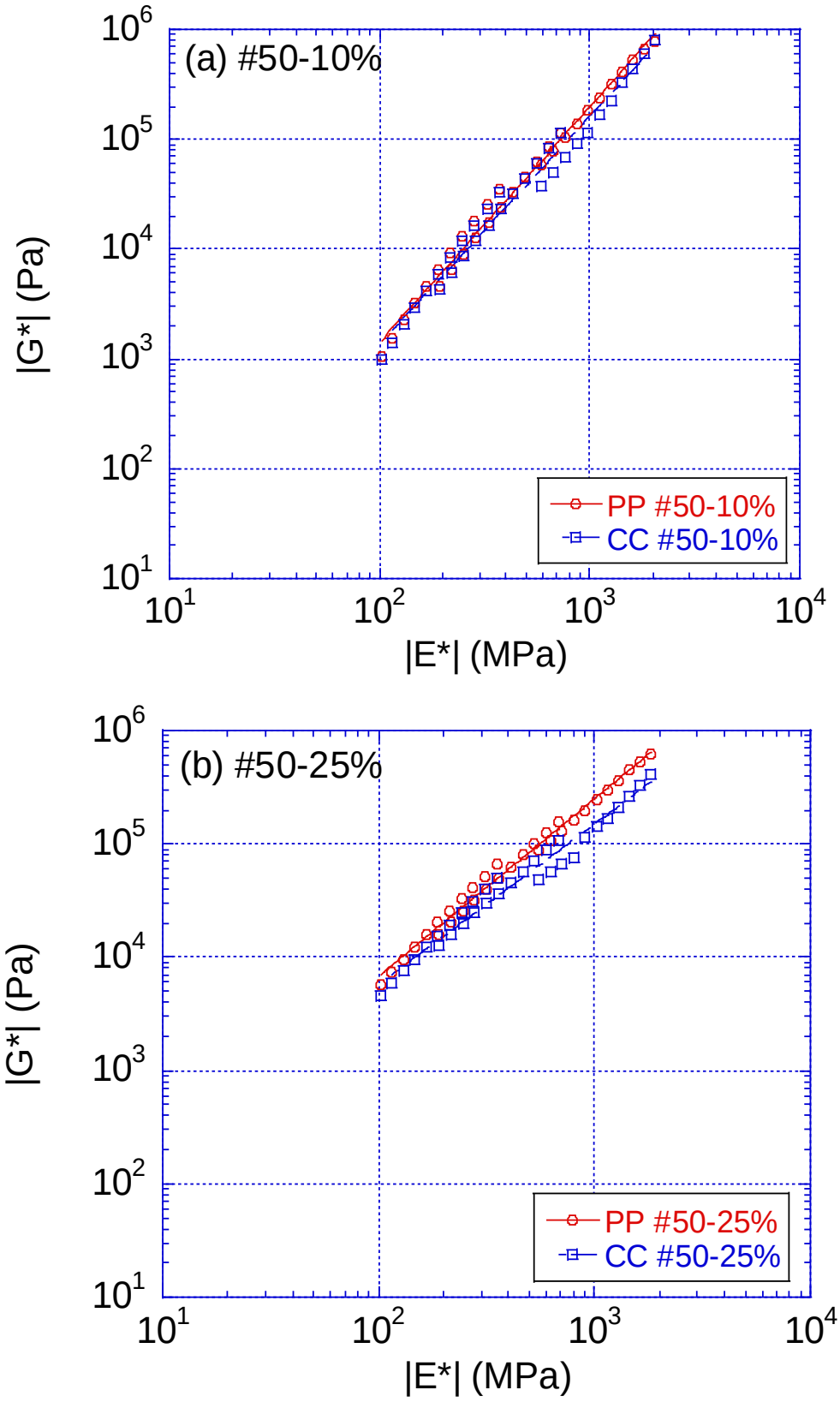

Figure 22: Log-log correlations between |E*| and |G*| for #50 CR (a) 10% and (b) 25%.

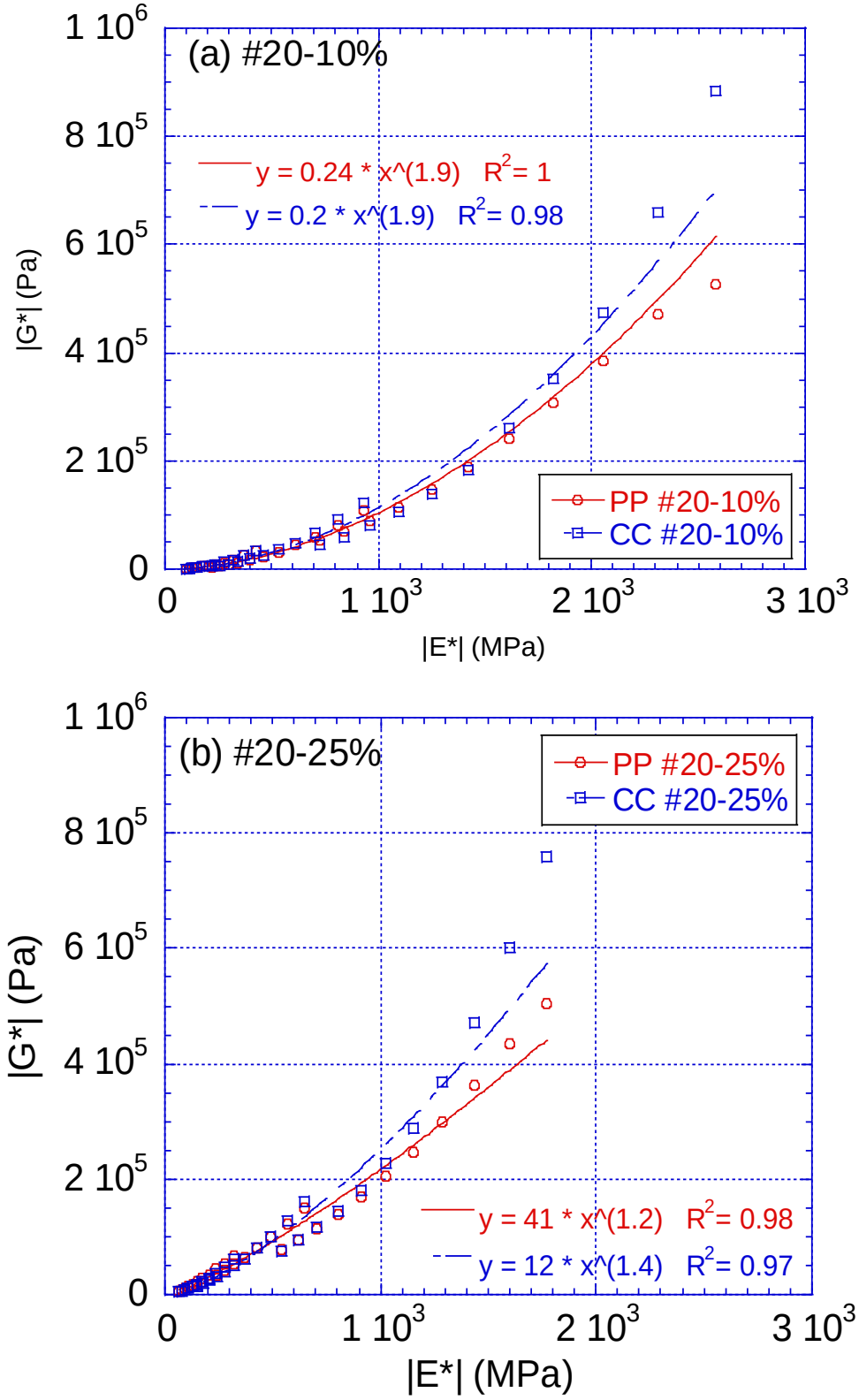

Figure 23: Linear-linear correlations between |E*| and |G*| for #20 CR (a) 10% and (b) 25%.

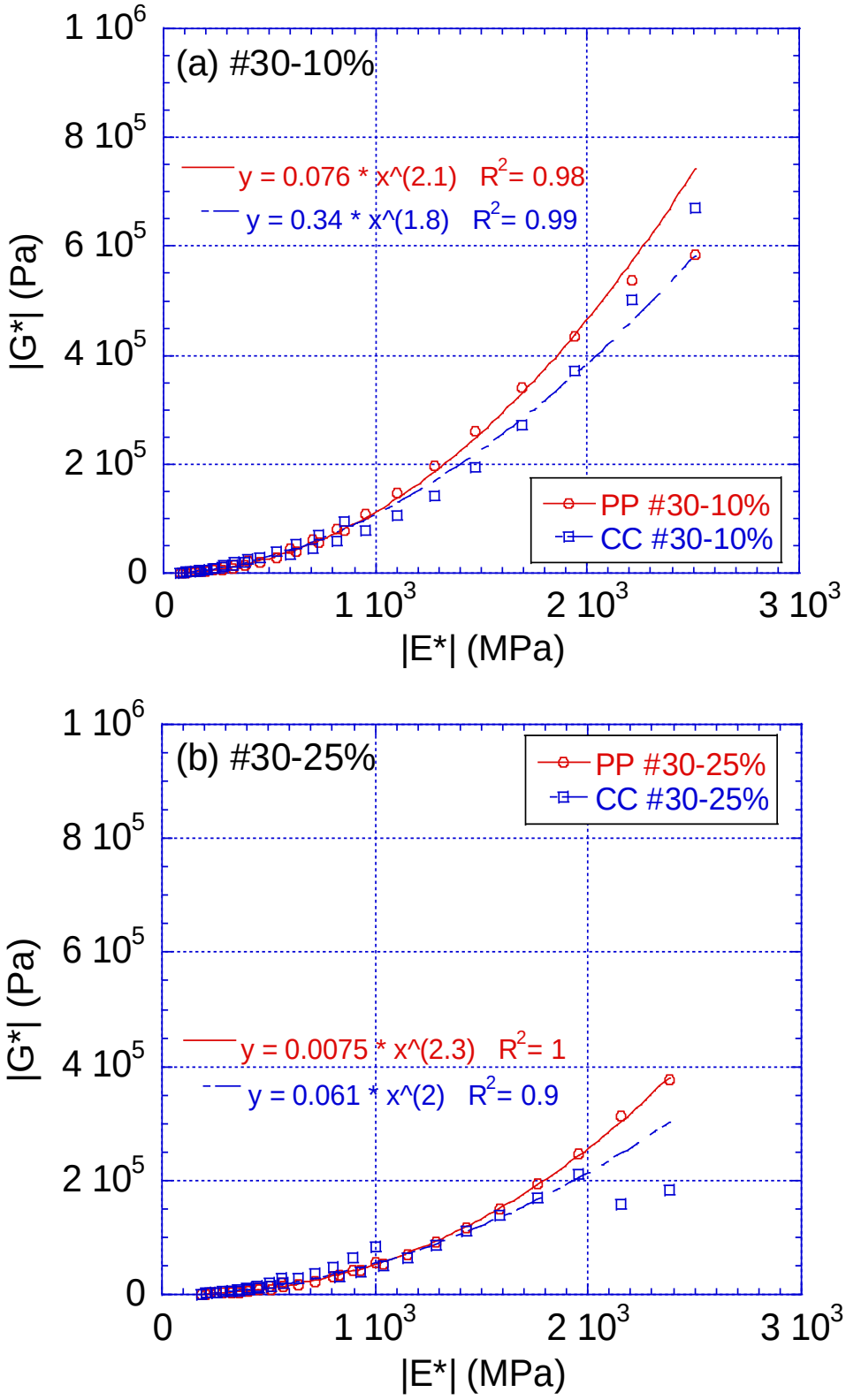

Figure 24: Linear-linear correlations between |E*| and |G*| for #30 CR (a) 10% and (b) 25%.

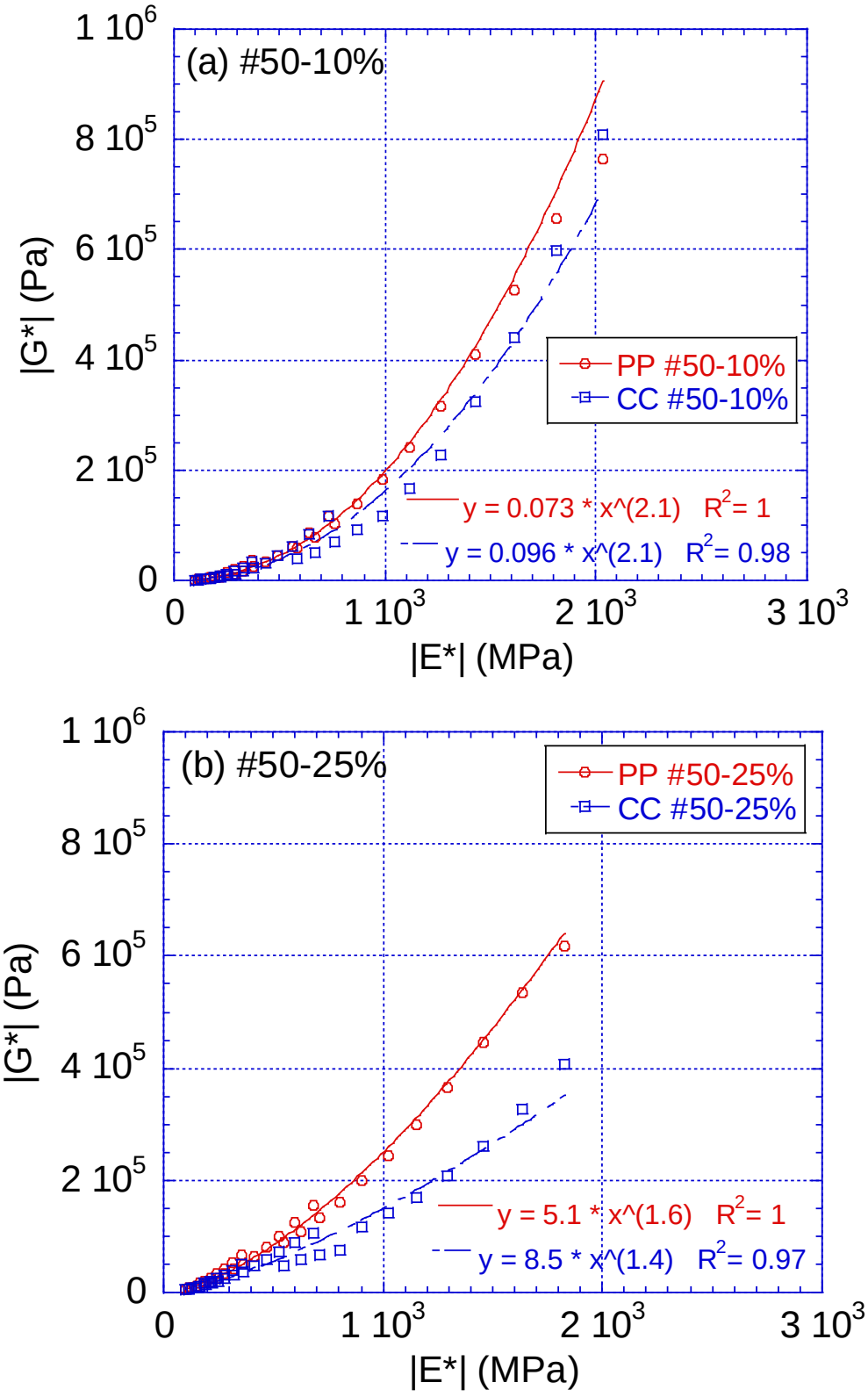

Figure 25: Linear-linear correlations between |E*| and |G*| for #50 CR (a) 10% and (b) 25%.

3.2.5 Mixture |E| Prediction from PP and CC Based |G*| Measurements*

To further evaluate the most feasible DSR testing geometry for CRM binders, binder |G*| measurements collected in this study were used to predict mixture dynamic modulus. The Modified Witczak model (Bari 2005) developed as part of NCHRP Project 1-40D was used for that purpose and is shown below:

$$\log_{10}|E^*| = -0.349 + 0.754\left(|G^*|_b^{-0.0052}\right)\left(6.65 - 0.032p_{200} + 0.0027(p_{200})^2 + 0.011p_4 - 0.0001(p_4)^2 + 0.006p_{3/8} - 0.00014\left(p_{3/8}\right)^2 - 0.08V_a - 1.06\left(\frac{V_{beff}}{V_{beff}+V_a}\right)\right) + \frac{2.558+0.032V_a+0.713\left(\frac{V_{beff}}{V_{beff}+V_a}\right)+0.0124p_{3/8}-0.0001\left(p_{3/8}\right)^2-0.0098p_{3/4}}{1+exp(-0.7814-0.5785\log|G^*|_b+0.8834\log\delta_b}} \quad (6)$$

where:

$|G^*|_b$ = Dynamic shear modulus of asphalt binder (pounds per square inch).

p_{200} = Percentage of aggregate passing #200 sieve.

p_4 = Cumulative percentage of aggregate retained in #4 sieve.

$p_{3/8}$ = Cumulative percentage of aggregate retained in 3/8-inch (9.56-mm) sieve.

V_a = Percentage of air voids (by volume of mix).

V_{beff} = Percentage of effective asphalt content (by volume of mix).

$p_{3/4}$ = Cumulative percentage of aggregate retained in 3/4-inch (19.01-mm) sieve.

δ_b = Binder phase angle associated with $|G^*|_b$ (degrees).

Since one control HMA mix designs was used in this study for each CR content, the only variables in the |E*| prediction model inputs were the binder |G*| and phase angle, as well as mixture V_a which was consistent at the target 7.0±0.5%. This allows for capturing the effect of the different |G*| measuring geometries on |E*| prediction. Figure 26 through Figure 28 show different comparisons of laboratory measured mixture |E*| versus predictions made based on CRM binder rheology obtained from PP and CC geometries. Similar trends are observed for both PP and CC based predictions in the log scale. However, when the data is plotted in linear scale, it is observed that PP based |E*| predictions (Figure 26b) are distributed more closely to the line of equality with less scatter than those from CC based predictions (Figure 27b). In addition, while both determination coefficients were fairly high; PP based predictions showed better correlation to laboratory measured |E*|. For comparison purposes, PP and CC based |E*| predictions are plotted on the same graphs in Figure 28a and Figure 28b. While PP based |E*| predictions generally under-estimated mixture |E*|, CC based predictions had a higher tendency to over-estimate mixture |E*|.

For a better understanding of the differences in mixture |E*| predictions from different DSR testing geometries, each dataset representing an individual CR size and concentration was plotted separately. Figure 29 through Figure 31 show a comparison of measured and predicted |E*| for 10% CR in all CR sizes. All determination coefficients were very high for both PP and CC geometries and for all CR sizes. When examined closely, it can be observed that for the #30 mesh CR containing the full range of rubber sizes, both DSR geometries produced almost identical |E*| predictions (Figure 30). More differences were however noted for the large (#20) and small (#50) CR sizes. While CC geometry seemed to over-estimate |E*| predictions compared to PP geometry (Figure 29), while PP geometry provided a better estimate for #50 CRM mixtures (Figure 31).

These findings are consistent with those noted in *Comparison of |G*| and phase angle mastercurves.*

Figure 33 through Figure 34 show a comparison of measured and predicted |E*| for 25% CR. Similar to predictions made for 10% CR, all determination coefficients were very high for both PP and CC geometries. However, clearer differences in |E*| predictions were observed at the higher CR concentration. The PP geometry surprisingly provided much closer |E*| predictions to those measured for #20 CR. When binder |G*| and phase angles were compared for #20 CR at this high concentration, it was noted that PP geometry measured a lower |G*| and phase angle due to an inter-particle interaction (or cushioning) phenomenon that caused an overall increase in CRM binder elasticity at lower temperatures. Mixture |E*| data suggests that this "cushioning" effect seen from PP measurements is more representative of mixture behavior. In addition, while binder rheology data suggested that both geometries were almost identical for 25% concentration of #30 CR, CC geometry seemed to provide more accurate |E*| predictions for #30 CR. Overall, at this concentration, CC geometry seemed to over-estimate |E*| for the large CR size, while PP under-estimated |E*| for the full range #30 CR. Both geometries provided almost identical |E*| predictions and very close to those measured for #50 CR. This is consistent with findings from *Comparison of |G*| and phase angle mastercurves*

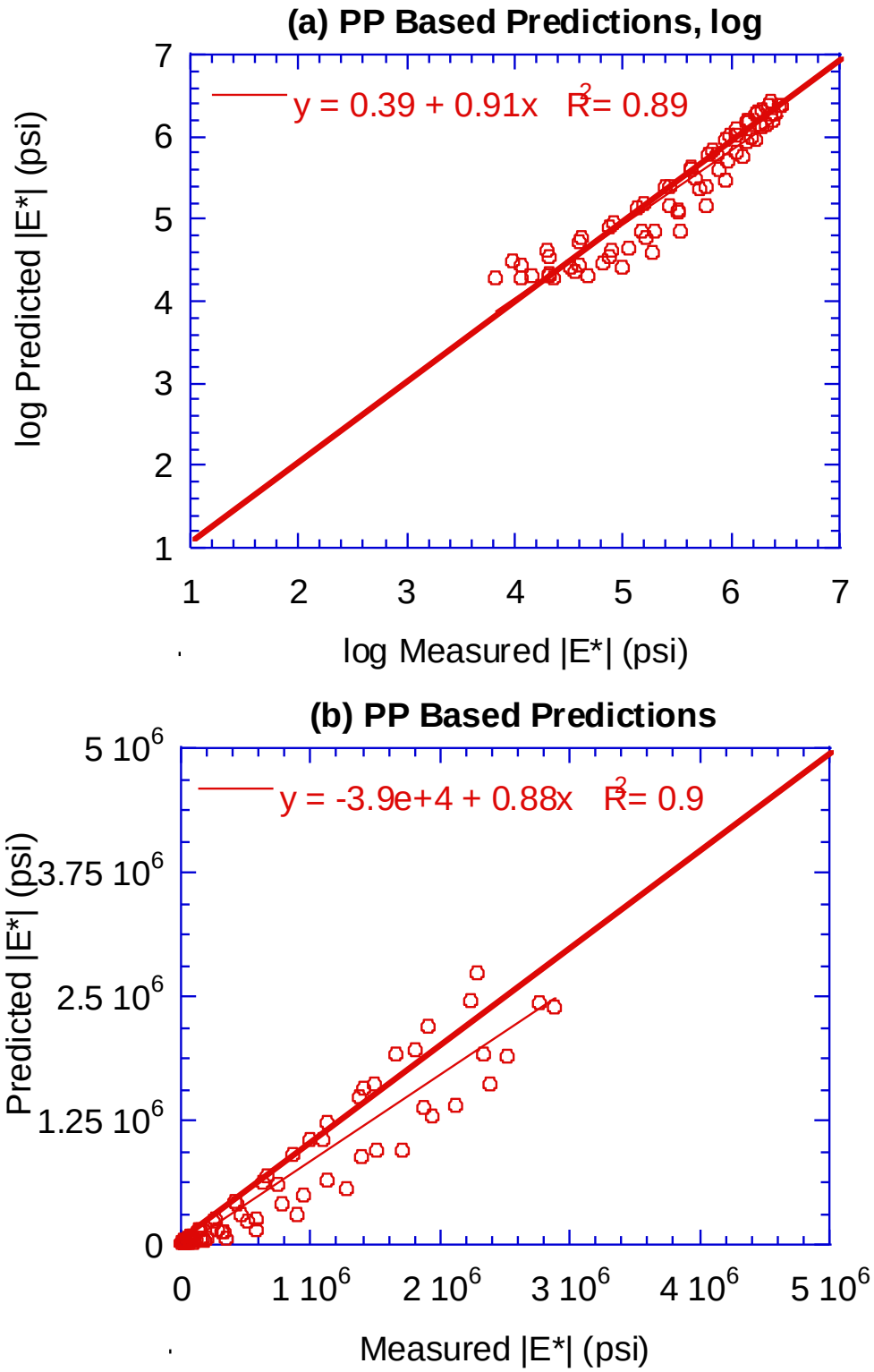

Figure 26: Measured versus predicted dynamic modulus |E*| for PP geometry in (a) log and (b) linear scales.

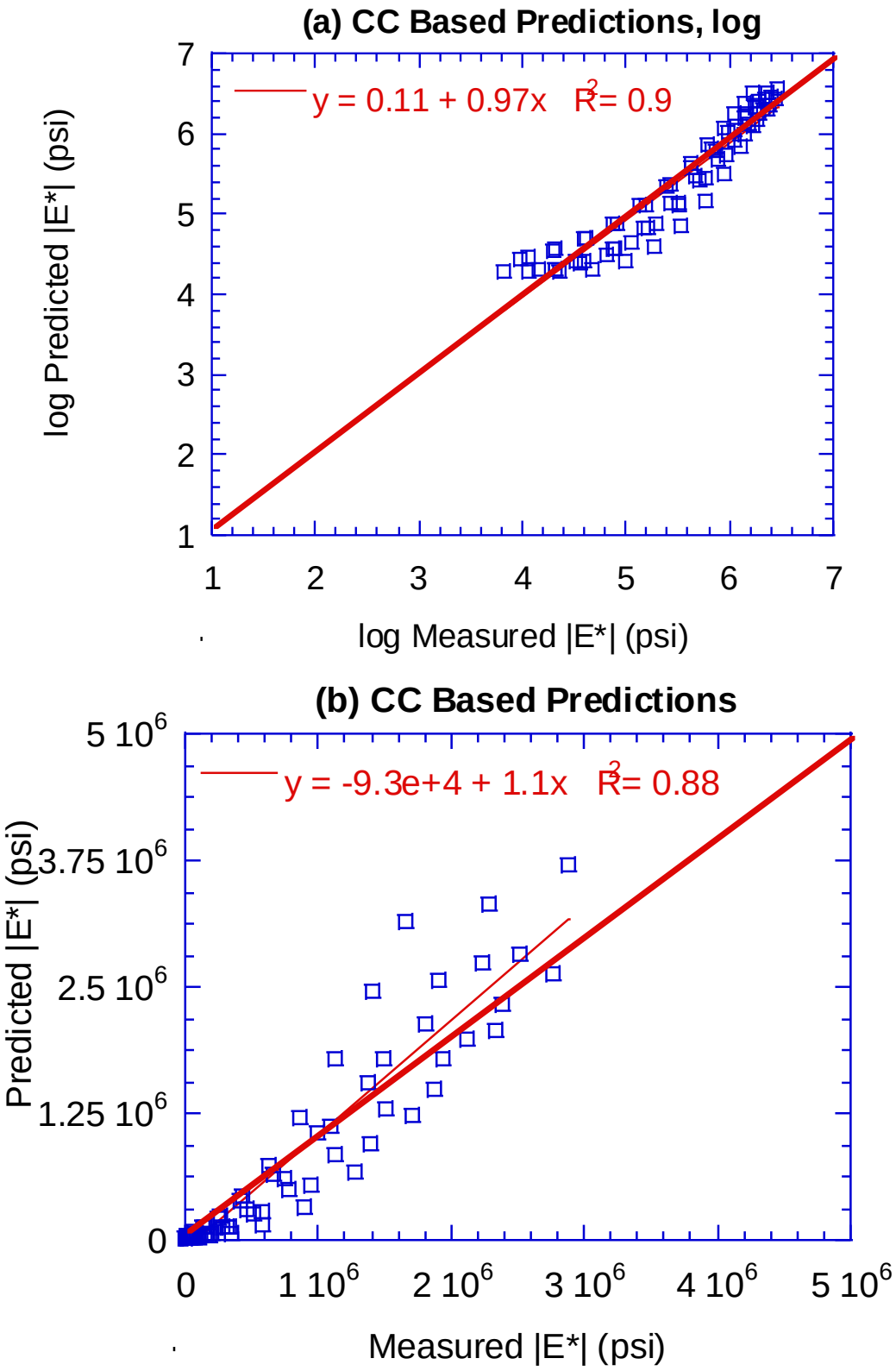

Figure 27: Measured versus predicted dynamic modulus |E*| for CC geometry in (a) log and (b) linear scales.

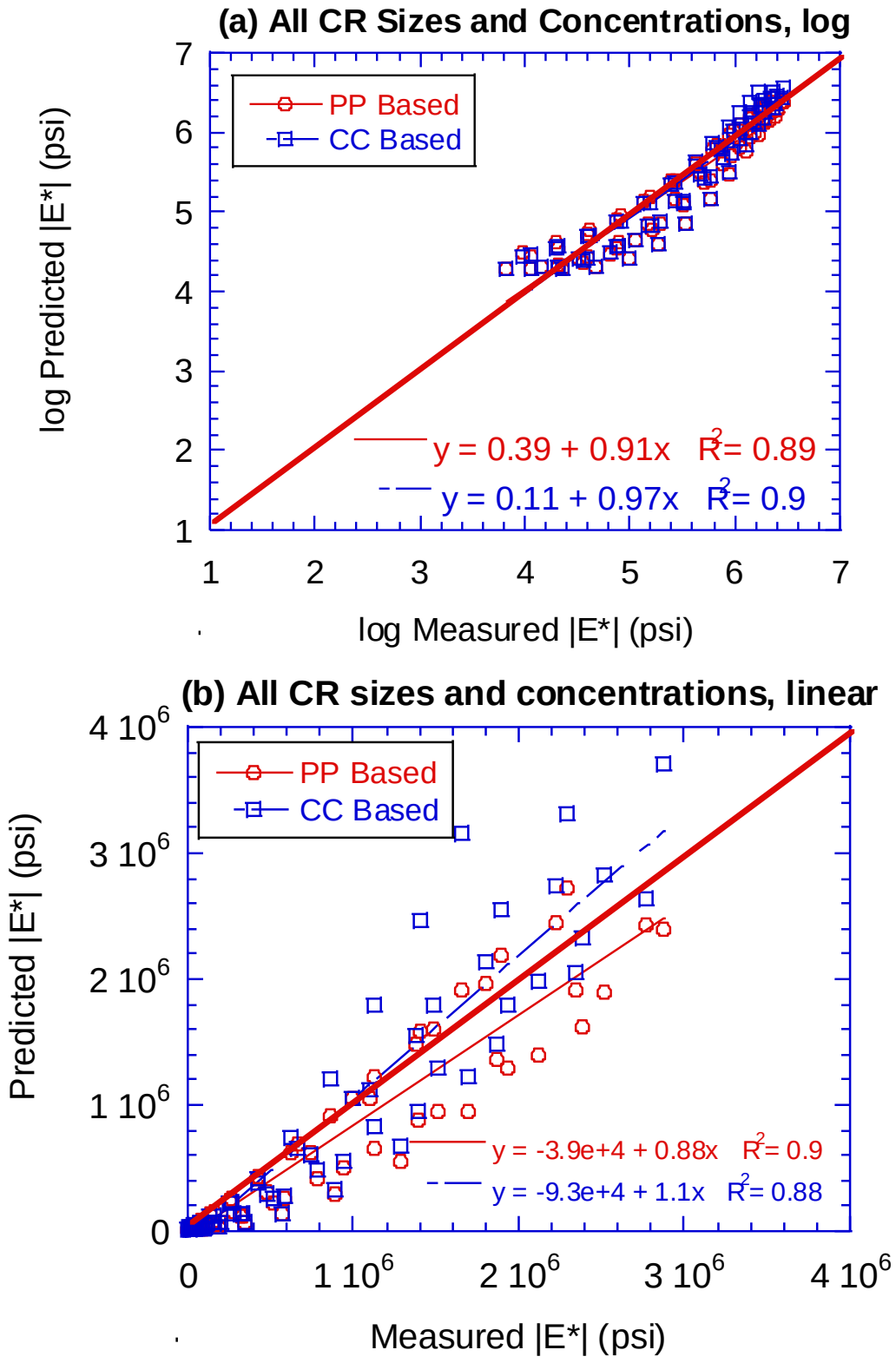

Figure 28: Measured versus predicted dynamic modulus |E*| for both DSR geometries in (a) log and (b) linear scales

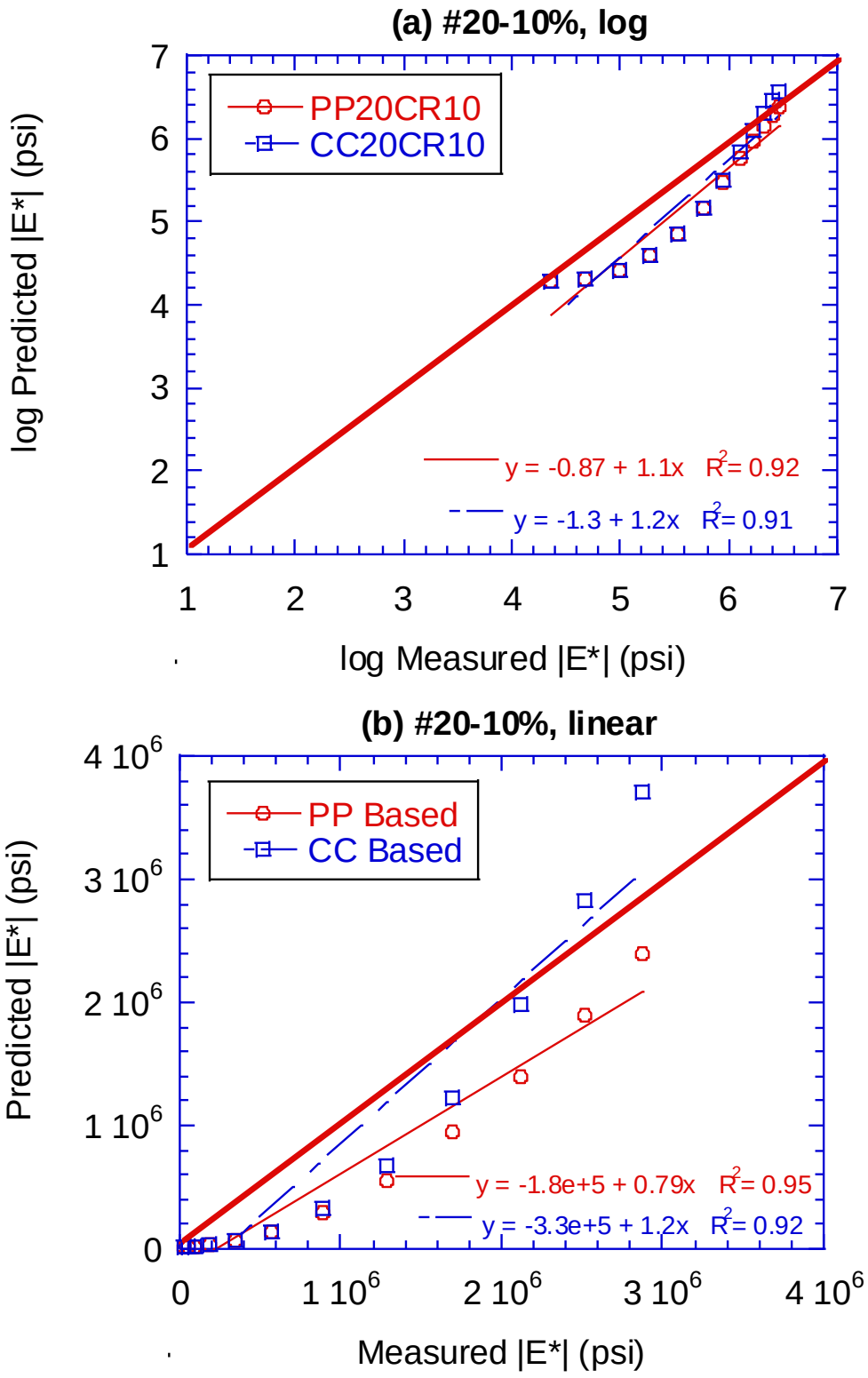

Figure 29: Measured versus predicted dynamic modulus |E*| from #20-10% rheology obtained from both DSR geometries in (a) log and (b) linear scales.

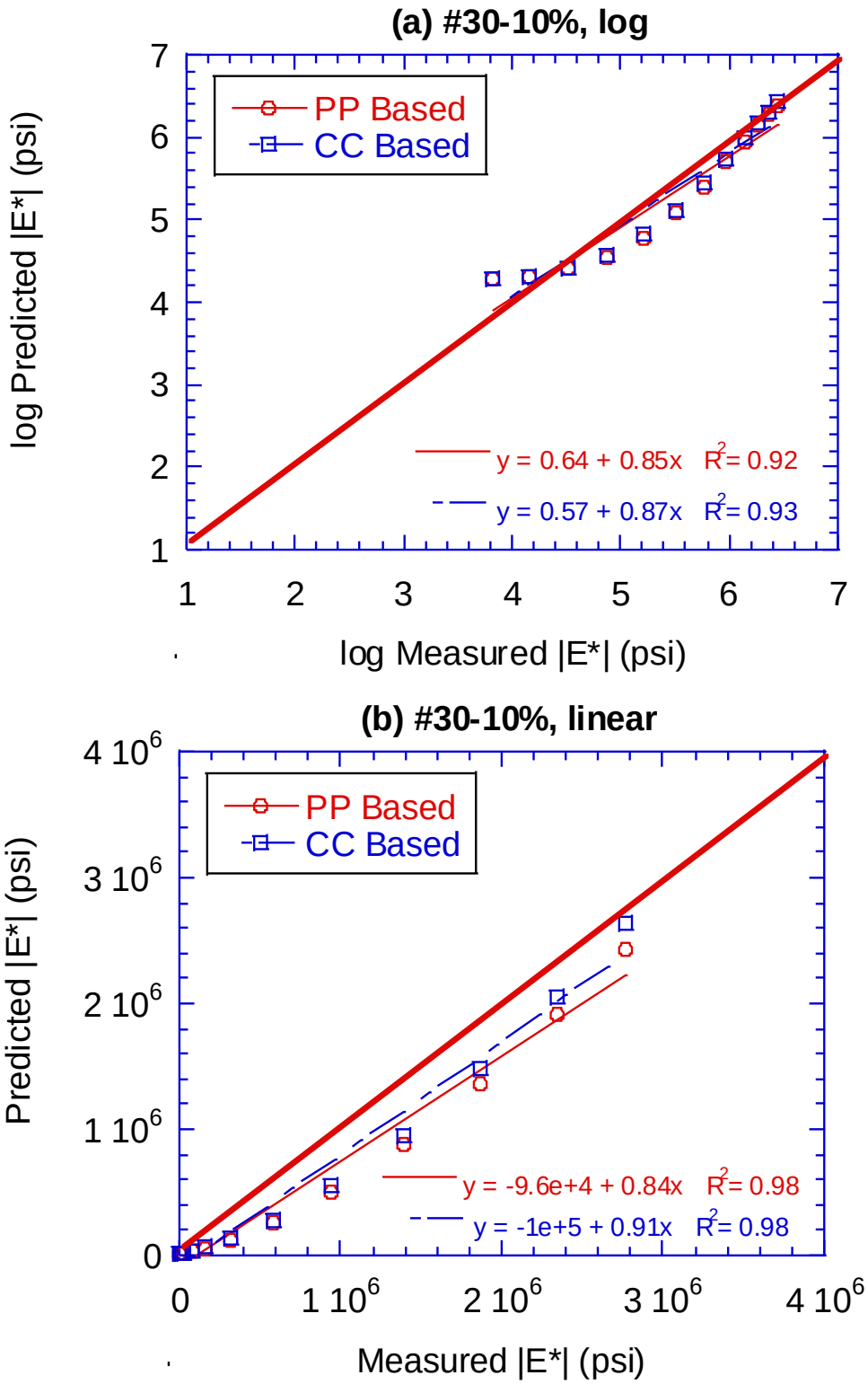

Figure 30: Measured versus predicted dynamic modulus |E*| from #30-10% rheology obtained from both DSR geometries in (a) log and (b) linear scales.

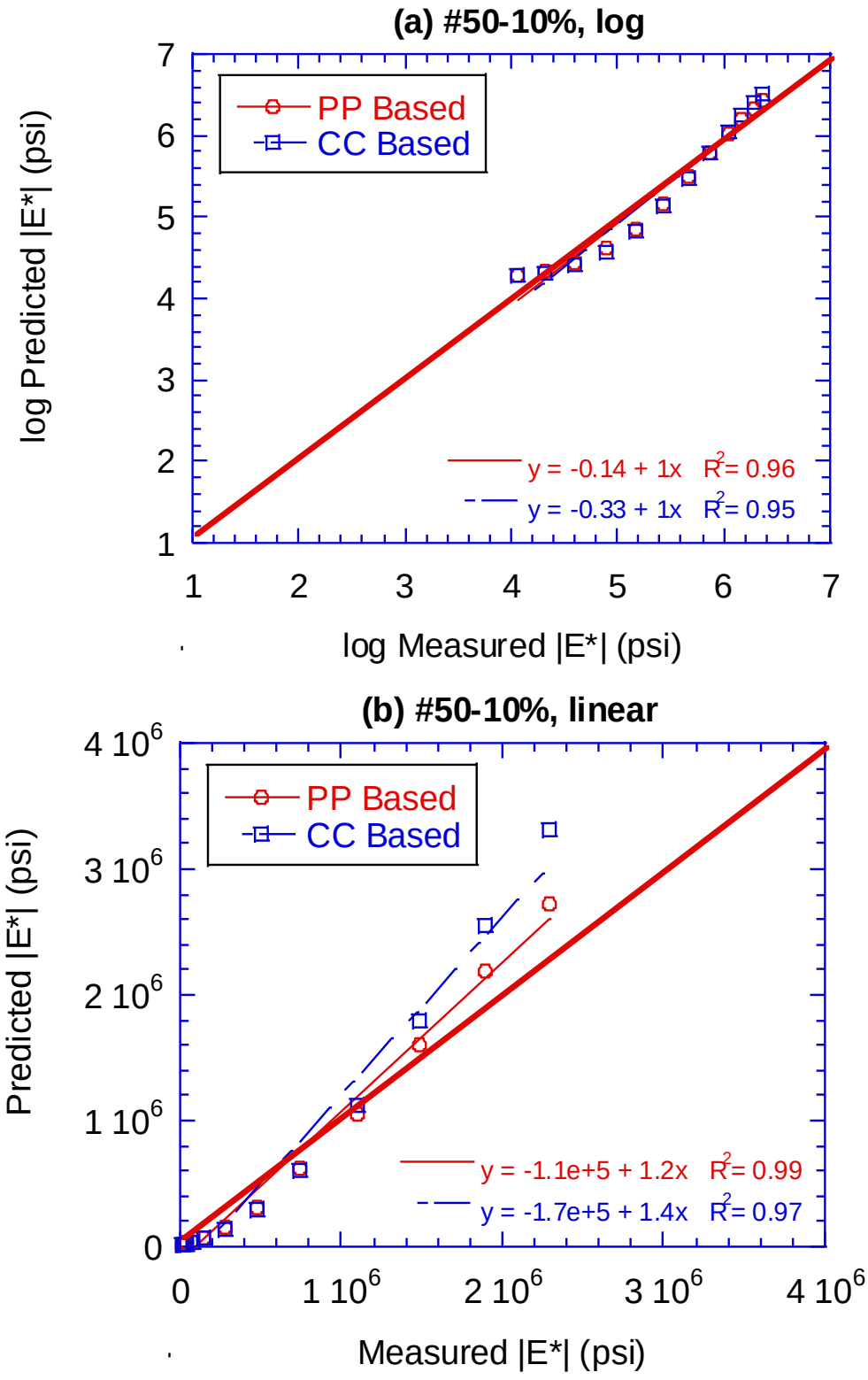

Figure 31: Measured versus predicted dynamic modulus |E*| from #50-10% rheology obtained from both DSR geometries in (a) log and (b) linear scales.

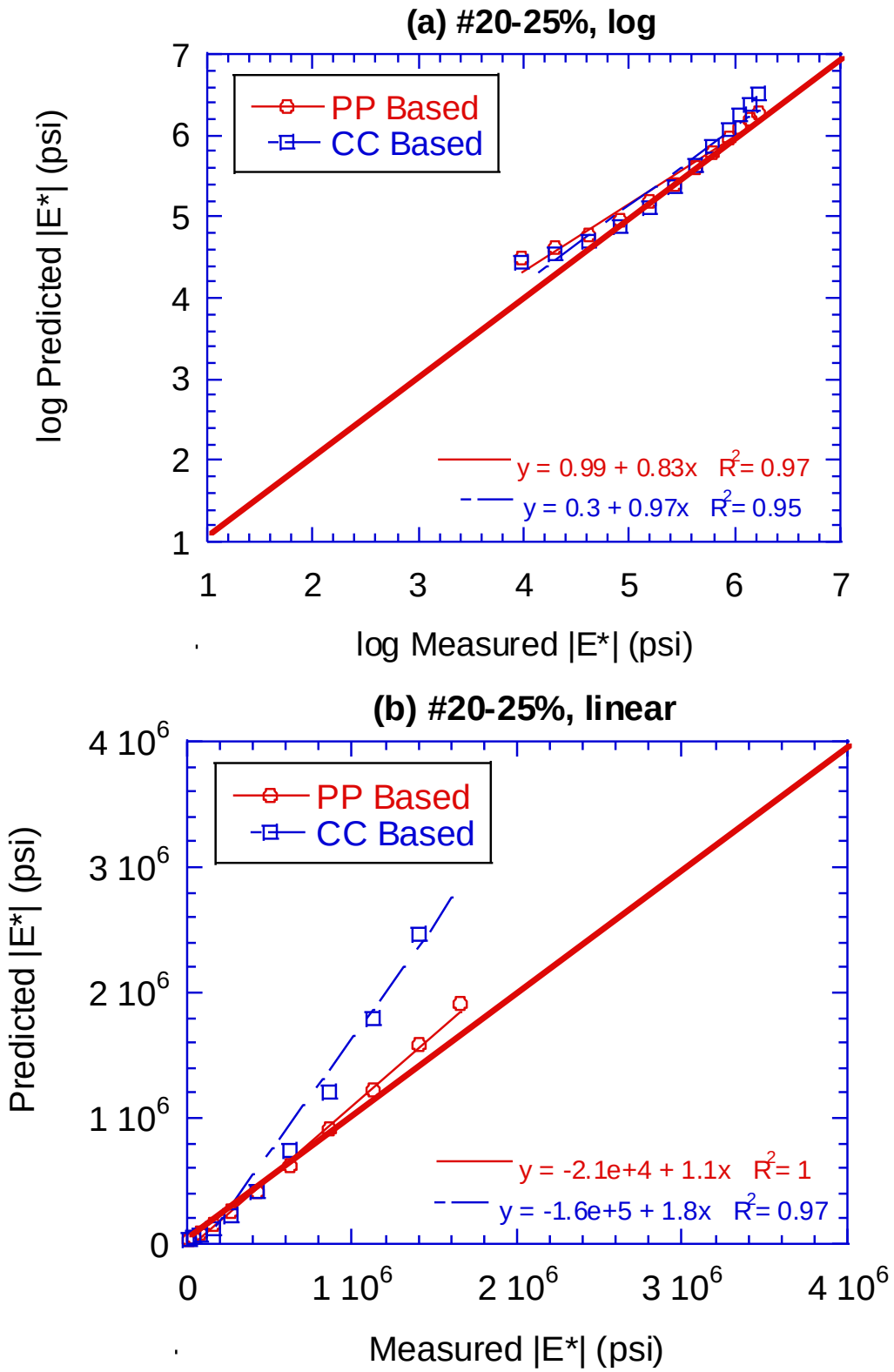

Figure 32: Measured versus predicted dynamic modulus |E*| from #20-25% rheology obtained from both DSR geometries in (a) log and (b) linear scales.

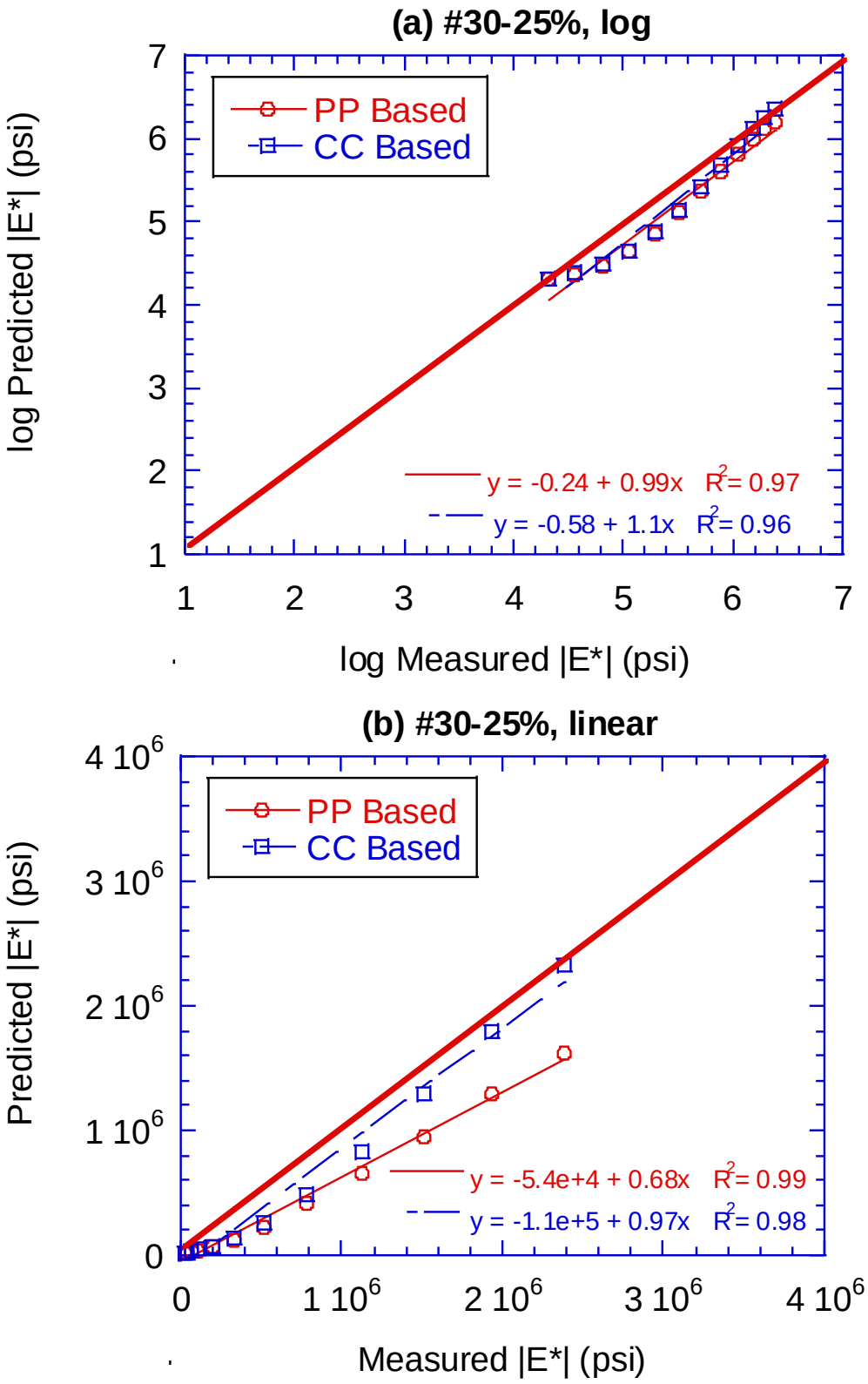

Figure 33: Measured versus predicted dynamic modulus |E*| from #30-25% rheology obtained from both DSR geometries in (a) log and (b) linear scales.

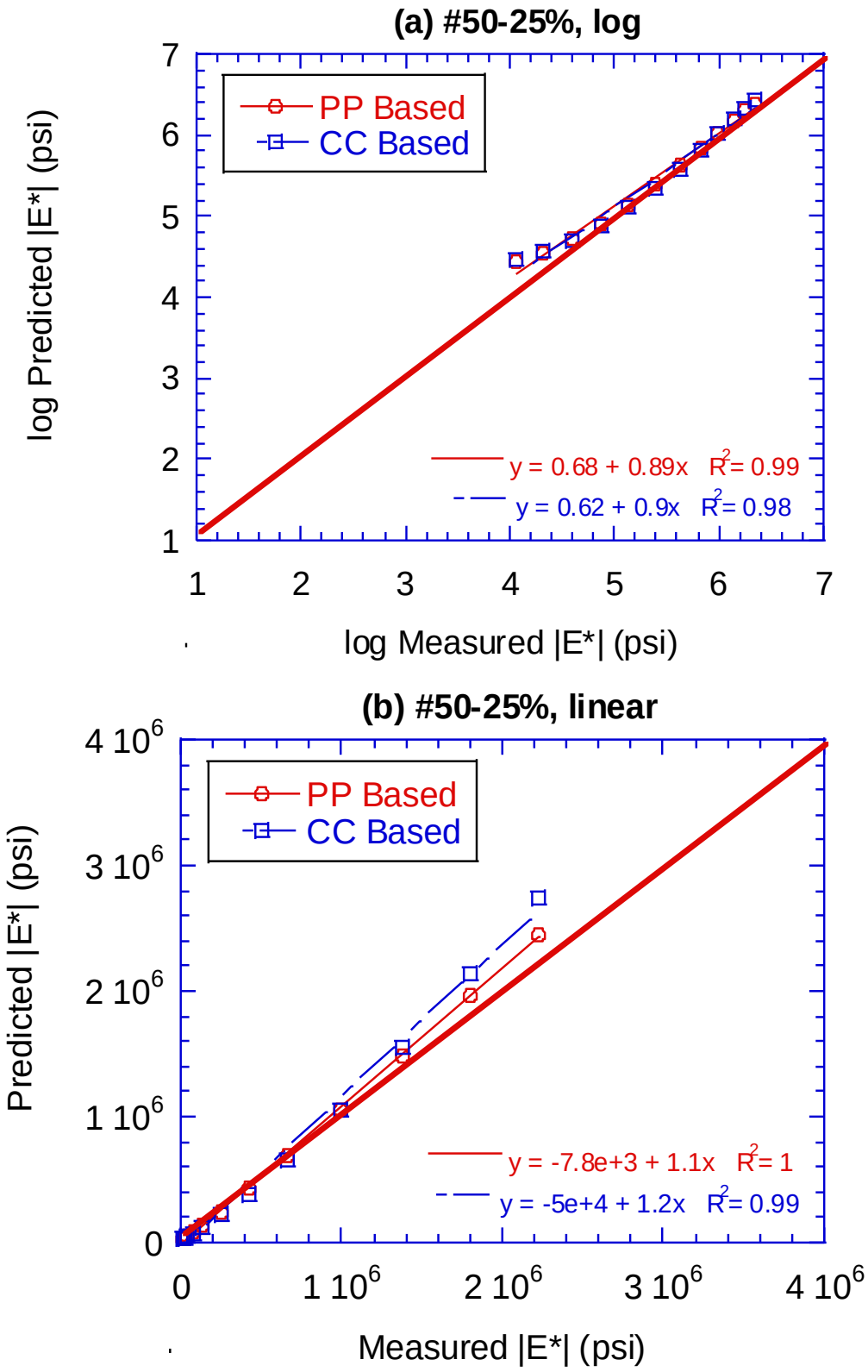

Figure 34: Measured versus predicted dynamic modulus |E*| from #50-25% rheology obtained from both DSR geometries in (a) log and (b) linear scales.

3.3 Chapter Conclusions

This section of the dissertation presents an experimental investigation of the feasibility of using the parallel plate DSR geometry for characterizing CRM binder rheology with an increased gap of 2.0 mm at high test temperatures. A comparison between asphalt binder rheological properties utilizing different sizes and concentrations of CR obtained from the parallel plate and concentric cylinder geometries was made. In addition, hot mix asphalt mixtures were designed, and performance samples were fabricated from six different CRM binders and tested for the dynamic modulus property over a wide range of temperatures and frequencies. Mixture mechanical properties were then used to identify the more suitable DSR testing geometry for characterizing CRM binders in relation to mix properties. Based on the experimental investigation presented herein, the following conclusions can be drawn for the CR sizes and concentrations used in this study:

- No significant variation was observed in measured CRM binder rheology between parallel plate and concentric cylinder geometries at 10% CR content on all sizes tested (i.e., #20, #50 and #30 mesh)
- Parallel plate DSR geometry provided slightly better or equal correlations to mixture performance in all size and concentration combinations of CRM in asphalt binder.
- Use of concentric cylinder may be required if CRM materials larger than #20 mesh are used. This needs to be validated.

From the preceding observations and due to the excessively long testing time and high variability in test replicate results at 30° C in the concentric cylinder geometry; this portion of the dissertation recommends using parallel plate DSR geometry for characterizing CRM binders instead of the concentric cylinder geometry for all sizes smaller than #20 mesh at 10%

concentration. While for #20 mesh size at 25% concentration, the PP geometry did not provide identical binder rheological results as the CC geometry; mixture |E*| predictions based on parallel plates measured |G*| and phase angle were closer to those measured in the lab. For the #30 and #50 mesh sizes, the CC and PP geometries produced very similar |G*| values at 25% concentration. Phase angles were also similar, except some differences were observed at low frequencies in #50 mesh size at 20% concentration.

An increased gap height of 2.0 mm in the parallel plate DSR geometry was found to provide a more accurate relationship to mixture mechanical performance for both high and low testing temperatures. In addition, it is recommended that when used, the DSR concentric cylinder geometry should be limited for use at 46° C or higher for characterizing CRM binders using the 14.46 mm cylinder.

CHAPTER 4. RELATING RUBBER SWELLING TO CRM BINDER PERFORMANCE

This chapter includes description of the portion of the study focusing on investigating the mechanisms of interaction between asphalt binders and CR. It is hypothesized that the extent to which CR swells can be related to fatigue properties of the overall modified binder. An experimental approach was carried out to investigate the nature of this interaction and the validity of the hypothesis. Asphalt binders were mixed with CR particles at different elevated temperatures (130, 160, and 190°C) by means of the wet process, and then filtered out such that no rubber particles were present in the residual asphalt binder. The base asphalt material, CRM asphalt blend, and the residual (drained) binders were then tested for |G*|, and fatigue characteristics using the Linear Amplitude Sweep (LAS) test in the DSR. The characteristics obtained were used to quantify the changes in the base asphalt rheology due to the absorption/diffusion of the light fractions (aromatic oils) of asphalt binder into CR. The properties of the swollen CR within the CRM binder were then derived and related to performance. The back-calculated CR modulus can be used as a Quality Control (QC) measure, which can be measured during construction.

4.1 Materials and Methods

The asphalt binder used in this study was a neat PG 58-28. The CR used was a 30-mesh material produced in the ambient procedure. Prior to testing, the material was sieved and only CR particles passing the No. 30 sieve and retained on the No. 40 sieve were used. Therefore, the CR particle size used in this study ranged between 0.425mm and 0.600 mm. Asphalt binder was blended with CR (15% by weight) by means of the wet process for a 30-minute interaction period at 750 rpm (rotation per minute) shearing speed. Three different mixing temperatures were selected (130, 160, and 190°C) to investigate the effect of temperature variation on CR swelling. A sample of the blended materials was collected for further testing.

A method similar to the “Basket Drainage Method” (Airey et al. 2003) was utilized to separate the swollen rubber particles from the asphalt binder after blending (Figure 35). In this method, the CRM binder was placed on a #50 sieve, then placed in an oven at a temperature of 150°C and the residual (drained) binder was collected on an aluminum pan. In order to isolate the effect of aging on the asphalt binder during mixing with CR, the base asphalt was aged by mixing it without the CR for the same amount of time (30 minutes) and at the same mixing temperatures (130, 160, and 190°C). This sample is called ‘binder aged (BA)’.

Figure 35: Filtering swollen CR out of CRM binders.

The base asphalt binder (B; Base), aged asphalt binder (BA; Base Aged), CR-asphalt composite (BAC; Base Aged with CR), and drained asphalt binder from BAC (BACD; Base Aged with Crumb Rubber and Drained) were tested for the dynamic shear modulus |G*| to quantify the rheological effects of CR modifier, and for damage tolerance (Linear Amplitude Sweep (LAS) test) as a measure of fatigue cracking performance in the DSR testing machine. In the DSR,

frequency sweep tests were conducted to determine |G*| at temperatures of 15, 30, 46, 60 and 76°C. At each temperature, tests were run at 11 frequencies varying between 1.0 and 100.0 rad/sec. Three test replicates of each asphalt binder were tested at each temperature and frequency. In addition, LAS tests were conducted on the asphalt binder samples after ageing using the Rolling Thin Film Oven (RTFO) and the Pressurized Aging Vessel (PAV). The LAS test is a strain-controlled test conducted with linearly increasing strain level from 0.1% to 30%. The collected data is then analyzed using the Viscoelastic Continuum Damage (VECD) theory. The outcome of the VECD analysis is the number of cycles to failure (N_f) for a given strain level, frequency and temperature. The N_f is used to characterize the cracking susceptibility of the tested binder. All binders were tested at the same intermediate temperature of 19°C, and three test replicates were used to generate the data. Details of the LAS test procedure and VECD theory are given in Hintz et al. (2011).

4.2 Results and Discussion of the |G*| Tests

4.2.1 Stiffening and Softening Effects of Mixing Temperatures on CRM Binders

Figure 36 shows the effect of mixing temperatures on |G*| of the CRM binder (BAC), aged binder (BA) and the residual (drained) binder BACD. It should be noted that, in order to eliminate the effect of binder aging occurring during blending CRM binders, comparisons should be made between the BA and the other binders (BAC and BACD). However, the |G*| of the base binder (B) is also provided as a horizontal red line for comparison purposes. As shown in Figure 36a (for |G*| at 15°C), at mixing temperature of 190°C, the CRM binder (BAC) is significantly softer than the aged binder (BA) and slightly softer than the original base binder (B). This is a desired behavior, where the CR particles have swollen enough to make the overall CRM binder soft (refer to Figure 3) and crack resistant. However, at lower mixing temperatures (at 130°C and 160°C), the BAC

samples are still stiffer than both the aged binder (BA) and base binder (B), possibly due to insufficient interaction/swelling of the rubber. Insufficient swelling means insufficient absorption of light fractions into CR, leaving the CR as hard as its original dry state. This indicates that the 'softening' effect in CRM binders mixed at 130°C and 160°C occurs at a much lower temperature than 15°C. Considering that the fatigue cracking temperatures are typically between 15 and 30C, beneficial 'softening' effect of rubber modified binder is not observed in CR modified binders mixed at 130°C and 160°C.

Figure 36b and Figure 36c show the effect of mixing temperature on the |G*| at 46°C and 76°C, respectively. In both cases, the stiffening caused by the CR is clearly visible and desirable for rutting resistance. It is interesting to note in Figure 36c that at mixing temperature of 190°C, the |G*| at 76°C value is the highest, indicating that 'good' swelling also leads to 'good' rutting resistance. Figure 36 also shows the |G*| values of the drained BACD binder (residual binder after CR is filtered out). As shown, at all |G*| testing temperatures (Figure 36a, b and c), the |G*| of the BACD is significantly higher than that for the BA. This indicates that the light fractions are absorbed by the rubber, leaving the residual binder with heavy fractions, which is consistent with the findings in the literature (Airey et al. 2003). Figure 36 also shows that |G*| of BACD increases with increasing CR mixing temperature, regardless of the |G*| temperature (see Figure 36a, b and c). This is meaningful since as the CR mixing temperature increases from 130°C to 190°C, better CR interaction occurs, and more light fractions are absorbed by the rubber. As a result, residual binder is stiffer at CR mixing temperature of 190°C as compared to the other mixing temperatures. It should be noted that stiff residual binder does not mean that the CRM binder is more prone to cracking. As shown in Figure 36a, the CR-asphalt composite (i.e., BAC) is much softer than both BA and BACD and even softer than the base binder B. More rigorous testing and details on the

cracking susceptibility of each of these binders are given in later sections of the dissertation (see section 4.5).

4.2.2 Binder Black Space Diagrams

Figure 37 shows the black space plots, i.e., phase angle versus |G*| relationships of all the binders tested. Rheological differences between the base binder (B) and the remaining binders BA, BAC and BACD are evident. At all CR mixing temperatures (Figure 37a through c) BAC (CRM binder) is significantly different than the rest of the binders. If each graph is examined closely, one can see the effect of CR mixing temperature. The BAC mixed at 190°C (Figure 37a) is significantly different than the B and BA binders. While BAC binders mixed at 160°C (Figure 37b) and 130°C (Figure 37c) are also significantly different than B and BA binders, they are closer, indicating less degree of interaction between the CR and the base binder.

4.3 Estimation of Swollen CR Modulus

Several 'rule of mixtures' (particulate filled composite) models have been proposed by researchers (Paul 1960, Shu 2007) to characterize properties of composite materials based on volume fractions and properties of the essential constituents. The use of these models to derive the properties of swollen CR within CRM binders are presented in this section. It is hypothesized that the modulus of the swollen rubber is an indicator of the performance of CRM binder and may be used as a measure of 'quality' of interaction between the rubber particles and the binder.

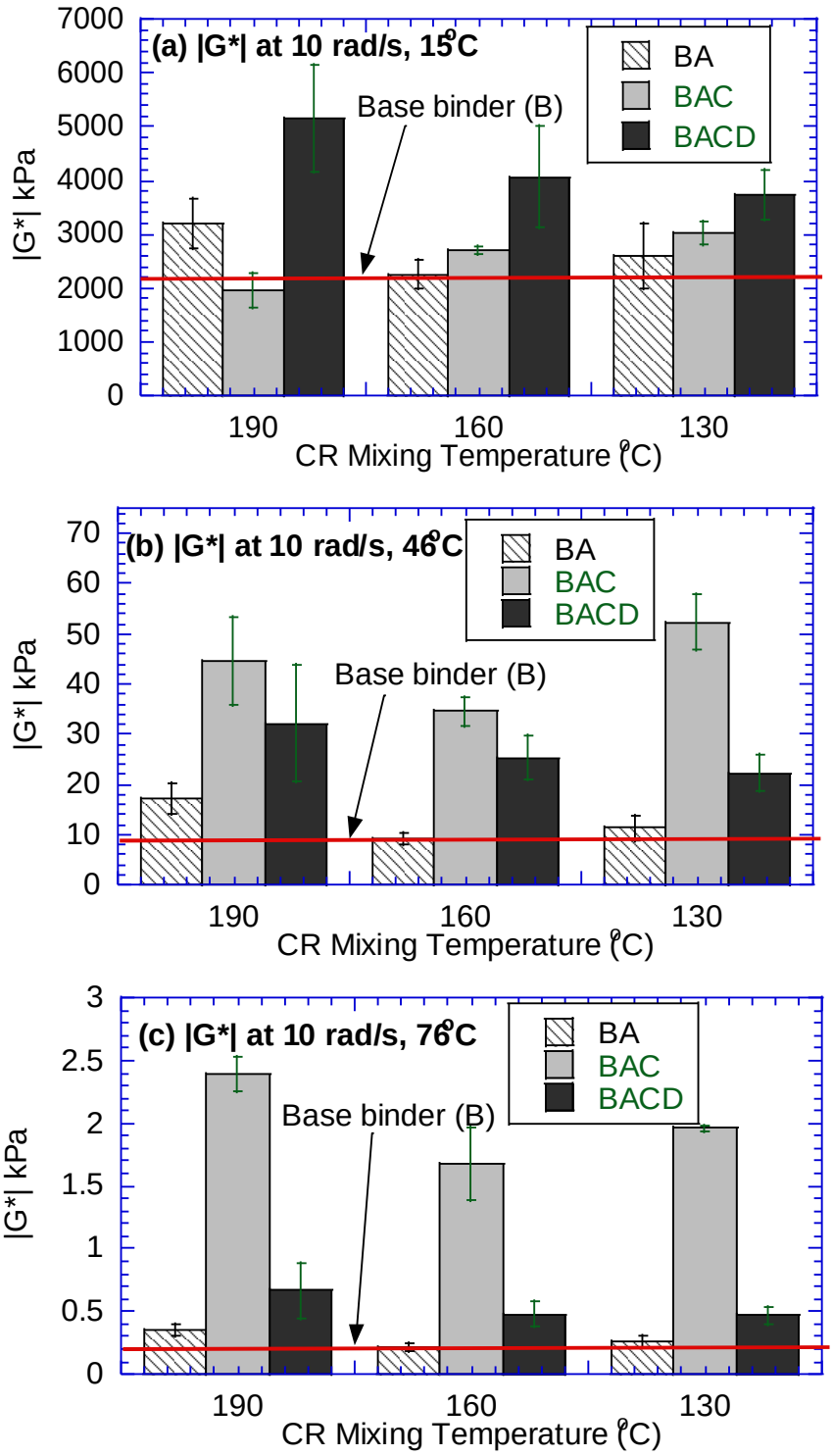

Figure 36: Effect of CR mixing temperature on |G*| at (a) 15°C, (b) 46°C and (c) 76°C.

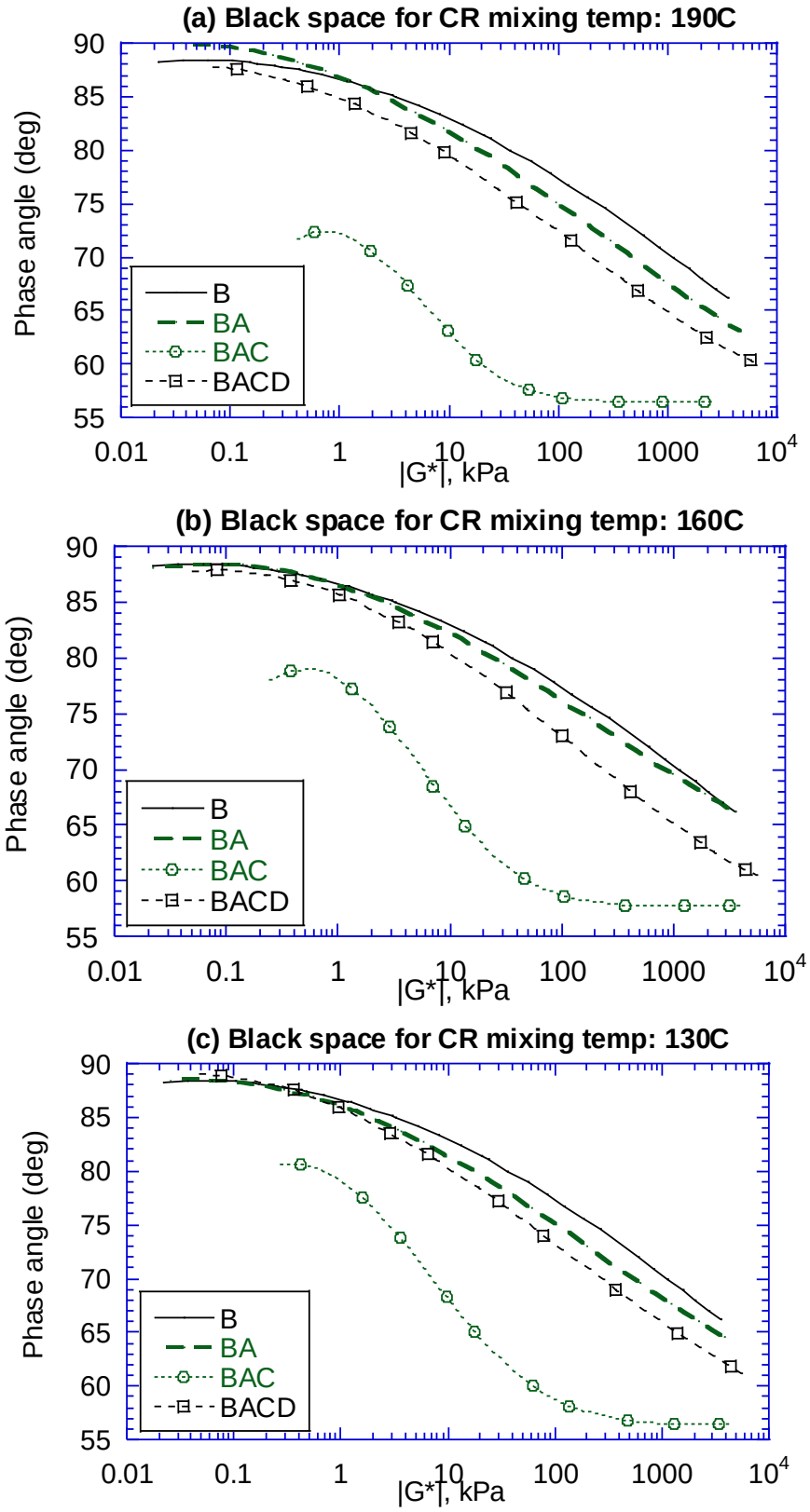

Figure 37: Black space plots for (a) 190°C, (b) 160°C and (c) 130°C mixing temperatures.

Figure 38 shows a plot of |G*| values versus testing temperature of BAC (Binder Aged with CR particles Composite) and BACD (Binder Aged Composite Drained) binders (for CR mixing temperature of 190°C). Recalling the illustration in Figure 3, BAC represents the behavior of the overall 'composite' while BACD corresponds to the behaviour of the 'fluid' portion, i.e., the asphalt binder. If the rubber particle in Figure 3 were to be a purely elastic rubber, i.e., did not interact with the binder and swell, it would have a constant modulus represented by the horizontal line shown in Figure 38. In such case, the point of intersection of the |G*| curves of the BAC and the BACD would correspond to the modulus of the rubber, where the two materials exhibit similar behavior. However, since rubber absorbs the light fractions of the asphalt binder and swells, its behavior should be viscoelastic, i.e., temperature and time dependent.

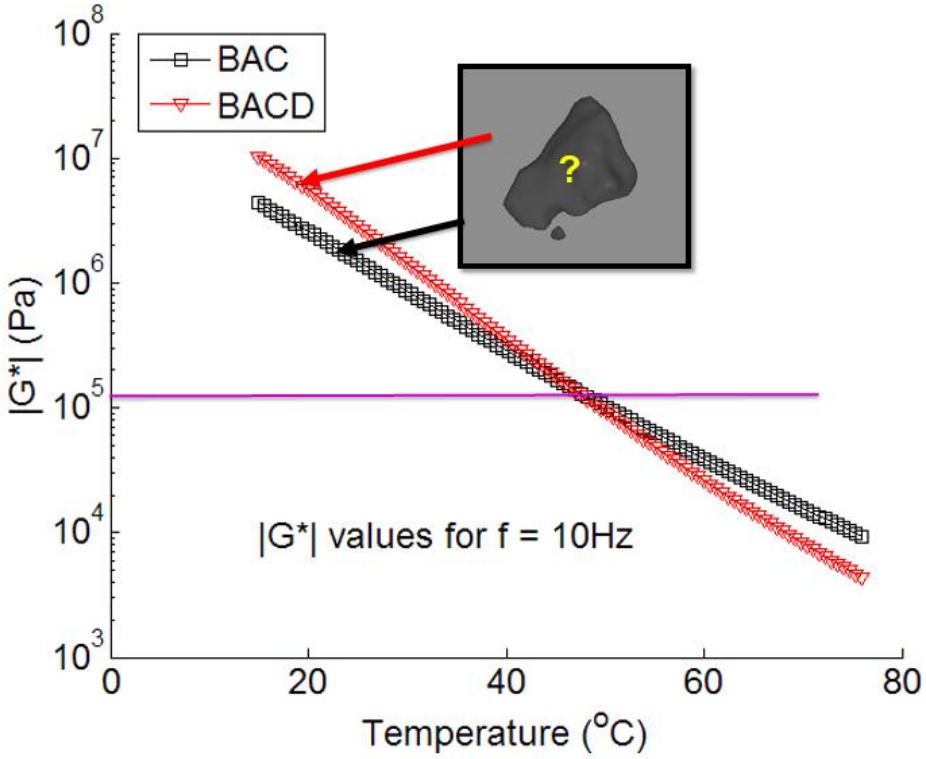

Figure 38: |G*| of BAC (CRM binder) and BACD (drained) mixed at 190°C.

Three different rules of mixtures models were investigated and used to back-calculate G_r^*: (i) parallel (upper bound) model (Paul 1960), (ii) series (lower bound) model (Paul 1960) and Shu

model (Shu 2007). The formulations in these models were rearranged such that effective moduli of inclusion (CR) within the composite (CRM binder) can be obtained.

4.3.1 Parallel model

The rubber modulus calculated by the parallel model corresponds to the lower bound (lower limit). The formulation for parallel model is given as follows:

$$\boldsymbol{G_c^* = G_r^* P_r + G_a^*(1 - P_r)} \qquad \textit{(7)}$$

where;

G_c^* = log(|G*|) of the rubber-asphalt binder composite (BAC);

G_r^* = log(|G*|) of the rubber particles;

G_a^* = log(|G*|) of the asphalt binder (BACD);

P_r = volumetric percentage of rubber.

Since the G_c^* and G_a^* are known and G_r^* is sought, equation 3 has been rearranged to yield the following formulation:

$$\boldsymbol{G_r^* = \frac{G_c^* - G_a^*(1 - P_r)}{P_r}} \qquad \textit{(8)}$$

4.3.2 Series model

The rubber modulus calculated by the series model corresponds to the upper bound (upper limit). The formulation for series model is given as follows:

$$\boldsymbol{\frac{1}{G_c^*} = \frac{P_r}{G_r^*} + \frac{1 - P_r}{G_a^*}} \qquad \textit{(9)}$$

where the variables used in the series model are the same as the ones used in the parallel model. Rearranging equation 5 yields:

$$G_r^* = \frac{P_r G_a^* G_c^*}{(1-P_r)G_c^* - G_a^*} \quad (10)$$

4.3.3 *Shu model*

Another method, proposed by Shu (2007), was originally developed to calculate of the effective shear modulus of an asphalt mixture from the constituents. This method was applied herein for deriving the CR modulus within CRM asphalt binder. The formulation derived by Shu is given as follows:

$$A\left(\frac{G_r^* - G_a^*}{G_r^* - G_c^*}\right) = \left(\frac{1}{1-P_r}\right) \quad (11)$$

where;

$$A = \left(\frac{G_c^*}{G_a^*}\right)^{\frac{8-10v_a}{15(1-v_a)}} \quad (12)$$

where v_a = Poisson's ratio of the asphalt binder, and the other variables are the same as defined for the parallel and series models. Equation 12 can be rewritten to compute the rubber modulus as follows:

$$G_r^* = \frac{A(1-P_r)G_a^* - G_c^*}{A(1-P_r) - 1} \quad (13)$$

Utilizing these three models described, the moduli of the swollen CR particles were back-calculated and compared to the moduli obtained from the |G*| curves of the rubber-asphalt binder composite (BAC), and drained binder from the rubber-asphalt composite (BACD). Figure 39 shows plots of the back-calculated swollen rubber moduli for the CRM binders mixed at different

temperatures. As shown, the back-calculated rubber modulus exhibits viscoelastic behavior. The degree of viscoelasticity/temperature dependency decreases with decreasing CR mixing temperature (comparing Figure 39a, Figure 39b and Figure 39c). Comparing Figure 39a, Figure 39b and Figure 39c, the slope of the G_r^* versus temperature curve generally decreases with decreasing crumb rubber mixing temperature. This indicates that at higher mixing temperatures (e.g., 190^{o}C) swollen CR is more viscoelastic/temperature dependent as compared to the G_r^* of the rubber within the binder mixed at lower temperatures (i.e., 160^{o}C and 130^{o}C). This is meaningful since the higher the mixing temperature, the more interaction/swelling occurs. As a result, the rubber becomes more viscoelastic/temperature dependent. The G_r^* curves in Figure 39 illustrate the effect of CR mixing temperature on the degree of interaction between the rubber and the binder. In order to investigate the validity of the |G*| values computed for the CR particles, a finite element analysis was performed, as described in the next section.

4.4 Finite Element Modeling of the DSR Test

A 3D Finite Element (FE) based micromechanical model of the |G*| test was developed using the ABAQUS software. As mentioned above, the primary goal was to verify the methodology presented earlier for backcalculation of CR modulus within the CRM binder. The secondary goal was to quantify the stiffening/softening effect caused by the CR particles within the binder, at different percentages of CR. Since the CR particles are asymmetrically distributed in the binder, the composite material was modelled as 3D solid elements. Eight-node continuum brick elements were used to mesh both the binder and the CR particles.

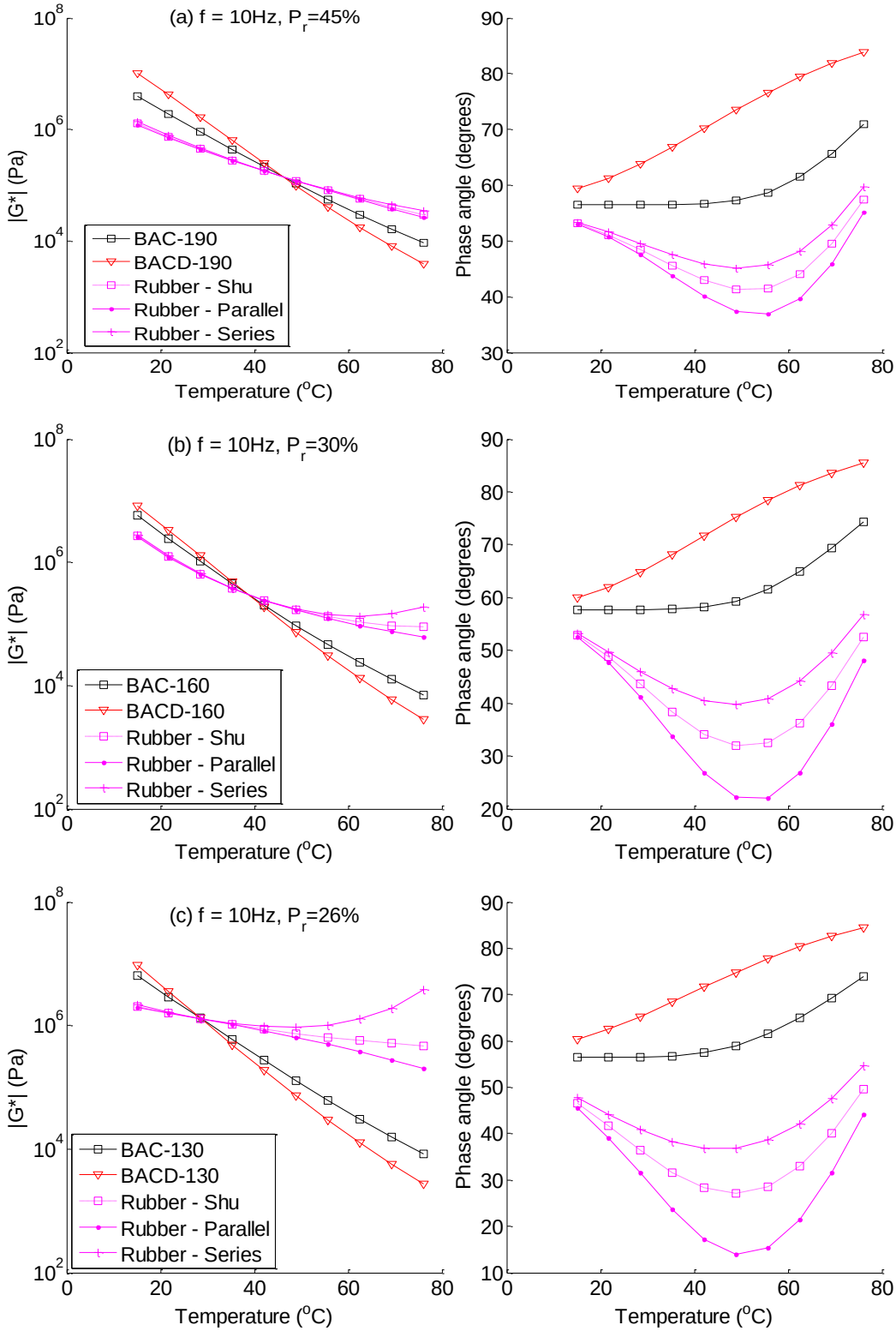

Figure 39: Back-calculated swollen CR moduli mixed at (a) 190, (b) 160, and (c) 130 °C.

The mesh size was selected such that the FE model is able to capture the geometry of CR particles and at the same time is computationally efficient. This was ensured by verifying the volume of CR in the FE model with geometry generated using CT-images. As for the boundary conditions, the vertical boundaries were free, and the bottom boundary was fixed. The micromechanical FE model of the DSR test sample included real 3D shapes of CR obtained using the non-destructive X-ray Microtomography (MT) imaging technique. In order to scan the samples using X-ray MT, CRM binders were poured into 7 mm diameter polypropylene micro-centrifuge tubes and instantly frozen using liquid nitrogen. The 3D images were obtained at the 5-BM-C Microtomography beam line at the Advanced Photon Source (APS) facility in Argonne National Laboratory (ANL). The sizes of the X-ray MT images were 1024x1024x1024 voxels, which leads to a spatial resolution of 6.8microns/voxel ($6.8x10^{-3}$mm/voxel). Figure 40a shows a 3D visualization of CR particles in the asphalt binder.

As illustrated in Figure 40, the internal structure of CRM binder was superimposed (overlapped) with a FEM mesh generated for the same size/height sample (7 mm diameter, 2mm high). Then the FEM elements that intersect with the CR particles were labeled as CR phase, and the remaining elements were labeled as the binder phase. The back-calculated CR modulus (G_r^*) was assigned at the elements occupied by the rubber, and the modulus of the residual (drained) binder (i.e., BACD) was assigned to the remaining elements. Then cyclic DSR test was simulated to compute |G*| of the CR-binder composite (i.e., the BAC) and compared to the measured |G*| of the composite. The DSR simulations were performed for test temperatures of 15°C and 76°C. The Poisson's ratio of the binder phase was set to 0.45 and 0.50 for 15°C and 76°C simulations, respectively. Poisson's ratio for the rubber was set to 0.50 for both temperatures. It has been reported in the literature that for an interaction period of 30 minutes and mixing temperature of

190°C, the rubber swells approximately 300% of its' initial volume (Dong et al. 2012). Therefore, the behavior was modeled with 45% incorporated CR particles by volume as opposed to 15% CR (by weight) added before interaction. Simulations were performed at different volumetric percentages of CR, in addition to the actual percentage (i.e., 45%) of the CRM binder sample. Different percentages of the CRM binders were artificially generated by editing the 3D X-ray MT images of the CR particles such that lower percentages of the CRM binder can be simulated. The goal was to show the stiffening and softening effects illustrated in Figure 36 at different CR percentages.

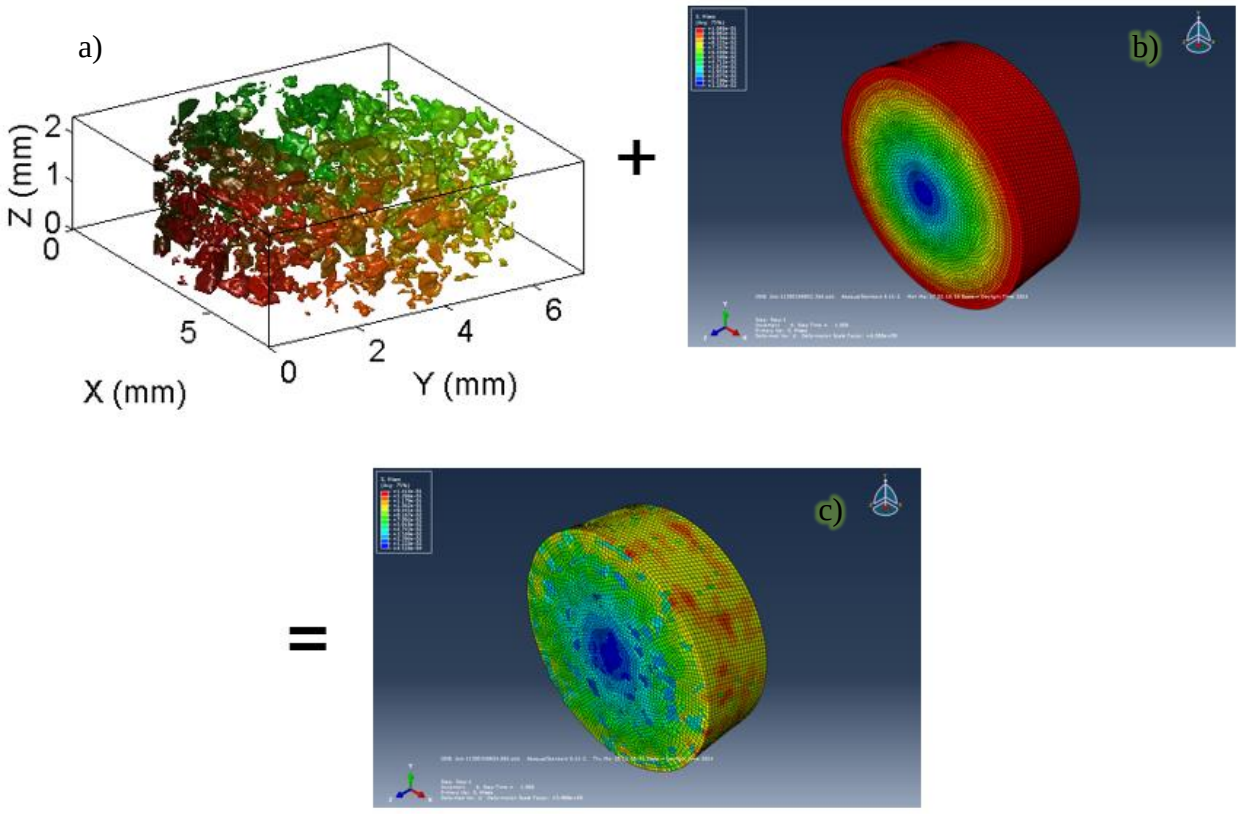

Figure 40: (a) 3D Visualization of CR particles in the asphalt binder, (b) template FEM mesh and (c) superimposed CR + FEM mesh.

To quantify stiffening and softening caused by CR inclusion in the asphalt binder, the following parameter was defined:

$$\Delta|\boldsymbol{G}^*| = \left(\mathbf{1} - \frac{|\boldsymbol{G}_c^*|}{|\boldsymbol{G}_a^*|}\right) \times \mathbf{100}\% \qquad \textit{(14)}$$

where;

$\Delta|G^*|$ = Percent change in dynamic shear modulus

$|G_c^*|$ = Dynamic shear modulus of the rubber-asphalt binder composite

$|G_a^*|$ = Initial dynamic shear modulus of the asphalt binder (0% CR)

Figure 41 shows the softening effect of CR modifier on asphalt binders at 15°C for asphalt binders mixed at 190°C. It is shown that the presence of CR particles softens the asphalt binder at low temperatures, which enhances the performance of CRM binders by making them less brittle at intermediate/low temperatures. In addition, the FEM agrees well with the laboratory measured data (see Δ|G*| values for 45% CR in Figure 41), which validates the procedure for backcalculation of |G*| of the rubber. Figure 41 also shows that there is a good correlation between the percentage of the rubber and the change in the |G*| value (i.e., Δ|G*|). Figure 42 shows the stiffening effect of CR modifier on asphalt binders for asphalt binders mixed at 190°C. It is clearly shown that CR modifier stiffens the asphalt binder at high service temperatures, which enhances the performance of CRM binders and makes it less prone to permanent deformation (rutting). Similar to the results obtained for 15°C, at 76°C the FEM also agrees well with the laboratory measured data (see Δ|G*| values for 45% CR in Figure 42), therefore validates the procedure for backcalculation of |G*| of the rubber. Similar to the results for 15°C, Figure 42 also shows that there is a good correlation between the percentage of the rubber and the change in the |G*| value (i.e., Δ|G*|) at 76°C.

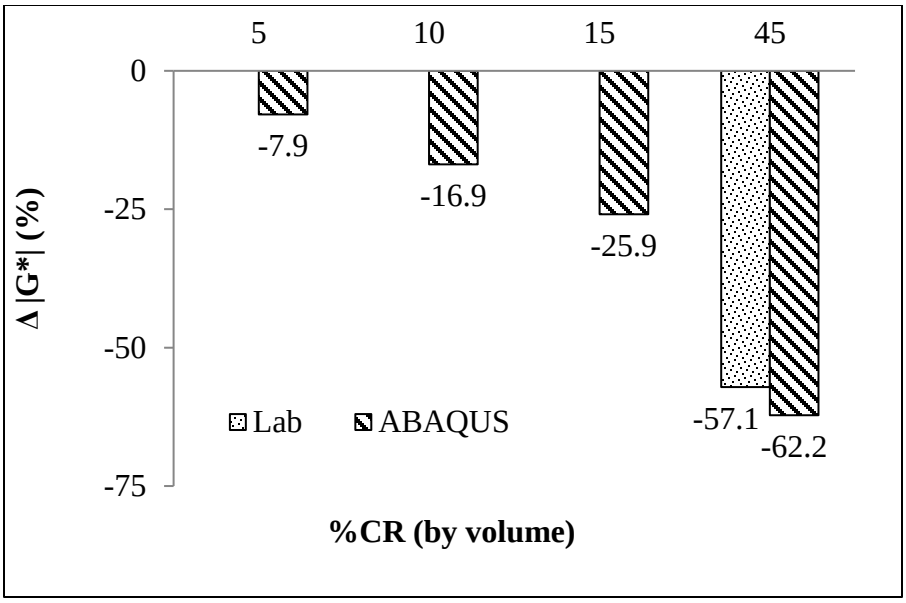

Figure 41: CR softening effect on asphalt binder at low temperatures (15 °C).

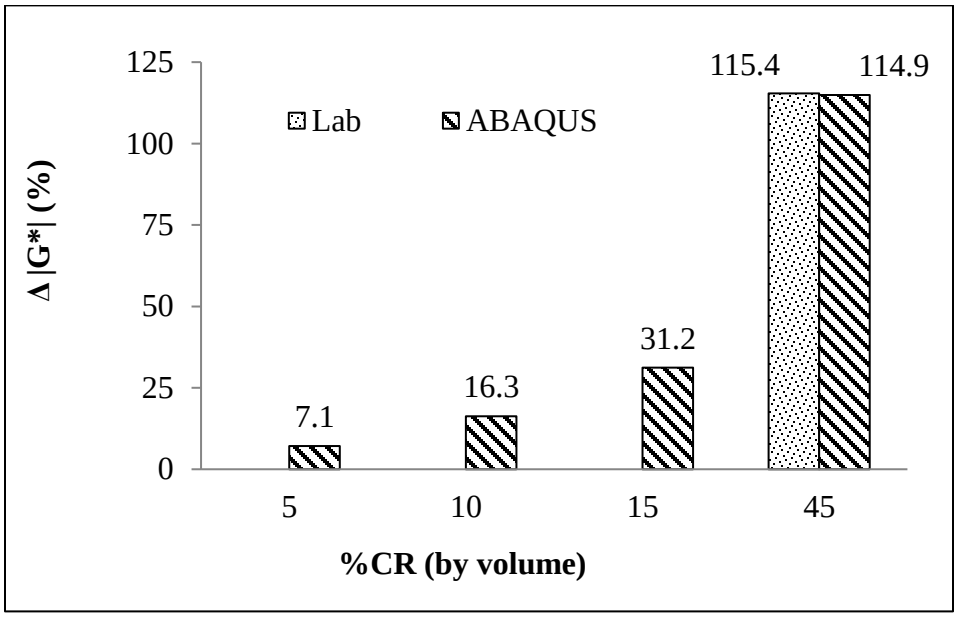

Figure 42: CR stiffening effect on asphalt binder at high temperatures (76 °C).

4.5 Fatigue Characteristics of CRM Binders

In this study, the LAS test was conducted on PAV aged binders to better simulate the aged conditions of CRM binders as the purpose of this test is measuring the fatigue life (N_f) of the material. Details on N_f calculation are given in AASHTO TP 101 (2014), therefore are not repeated

here for brevity. Figure 43a and Figure 43b show the results of the LAS test for 2.5% and 5.0% strain levels, respectively. The results clearly illustrate the effect of CR on the fatigue life of asphalt binder. Binders tested with CR particles present in the composite (BAC) exhibit a much better fatigue resistance. In addition, the figures also show the effect of mixing temperature ($T_{CR\text{-}mix}$) on the extent of benefits of CR on asphalt binder. While the test variability is relatively high, improvement in fatigue life is visible as the mixing temperature ($T_{CR\text{-}mix}$) increases. It should be noted that temperatures greater than 200°C may cause CR depolymerization which can lead to decreased fatigue resistance (Attia and Abdelrahman 2009).

Another observation that can be made from the bar graphs in Figure 43 is that the BACD has less N_f as compared to BAC. This is because CR particles absorb the light asphalt components (aromatic oils and resins). Once the material is drained, the remaining material is an asphalt binder with a much higher level of heavy fractions (asphaltenes). This explains why BACD binders have a significantly lower fatigue life as compared to BAC binders. However, when BACD and BA are compared, the BACD is better than (or as good as) the BA. The reason for this is believed to be the antioxidants released by CR into the binder, which may be balancing for the light fractions lost to the rubber. Figure 43 also shows that the gap between the BAC and BACD increases with increasing mixing temperature ($T_{CR\text{-}mix}$), which further illustrates the higher extent of absorption of light fractions and swelling of the rubber at high temperatures.

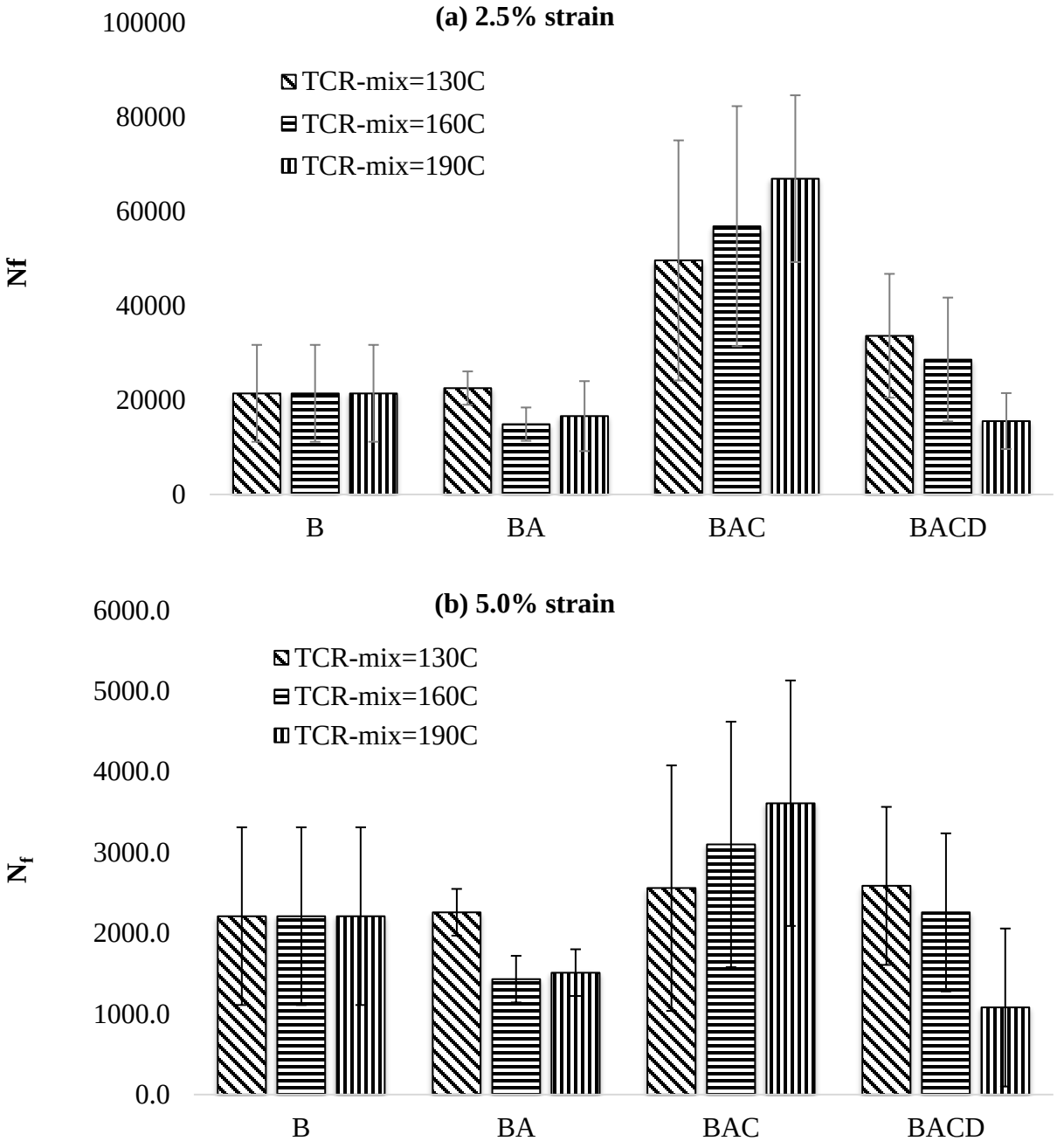

Figure 43: LAS results at (a) 2.5% strain, and (b) 5.0% strain for all binders.

Figure 44 and Figure 45 show the relationship between three different moduli ($|G^*|_r$ (= $|G^*|$ of rubber obtained from the Shu model), $|G^*|$-BAC and $|G^*|\sin\delta$-BAC) values and the fatigue life parameter N_f determined from the LAS test. For 2.5% strain level (Figure 44), good correlation coefficients (R^2) are observed for all three moduli relationships; with the relationship between N_f

and $|G^*|_r$ being the best (95% R^2). However, when the strain level is increased in the damage analysis, poorer correlations between N_f and |G*|-BAC and |G*|sinδ were observed, as shown in Figure 45. In contrast, the relationship between N_f and $|G^*|_r$ shows improved correlation at higher strain levels with a R^2 value of 99%. This confirms the hypothesis that the modulus of the swollen rubber is an indicator of CRM binder performance and may be used as a measure of 'quality' of interaction between the rubber particles and the binder.

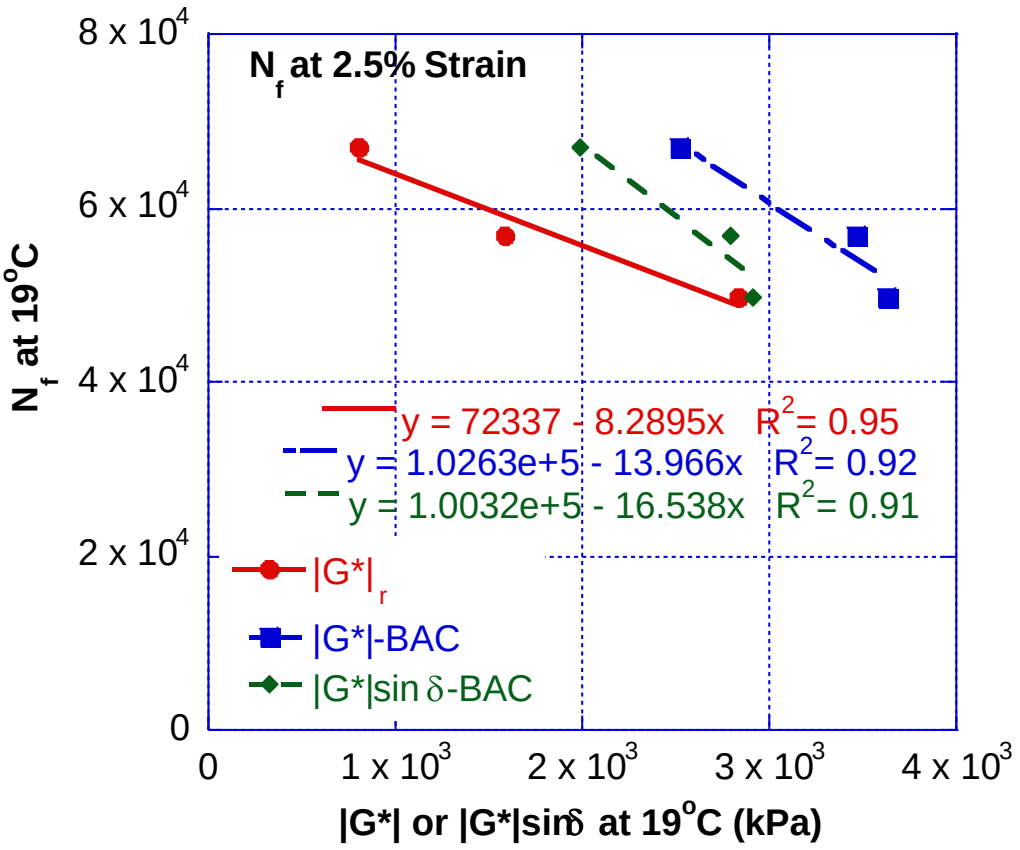

Figure 44: Relationship between different moduli values and damage tolerance at 19 °C for 2.5% strain.

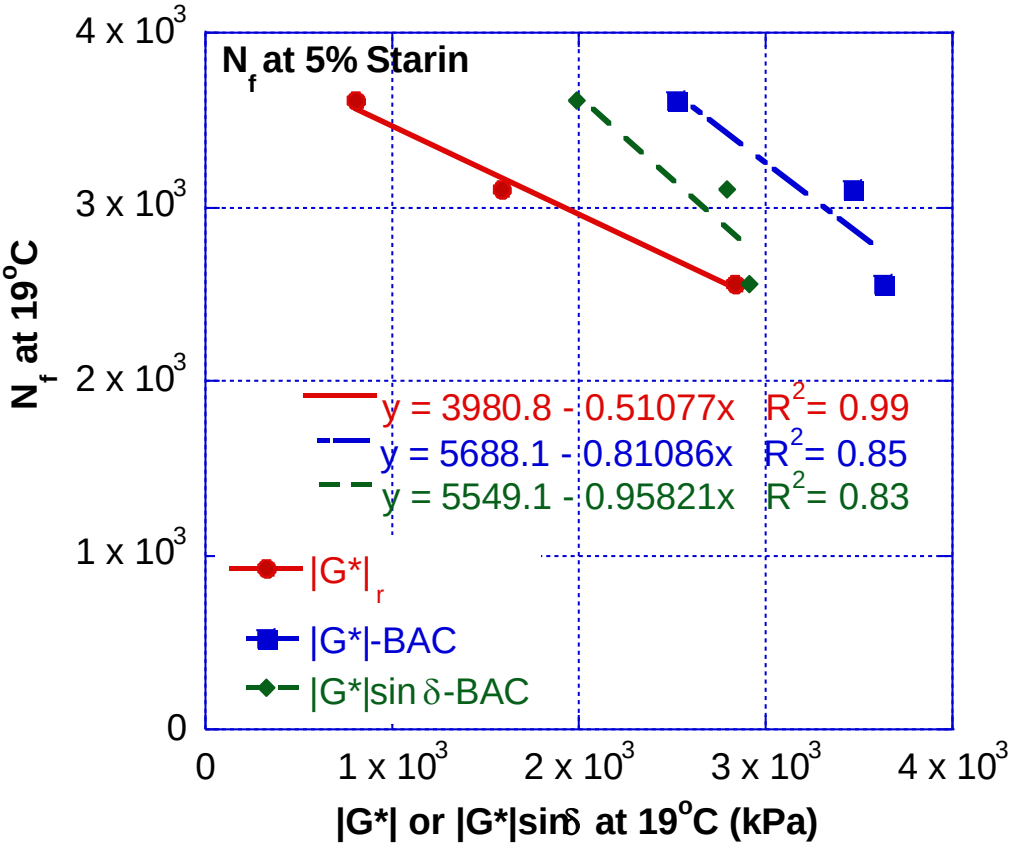

Figure 45: Relationship between different moduli values and damage tolerance at 19 °C for 5.0% strain.

4.6 Chapter Conclusions

The mechanisms of interaction between asphalt binders and CR were investigated in this portion of the dissertation. An experimental approach was used to quantify the rheological changes in CRM binders using the |G*| test. In addition, the damage tolerance of modified and unmodified binders was investigated using the LAS test. Based on the foregoing, the following conclusions were drawn:

- Effect of CR mixing temperature on CRM binder rheology was investigated. It was shown that at 190°C the rubber particles have swollen enough to make the overall CRM binder soft and crack resistant at low temperatures. However, insufficient swelling in CRM

binders mixed at 130°C and 160°C indicates that the 'softening' effect occurs at a much lower temperature than 15°C.

- As mixing temperature increased from 130°C to 190°C, better interactions occur, and more light fractions are absorbed by the rubber.
- Black space plots show that at all CR mixing temperatures; CRM binder is significantly different than the other binders. It was observed that the higher the mixing temperature is, the further/more different the CRM binder gets from the base binder. This indicates a higher degree of interaction between CR and the base binder.
- |G*| values produced by the FE model confirmed that the micromechanical model developed by Shu can be applied to CRM binders to back-calculate the swollen CR modulus.
- Rubber inclusions in a CRM binder clearly exhibit viscoelastic behavior. The degree of viscoelasticity/temperature dependency of CR increases with increasing mixing temperatures.
- Stiffening and softening effects of CR on asphalt binders were shown in the FE model of the DSR tests developed in this study. In addition, the FEM agrees well with the laboratory measured data.
- Results of the LAS test illustrated the positive effect of CR on the fatigue life (N_f) of an asphalt binder. It was also observed that better improvement in fatigue life of CRM binders is achieved with increased mixing temperature.
- The relationship between performance (N_f) and different material characteristics were investigated. The best correlation was found between N_f and back-calculated CR modulus, especially at higher strain levels. This confirms the hypothesis that the modulus of swollen

CR is a good indicator of CRM binder performance and may be used as a measure of quality of interaction between asphalt binder and CR.

CHAPTER 5. RELATING RUBBER SWELLING TO CR PRETREATMENT

As briefly mentioned in Chapter 1, there are two main methods of incorporating CR into asphalt pavements. The most common modification method is the wet process, where CR is used as a binder modifier and is blended with the hot asphalt liquid at elevated temperatures (160-220°C). This method utilizes 15 to 25% CR by weight of the binder. The second method is the dry process, where CR materials are used as a fine aggregate replacement and are directly added to the asphalt mixture during HMA production, and before the asphalt binder is introduced. While the wet process has been proven to have superior performance, special equipment and mixers are required to produce the CRM binder, which can lead to an increase in the overall cost of the HMA mixture. The dry process does not require any special mixing equipment and has a higher recycling potential in asphalt pavements. However, the limited success and inconsistent performance of the dry process has raised concerns among researchers and practitioners.

To overcome the issues in both the wet and dry processes, pre-treated CR modifiers have been developed. CR pre-treatment is done by mixing CR particles with low viscosity petroleum-based products or aromatic oils compatible with the lighter asphalt fractions. The treatment oil is added to the rubber (percent by weight) and the two materials are mixed together at around 135°C until the rubber particles are fully mixed, and no oils are remaining (Newcomb et al. 1994). This process is done at least 24 hours prior to using the CR modifier in asphalt mixtures. The main goal of CR pre-treatment, or surface modification, is to enhance the compatibility of CR with the modified binder matrix (Kocevski et al. 2012). In addition, pre-treatment blocks the penetration of asphalt liquid into CR and prevents the rubber particles from absorbing the light fractions of asphalt binder during and after mixing (Chapter 4). After the pre-treatment process is completed, CR is incorporated into the asphalt mixture in a manner similar to that of the dry process.

The relationship shown in Chapter 4 between swollen CR modulus and the overall properties of the modified material can be used to quantify the extent of CR pre-treatment and to identify sufficiently pre-treated CR materials in the laboratory before being incorporated in CRM HMA mixtures. For that, an experimental approach is presented. A PG 58-28 asphalt binder was blended with an ambient 30-mesh CR material by means of the wet process. The same CR material was treated by two different manufacturers (Source A and Source B) and blended with the same base asphalt. These blends were also used in the analyses. CR particles were filtered out of the CRM binders using the draining procedure referenced in Chapter 4. The experimental program included rotational viscosity (η) and dynamic shear modulus, |G*| on the base binder and the sampled CRM binders (both rubberized and residual). The viscosity of the modified materials was monitored, and the study suggested that one pre-treatment (Source B) was more sufficient than the other (Source A). This was evidenced by a viscosity increase in Source A CRM binder, and was confirmed by dynamic shear modulus tests.

5.1 Introduction

Since pre-treated CR is used to modify asphalt mixtures in the dry process, a limited interaction time between CR and asphalt binder (as opposed to the longer interaction time in the wet process) is expected. This allows the rubber particles to maintain their physical shape and elastic performance in the voids between the aggregates (Figure 46). The ability of the asphalt liquid to penetrate into CR particles is controlled by the osmotic pressure. Therefore, it is assumed that the asphalt liquid will produce a vapor pressure that would force the petroleum-based product used for pre-treatment into the rubber particles rather than allowing it to modify or contaminate the asphalt binder (Newcomb et al. 1994). If the CR material is sufficiently pre-treated, this should

be seen as a reduction of the viscosity increase observed in typical CR modified binders (Newcomb et al. 1994).

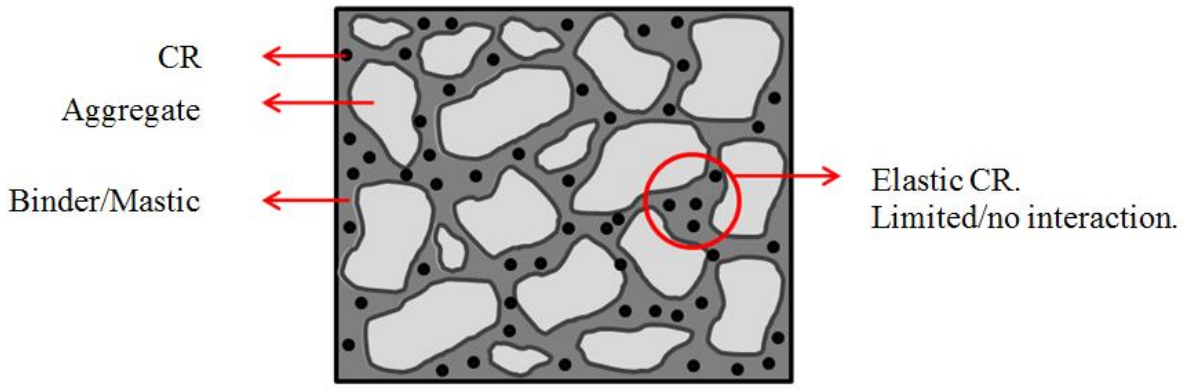

Figure 46: Schematic explanation of asphalt- rubber interaction in a dry process asphalt mixture.

Stroup-Gardiner et al. (1996) investigated the effects of pre-treated CR modifier on the performance of asphalt mixtures using both laboratory fabricated specimens and field sections. The study found that mixtures incorporating pre-treated CR exhibited the highest ability to reduce thermal stresses when compared with control (unmodified) mixtures, and mixtures modified using the dry process (untreated CR). This indicates a potential for reduced thermal cracking in pre-treated CRM mixtures. In a study on the properties of pre-treated CRM binders, Campillo (2014) found that pre-treated CR improved the temperature susceptibility of asphalt binders. In addition, it was concluded that pre-treated CR improves the overall consistency of binders and improves the temperature susceptibility.

Despite the potential benefits and improved properties, a fundamental method of quantifying the extent of pre-treatment levels on CR has not yet been established. Establishing such methods will help identify sufficiently pre-treated CR materials in the laboratory before incorporating the modifier into asphalt mixtures.

5.2 Materials and Methods

The asphalt binder used in this study was a neat PG 58-28. The raw untreated CR material utilized was a 30-mesh material, produced using the ambient process. In addition, the same CR material was pre-treated by two different manufacturers (Source A and Source B) and used in the proceeding analyses. Since CR pre-treatment blocks the penetration of asphalt liquid into the rubber particles, no interaction between the binder and the pre-treated CR particles is expected to take place after adding the rubber into the asphalt mixture. To quantify the extent of CR pre-treatment and interaction effects between the pre-treated CR and the asphalt liquid, an experimental approach is presented.

Untreated CR modifier shows clear rheological and interaction (stiffening and softening) effects on asphalt binder (Chapter 4). This phenomenon is not expected to take place in pre-treated CRM asphalt binders as the rubber particles have inherent light asphalt components absorbed during the treatment process. Hence, no interaction in the rubber-asphalt blend is expected. Asphalt binder was blended with 10% CR by means of the wet process at 190°C for a 30-minute interaction period at 750 rpm shearing speed. This process was applied on the untreated as well as pre-treated CR materials. Then, CR particles were filtered out of the CRM binder after blending. The CRM binder was placed on a #100 sieve then placed in an oven at a temperature of 155°C. The residual (drained) binder was collected on an aluminum pan. Samples of both the CRM binders "Rubberized binder" and the drained binders "Residual binder" were collected for further testing. The base binder and the sampled CRM binders (both rubberized and residual) were tested for rotational viscosity (η) and $|G^*|$.

5.3 Results and Discussion

5.3.1 Rotational Viscosity

A Brookfield Rotational Viscometer was utilized for viscosity measurements of the base binder and the CRM binders. The rotational viscosity tests were conducted in accordance with AASHTO T316 "*Standard Method of Test for Viscosity Determination of Asphalt Binder Using Rotational Viscometer*" on two test replicates at 135°C and are shown in Figure 47. A substantial increase in viscosity is observed for the asphalt binder modified with untreated CR. As previously noted; this phenomenon is expected to take place and is a typical material behavior. On the other hand, pre-treated CR modifiers are not expected to exhibit the same behavior. Pre-treated CRM binders exhibited two different behaviors. Source A pre-treated CRM binder had a viscosity ratio of 2.07 to that of the base binder. This suggests an insufficient pre-treatment level. Such high viscosity increase indicates that either the oil used in the pre-treatment process was not suitable, or that low percentages (below optimum) of oil pre-treatment were used. On the other hand, Source B pre-treated CRM binder had an almost identical viscosity of that observed for the base asphalt binder. This indicates sufficient pre-treatment used for this material and that the oil used did in fact block the penetration of lighter asphalt components into the CR particles.

Unlike the pre-treated CR from Source B, the preceding observations suggest that if the pre-treated CR from Source A is incorporated into the asphalt mixture without prior blending with asphalt binder (dry process), the rubber particles will interact with the binder and it will no longer be serving as an elastic aggregate in the voids between the aggregates. The fact that the two materials interact may have several potential negative effects on the performance of the asphalt mixture in the field. For example, while mixing the binder and aggregates, if insufficiently treated CR is at the interface between the binder and aggregate, it may absorb the light fractions leaving

the stiff and brittle binder at the interface. This can potentially create a brittle bond between the aggregate and the binder.

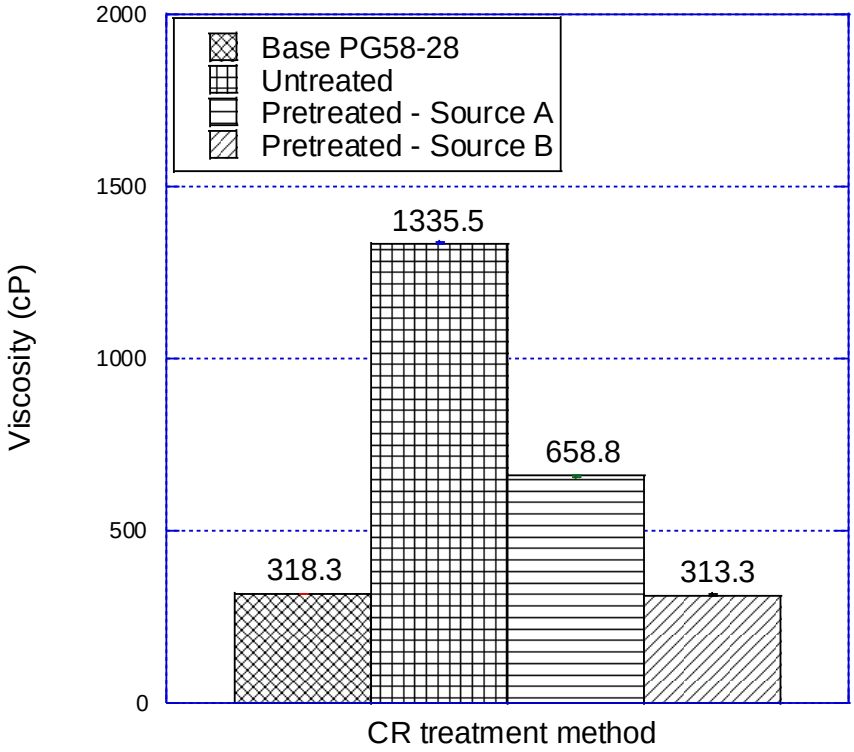

Figure 47: Viscosity of virgin and rubberized binders.

5.3.2 Dynamic Shear Modulus

To further quantify the extent of CR pre-treatment on the materials investigated, the interaction between asphalt liquid and CR were further examined using the |G*| test at different temperatures. This helped capture the effect of interaction between the two materials on the final CRM blend and helped eliminate the concerns over the possible effects the presence of rubber particles may have on viscosity measurements.

DSR testing was completed using parallel plate geometry on three test replicates at 15, 46, and 76°C and a frequency of 10 Hz. The 25 mm plate geometry with 2.0 mm gap was used for |G*| measurements at 46 and 76°C, while the 8 mm plate geometry with 2.0 mm gap was used for measurements at 15°C. Figure 48 shows the effects of different CR modifier types on the stiffness

of the base asphalt binder. As shown in Figure 48a (for |G*| at 15°C), the rubberized binder for untreated rubber is significantly softer than the base binder, whereas the residual binder is significantly stiffer. This is an expected result for the raw untreated rubber material. As described in the previous section, untreated rubber absorbs the light fractions, leaving the residual binder with heavy, stiff fractions.

As for the pre-treated CRM blends; a clear interaction between the binder and Source A pre-treated CR was observed from the significant differences in stiffness of the rubberized and residual binders. Figure 48b and Figure 48c also show the clear interaction effects of untreated and Source A pre-treated CR on the base asphalt binder. The rubberized binder is significantly stiffer than the base binder at higher temperatures (e.g. 46 and 76°C). On the other hand, no absorption of light fractions is observed for Source B pre-treated CR. The rubberized and residual binders produced using Source B pre-treated material exhibit very similar behavior and show insignificant differences in rheology. The two materials exhibited statistically identical behavior. This confirms that sufficiently pre-treated CR does not absorb the light fractions of the asphalt liquid when incorporated into the asphalt mixtures. It should however be noted that the residual binder of Source B pre-treated CR exhibited lower |G*| values as compared to the base binder. This may be caused by the release of the 'treatment fluid' into the binder.

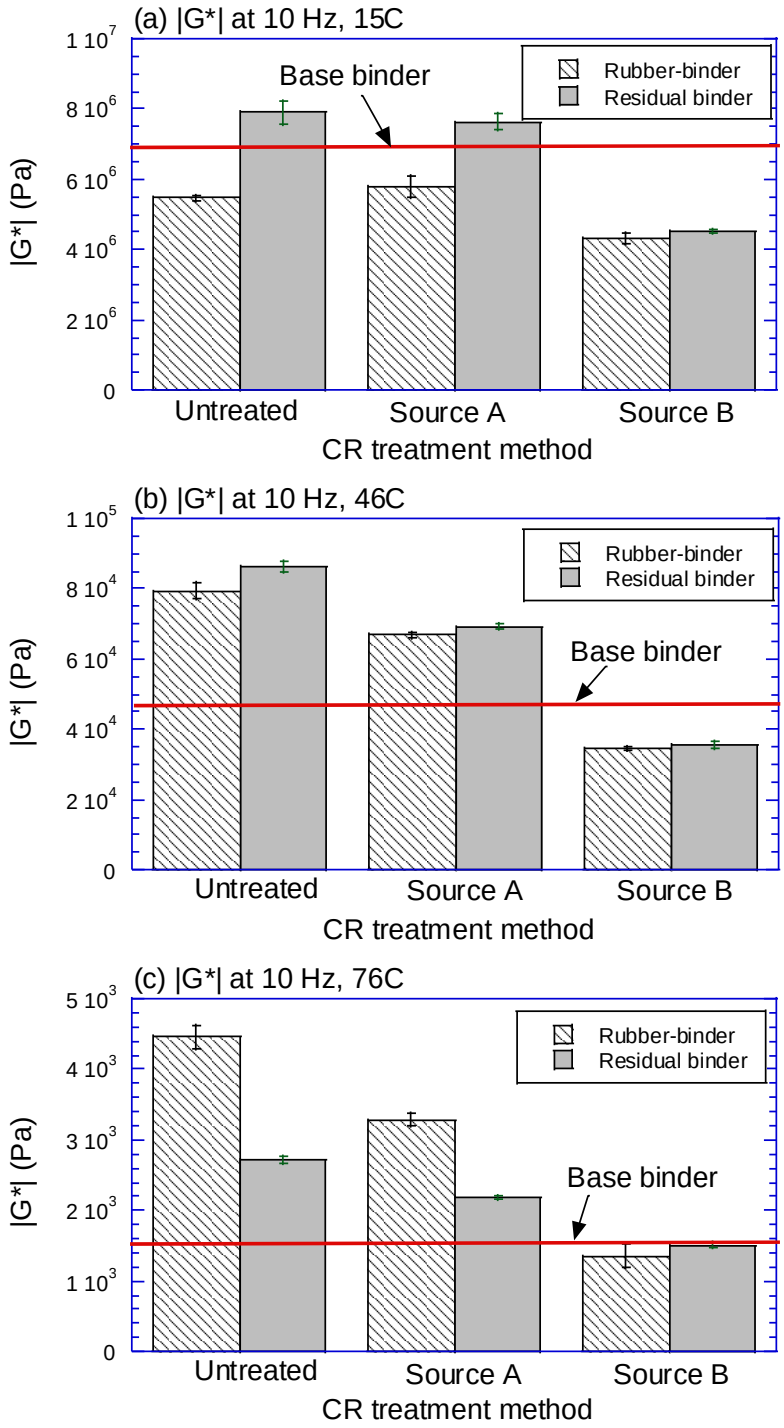

Figure 48: Effects of different CR treatment methods on asphalt-rubber interaction at (a) 15°C, (b) 46°C and (c) 76°C.

Rheological testing of CRM binders provides fundamental characterization of the material. But to capture the complete effect of pre-treatment on CRM asphalt blends, HMA mixture testing is needed to confirm the validity of the evaluation process proposed in this part of the study.

5.4 Chapter Conclusions

Based on the preceding analyses, the following conclusions are made:

- Source A pre-treated CR produced a rubberized binder with a viscosity ratio of 2.07 to that of the base binder. Such high viscosity increase indicates that either the oil used in the pre-treatment process was not suitable, or that low percentages of oil pre-treatment were used. This was also confirmed by the significant differences in |G*| for the rubberized and residual binders. The opposite was true for Source B pre-treated CR.
- Findings from the |G*| tests were consistent with the findings from the rotational viscosity measurements.
- Findings from the rheological tests suggest that incorporating pre-treated CR from Source A into the asphalt mixture in a manner similar to that of the dry process may not provide the anticipated benefits of CR modifiers in terms of fatigue/low temperature cracking.
- Further testing is needed on asphalt mixtures to confirm the validity of the proposed process.

CHAPTER 6. NEW RHEOLOGICAL PARAMETERS TO EVALUATE CRM BINDER PERFORMANCE

Crumb Rubber Modified (CRM) binder testing and characterization methods continue to rely on empirical tests that provide an indication of existence of modification, but do not always address fundamental engineering behavior linked to pavement performance. A better understanding of CR modification techniques within the context of performance-based specifications on asphalt binders will encourage the overall adoption of CRM material in paving applications. This study produced a new analysis methodology for evaluating performance characteristics in CRM binders based on the temperature when the rubber and binder stiffnesses coincide. A new rheological parameter *"Crossover Temperature"* has been introduced, based on the stiffnesses of CRM binder and residual binder (rubber filtered out after interaction). This new parameter provided strong correlations to CRM binder fatigue and rutting characteristics, without the need for micromechanical modeling or advanced testing/characterization techniques. This new parameter is recommended for Quality Control screening of CRM binders. During development of the parameter, a wide range of base asphalt binder Performance Grades, and CR sizes were utilized.

6.1 Introduction

As mentioned in Chapter 2, the most successful method of incorporating CR into asphalt paving mixtures is the wet process, where CR is used as an asphalt binder modifier and is added to the asphalt liquid and is blended at elevated temperatures (160-220 °C). Despite the proven success of this technology on the mixture level, CRM binder testing and characterization continues to rely on empirical tests (mainly viscosity and penetration) that can indicate modification, but do not address fundamental engineering behavior relating to pavement performance (Heitzman 1992,

Epps 1994, Lougheed and Papagiannakis 1996, and Jones et al. 2017). A better understanding of CR modification techniques relative to performance-based specifications on asphalt binders will encourage the overall adoption of CRM material in paving applications.

Several fundamental rheological tests demonstrating correlation to field performance have been developed to evaluate rheological properties of asphalt binders in the Dynamic Shear Rheometer (DSR). In addition, alternatives to DSR test methods that can provide strong relationships to CRM binder behavior (as influenced by different material variables) are of high value to the industry. For this, an experimental approach was undertaken to evaluate rheological behavior, including performance characteristics of CRM binders produced using a wide range of material variables. Material variable included two different CR mesh sizes, and three base asphalt binders covering a wide range of Superpave Performance Grade (PG) binders. Performance tests included Linear Amplitude Sweep (LAS) to evaluate fatigue resistance (AASHTO TP 101-12 2016), and Multiple Stress Creep Recovery (MSCR) to evaluate rutting characteristics (AASHTO T 350-14 2014). The DSR parallel plate testing geometry was utilized for all rheological tests, with a modified geometry utilizing a 2.0 mm gap height for both low and high-test temperatures (Bahia and Davies 1994, Tayebali et al. 1997, Putman et al. 2005, and Jamrah et al. 2015). In addition, alternative parameters derived from rheological characteristics of CRM binders were evaluated as indicators of overall performance.

The objectives of this component of the study were to (i) quantify the rheological changes in CRM binders from different material variables in both unaged and short term aged conditions, (ii) evaluate the influence of CR mesh size and base asphalt binder on CRM binder performance, and (iii) establish reliable relationships between CRM binder performance and rheological

parameters derived from DSR testing for timely determination of Quality Control (QC) parameters to be adopted in the field.

6.2 Materials and Methods

6.2.1 Materials

To account for possible effects of base asphalt binder and CR size, three different binders and two CR sizes were utilized to prepare six different combinations of modified binders in the experimental portion of this study. The stiffness of base binders varied from very soft, to relatively stiff materials including PG 46-34, PG 52-28, and PG 64-22. The CR material used was a 30-mesh material produced using the ambient grinding process (Thodesen 2008). Prior to testing, the CR material was sieved and separated into two size fractions: (i) a coarse fraction passing No. 16 – retained No. 20 sieve (1.18 to 0.85mm), and (ii) a fine fraction passing No. 40 – retained No. 50 (0.42 to 0.30mm).

6.2.2 CRM Binder Blending

Base binders were blended with CR (15% by weight) by means of the wet process at 190 °C and 1,000 rpm (rotation per minute) shearing speed. Table 8 below shows CRM binder IDs as a function of blend constituents. Binder IDs will be used to reference these CRM binders throughout this section.

Recognizing that optimum CR swelling is key for superior CRM binder performance (Jamrah et al. 2015), trial blends with each binder/CR combination were blended at these controlled conditions and sampled at different time intervals to monitor the change in rheological properties dynamic shear modulus ($|G^*|$) divided by sine phase angle ($\sin\delta$) in the DSR and determine optimum mixing time (T_{opt}). Figure 49 shows rheological property development in these

blends at equi-viscous DSR testing temperatures (T_{eq}) where |G*|/sinδ equals to 1.00 kPa. Equi-viscous DSR testing temperatures for each base binder are shown below in Table 9.

Table 8: Details of CRM binder constituents.

Base Asphalt	CR Size	Binder ID
PG 46-34	#20 mesh	2046
	#50 mesh	5046
PG 52-28	#20 mesh	2052
	#50 mesh	5052
PG 64-22	#20 mesh	2064
	#50 mesh	5064

Table 9: Equi-viscous test temperatures for unaged base binders.

Base Binder	**Equi-viscous Temperature (° C)**
PG 46-34	52.4
PG 52-28	57.2
PG 64-22	67.6

As shown in Figure 49, |G*|/sinδ stabilized at 60 minutes and was used as T_{opt} in preparing the CRM binders used in the remaining experimental portion of this study. It is noted here that two unique blends were prepared for each binder/CR combination to account for material variability.

Moreover, a method similar to the "Basket Drainage Method" first utilized by Airey et al. and others (Jamrah et al. 2015, Medina and Underwood 2017) was utilized to separate swollen CR

particles from the modified binder after blending. In this method, the CRM binder composite (BAC) is transferred onto a #100 sieve and covered with an aluminum pan (to eliminate potential oxidation effects), then placed in an oven at a temperature of 150 °C and the residual (drained) (BACD) binder was collected for further testing.

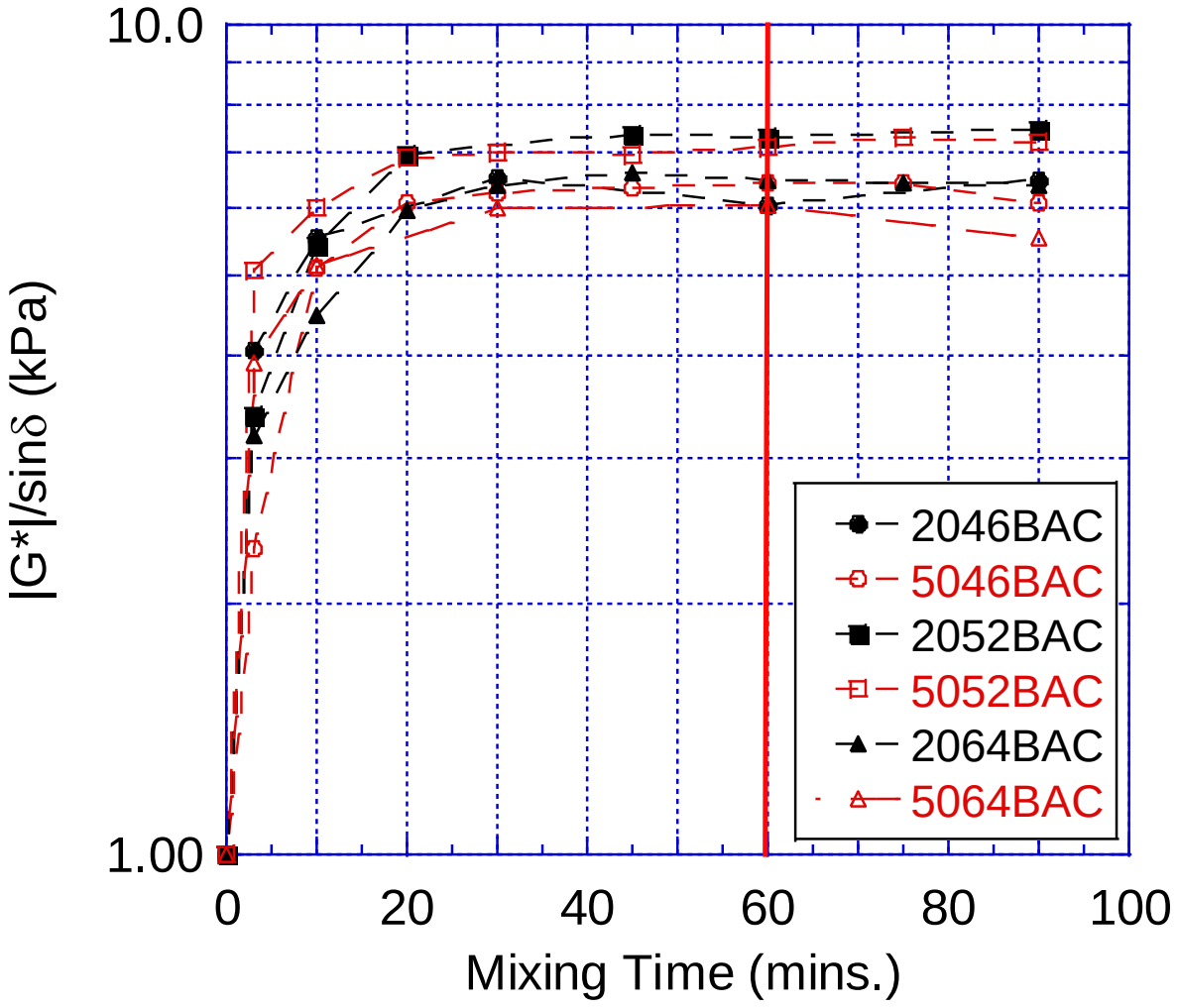

Figure 49. Rheological property development in CRM binders at equiviscous conditions.

6.2.3 Test Methods

Base asphalts and CRM binders (BAC and BACD) were tested for the dynamic shear modulus |G*| to quantify the rheological effects of CR modifier. Additionally, all CRM binders were tested for fatigue resistance by means of the Linear Amplitude Sweep test, and rutting

characteristics as indicated by the Multiple Stress Creep and Recovery test. A test matrix describing CRM binder preparation and rheological testing is summarized in Figure 50. DSR Temperature/Frequency Sweep Testing

An Anton Paar MCR 302 Dynamic Shear Rheometer (DSR) was used for all rheological tests performed in this study. Strain controlled frequency sweep tests were conducted on CRM binders, including BAC and BACD materials. Testing was conducted in accordance with AASHTO T 315 (AASHTO T 315 2014) at 10% strain level for two test replicates of each CRM binder. A third replicate was tested for CRM binders that showed variability outside of the single operator precision defined by the test method. Data collected included $|G^*|$ and δ at 15, 30, 46, 58, 70, and 82 °C for eleven frequencies ranging from 1.0 to 100.0 rad/sec. A 2.0 mm gap height was used with 8 mm test plates at 15 and 30 °C. Similarly, a modified gap height of 2.0 mm was used in all 25 mm high temperature tests to accommodate CR particulates in BAC materials.

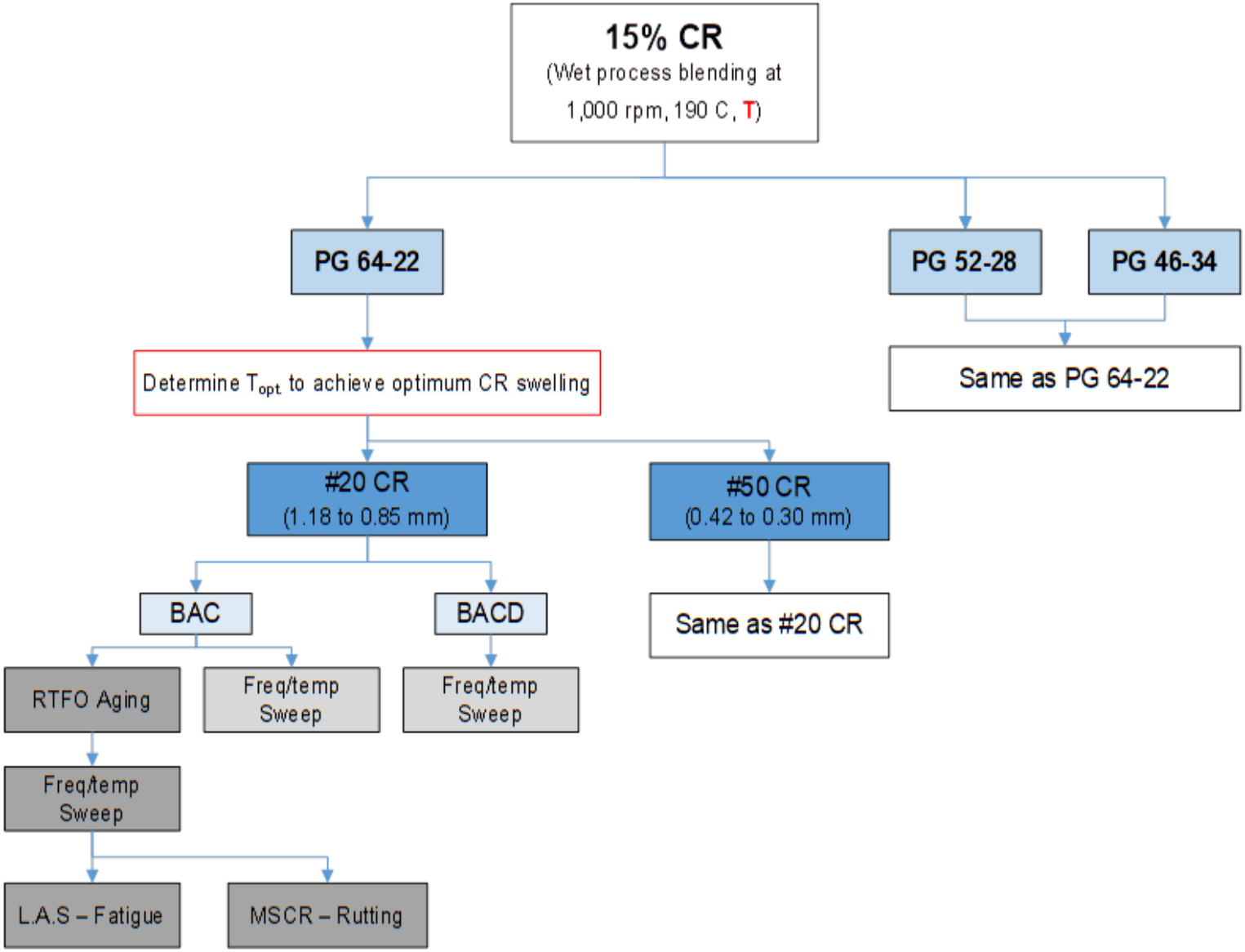

Figure 50: Test matrix for CRM binders used in this study

To combine the effects of frequency and temperature on |G*|, master curves were generated from the collected data using the time-temperature superposition (TTS) principle (Kim 2009). This was achieved by horizontally shifting measured data for each frequency until a good |G*| sigmoid fit was obtained. The same equations described in Chapter 3 were used in this portion of the study.

6.2.4 Fatigue Characterization in LAS

The Linear Amplitude Sweep (LAS) test was utilized in this study as a measure of fatigue cracking resistance in the DSR under cyclic loading with increasing shear strain amplitudes (Hintz et al. 2011). The first portion of the test consists of a frequency sweep to determine undamaged material properties as quantified by an "α" parameter. This is done by applying a 0.1% strain level over a range of 12 frequencies (from 0.2 to 30 Hz). The second portion of the test is a linearly increasing strain amplitude (from 0.1 to 30%) at 10 Hz. Peak shear strain and stress, as well as phase angle and |G*| are recorded at 1 second intervals (AASHTO TP 101 2016). This test is conducted on CRM binders after short-term ageing in the Rolling Thin Film Oven (RTFO) and utilizes the 8 mm DSR parallel plate geometry with 2.0 mm gap height at intermediate test temperatures. Once the data is collected, Viscoelastic Continuum Damage (VECD) theory is used to determine Number of cycles to Failure (N_f) for a given strain level, frequency and temperature. In this study, equi-viscous intermediate temperatures in RTFO aged conditions, as determined by |G*| master curves were used. Two replicates of each binder were used to generate the data, with a third replicate utilized when the initial two samples are outside of acceptable Single Operator Precision.

6.2.5 Rutting Characterization in MSCR

MSCR test was conducted according to AASHTO T 350-14 specification at the high Superpave PG temperature on RTFO aged CRM binders to evaluate rutting properties (D'Angelo

2009). Similar to high temperature CRM binder DSR testing described in this section, a modified 2.0 mm gap in the 25 mm parallel plates was used. Binders were subjected to loading unloading cycles of 1 and 9 seconds respectively. This creep and recovery testing mode is done at two shear stress levels of 0.1 and 3.2 kPa. The resulting shear strain is recorded and used to evaluate rutting characteristics as indicated by elastic response (%Recovery) and stress dependency (J_{nr}) in these asphalt binders. Details on calculating these parameters are included (AASHTO T 350-14). Testing was completed on RTFO aged samples at high PG equi-viscous temperature conditions. Two replicates of each binder were used to generate the data, and a third replicate was utilized when the initial two samples are outside of acceptable Single Operator Precision.

6.3 Estimation of the Modulus of the Swollen Rubber within the CRM Binder

Several micromechanical models have been successfully utilized by researchers (Paul 1960, Shu 2007, and Medina and Underwood 2017) to characterize properties of composite materials based on volume fractions and properties of the essential constituents. Applications of such models to CRM binders to estimate swollen rubber modulus are published in the literature (Jamrah et al. 2015) and have shown that this parameter is indicative of overall CRM binder performance. This study utilizes a rearranged formulation of the Shu model (Shu 2007) referenced in Chapter 4 to obtain effective moduli of swollen CR particles within CRM binders.

6.4 Results and Discussion

6.4.1 CR Effect on Base Asphalt

Figure 51 shows the stiffening and softening effects of CR on base asphalt rheology for the three binders modified in this study. As shown, CRM binders produced with either CR size are significantly softer than the base asphalt at high reduced frequencies; corresponding to low

temperatures and are stiffer than the base binder at low reduced frequency; corresponding to high temperatures. This is true for all base binders evaluated in this study and is a desired behavior. In the reaction process with asphalt at elevated temperature, CR swelled enough to make the overall CRM binder soft and crack resistant at low temperatures, and stiffer than the base asphalt for desired improvements in rutting resistance. Moreover, it is observed from the data presented in Figure 51a that CR has the most significant softening/stiffening effects on PG 46-34 base binder. This is caused by higher level of absorption/diffusion of light asphalt fractions into CR, leading to a more successful modification process for both CR sizes.

To further examine CR effects on the rheology of asphalt binder, Figure 52 shows the change in |G*| as a ratio between CRM binder |G*| and base binder |G*| (at 10 rad/sec) as a function of CR size. This data highlights observations made in Figure 51 above, where the ratio is below 1.0 at low temperatures, and increase with increasing temperature; indicating the desired stiffening and softening effects of CR. It is also noted that the influence of base PG binder is more pronounced with large #20 CR mesh size. Similar to Figure 52, Figure 53 shows the influence of CR size on base binder rheology at 10 rad/sec. Overall, it is observed that the influence of CR size is more pronounced in softer base binder (e.g. PG 46-34 vs. PG 64-22).

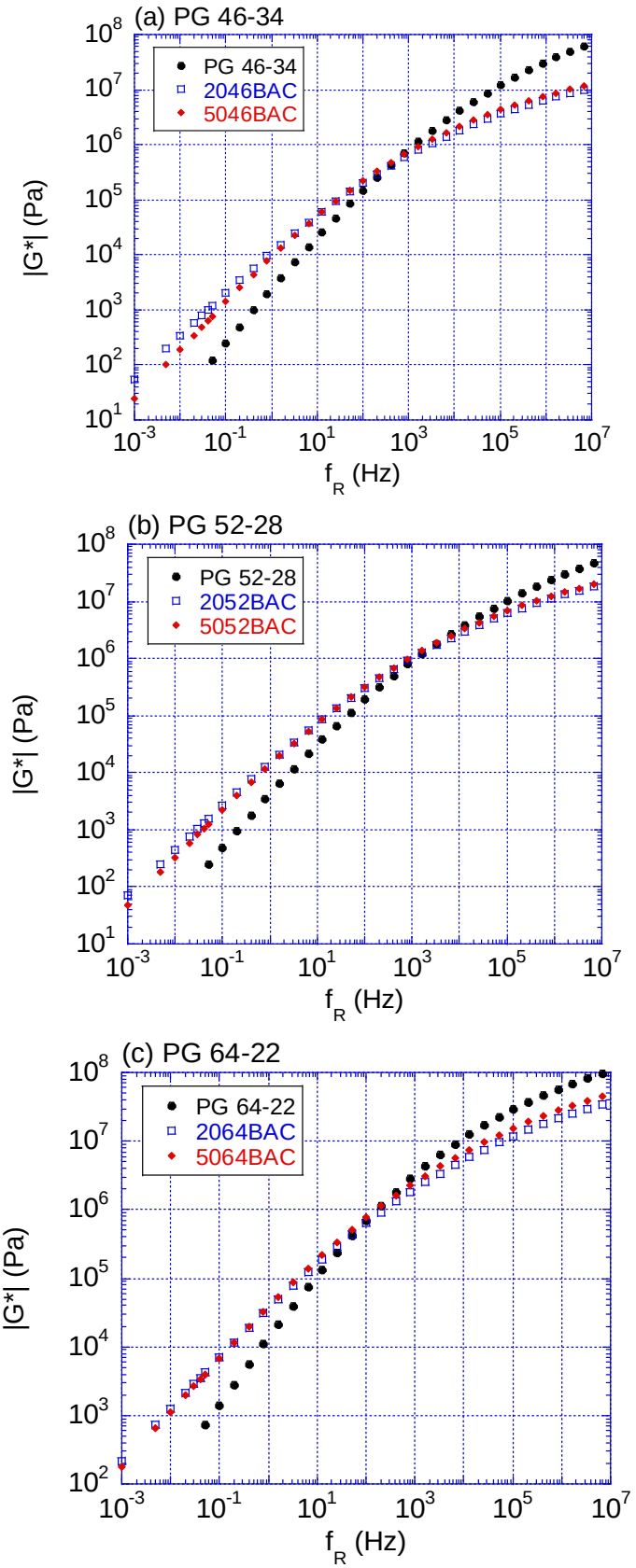

Figure 51. Stiffening/softening effects of CR on base asphalts.

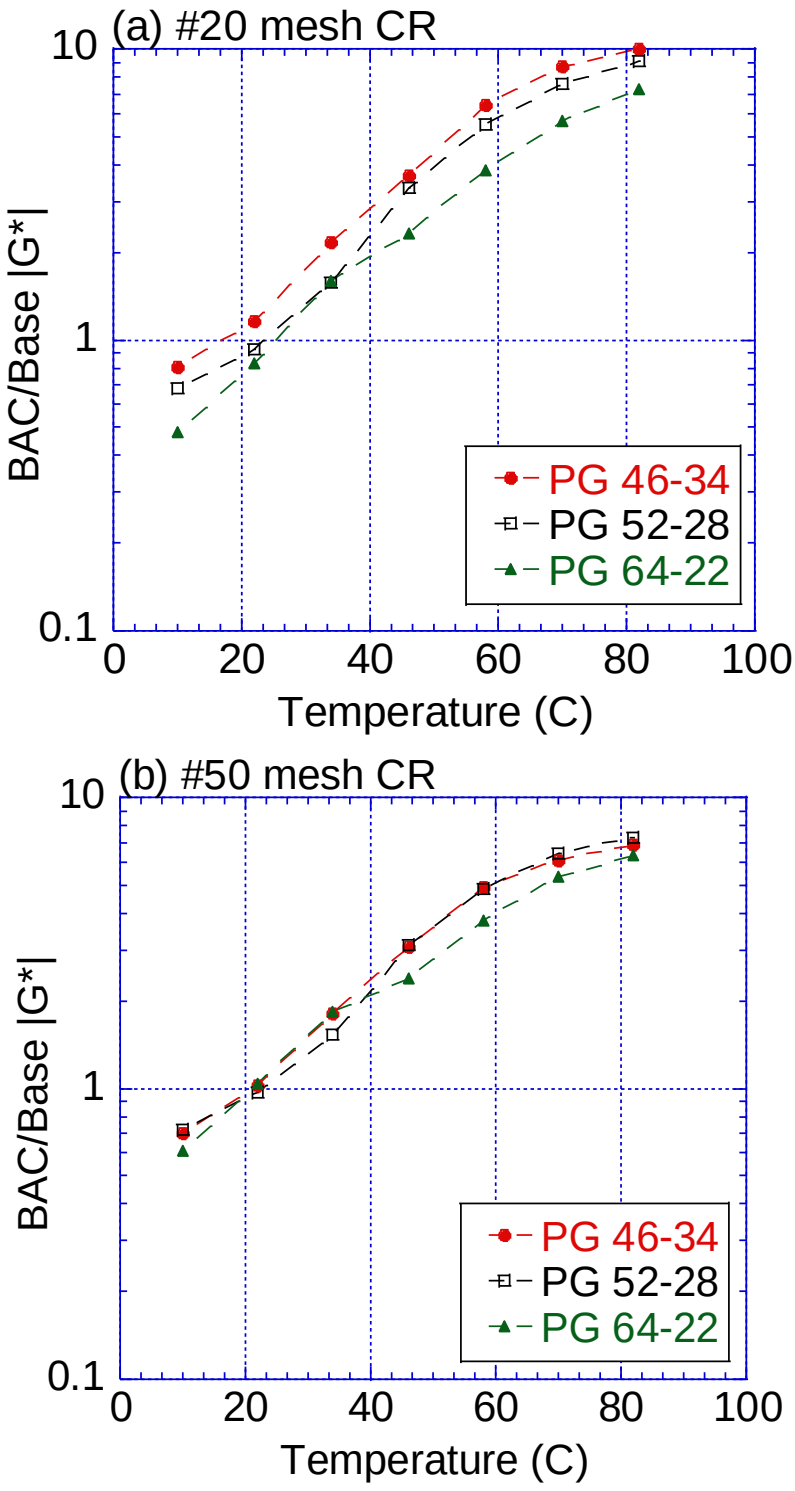

Figure 52. Change in base binder |G*| for (a) #20 mesh, and (b) #50 mesh CR.

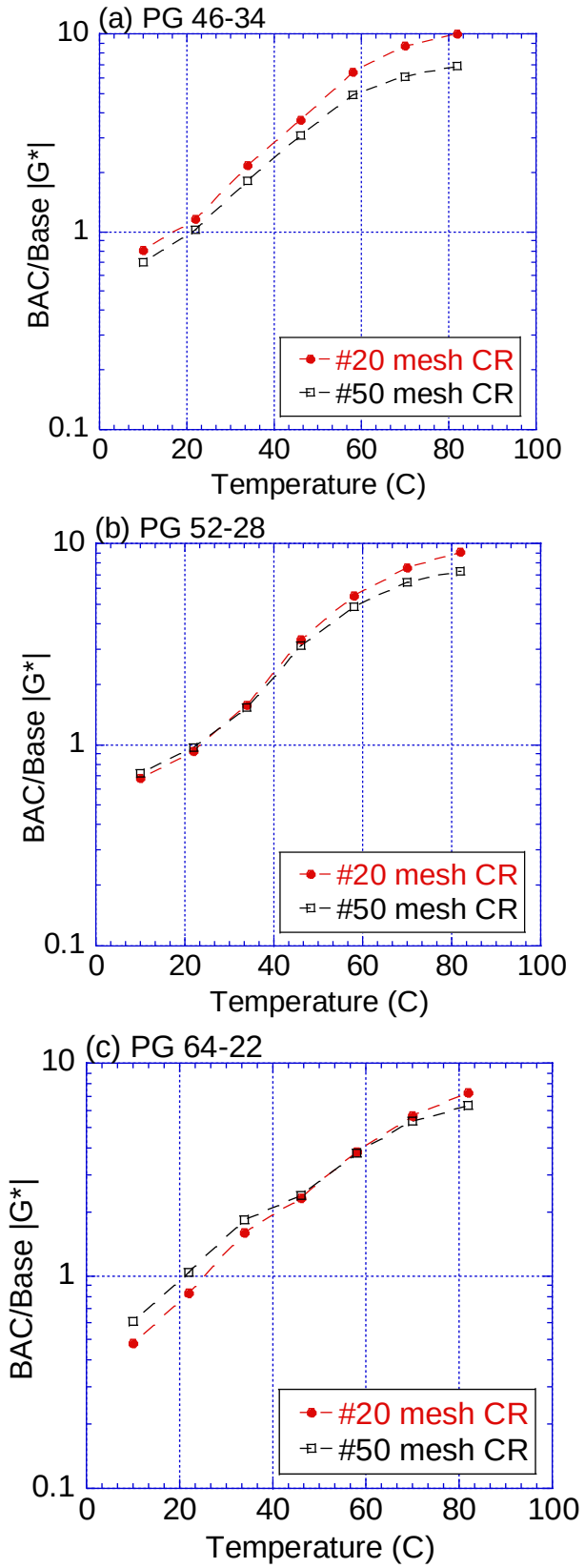

Figure 53. Change in base binder |G*| for (a) PG 46-34, (b) PG 52-28, and (c) PG 64-22.

6.4.2 CRM Binder Aging

Figure 54 shows the changes in CRM binder rheology after short term aging in the RTFO, relative to base binder rheology. It is observed from this figure that the desired stiffening/softening effects are consistently present in all base binders, but with slight changes to the trends observed for the unaged rheology (Figure 51). Better softening effects were observed in PG 52-28 and PG 64-22 CRM at low temperatures, while the best stiffening effect was seen in PG 46-34 at high temperatures.

To further examine rheological changes in RTFO aged binders, Figure 55 shows the change in RTFO aged base binder |G*| (at 10 rad/sec) as a function of CR size. The influence of base PG binder is more pronounced with large #20 CR mesh size. In addition, better softening effects are achieved in softer base binders (PG 46-34 and PG 52-28), while better stiffening effects are achieved with the larger #20 mesh CR. Figure 56 shows the influence of CR size on each RTFO aged base binder at 10 rad/sec. Overall, CR size effect becomes more significant with increasing DSR test temperatures; where the larger CR mesh size leads to better stiffening effects. In addition, the two CR sizes have a similar effect on low temperature properties in both PG 52-28 and PG 64-22, whereas #50 mesh CR has a much more pronounced softening effect in PG 46-34.

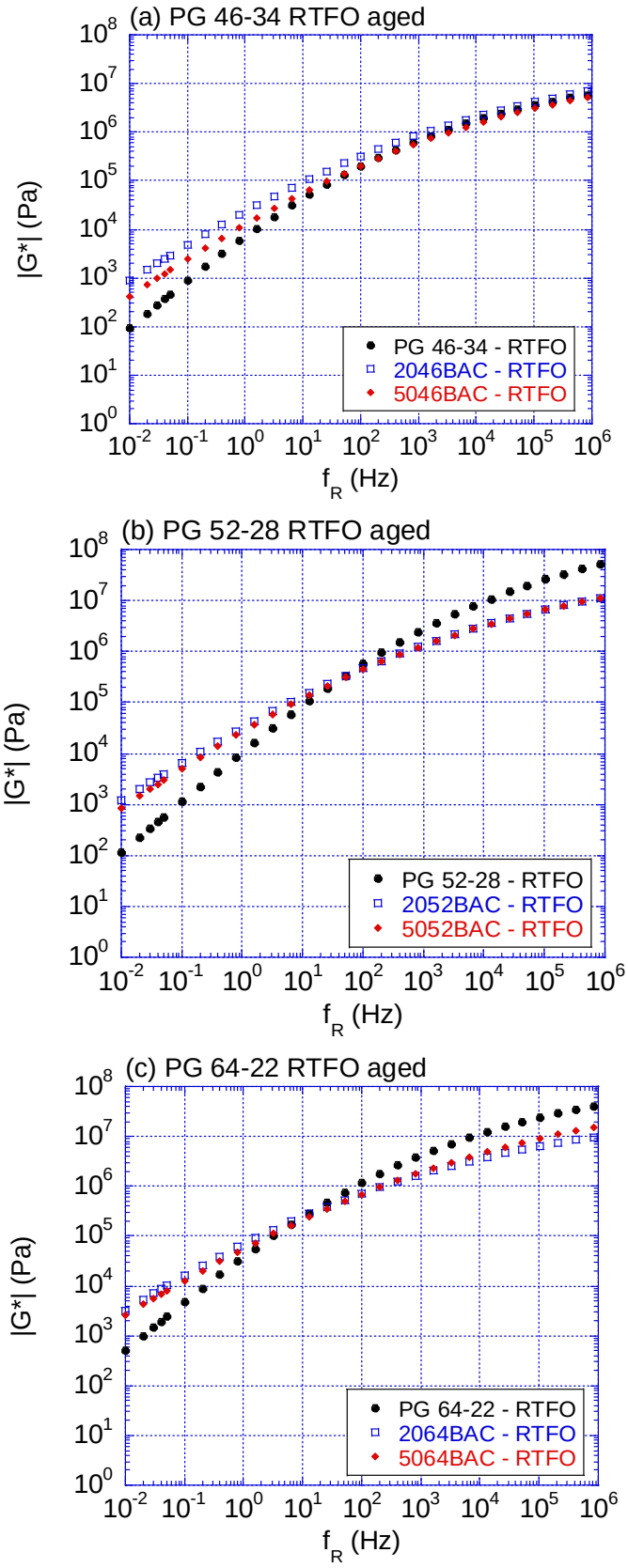

Figure 54. Changes in CRM binder rheology after RTFO aging.

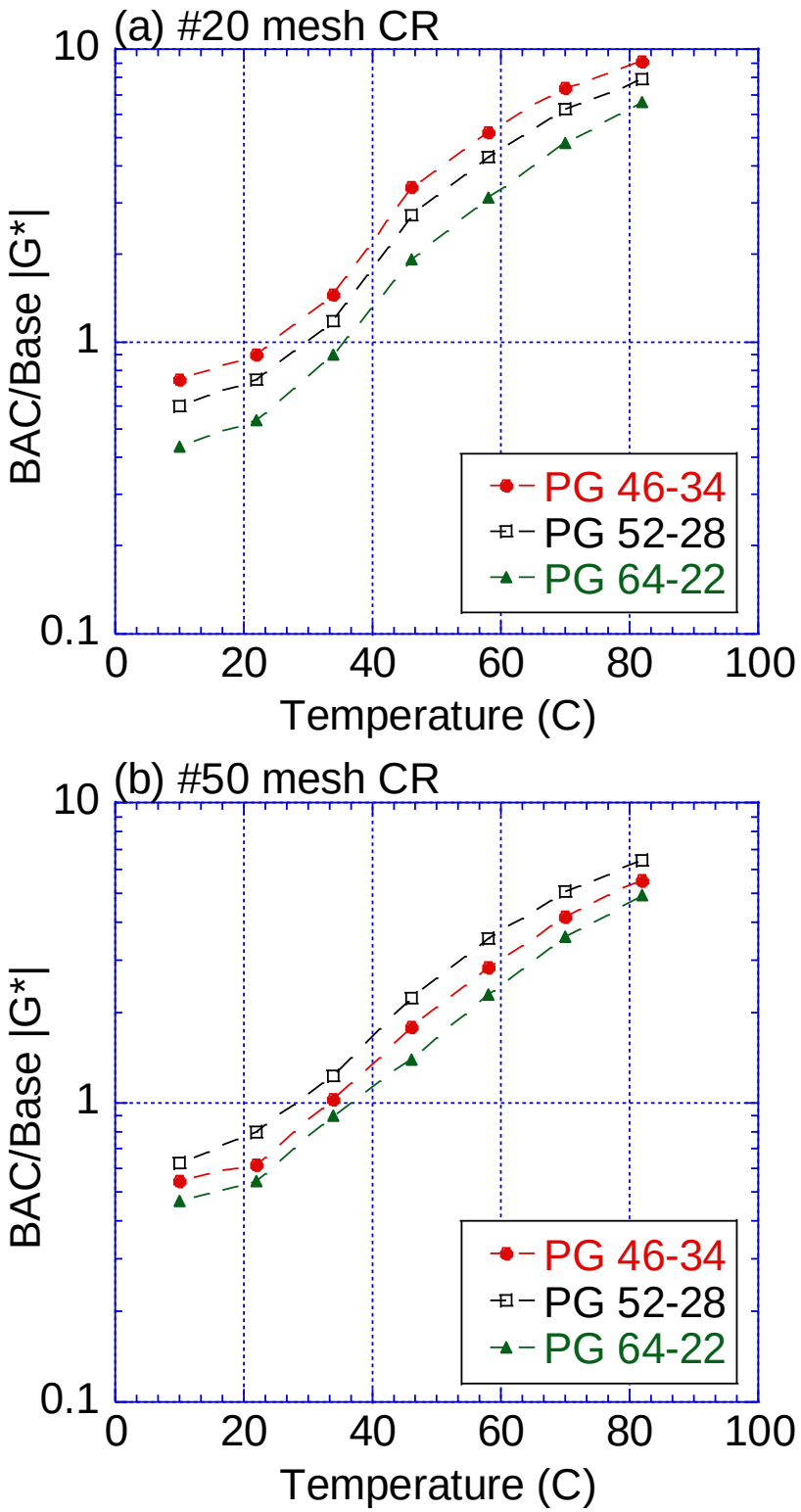

Figure 55. Change in RTFO aged base binder |G*| for (a) #20 mesh, and (b) #50 mesh CR.

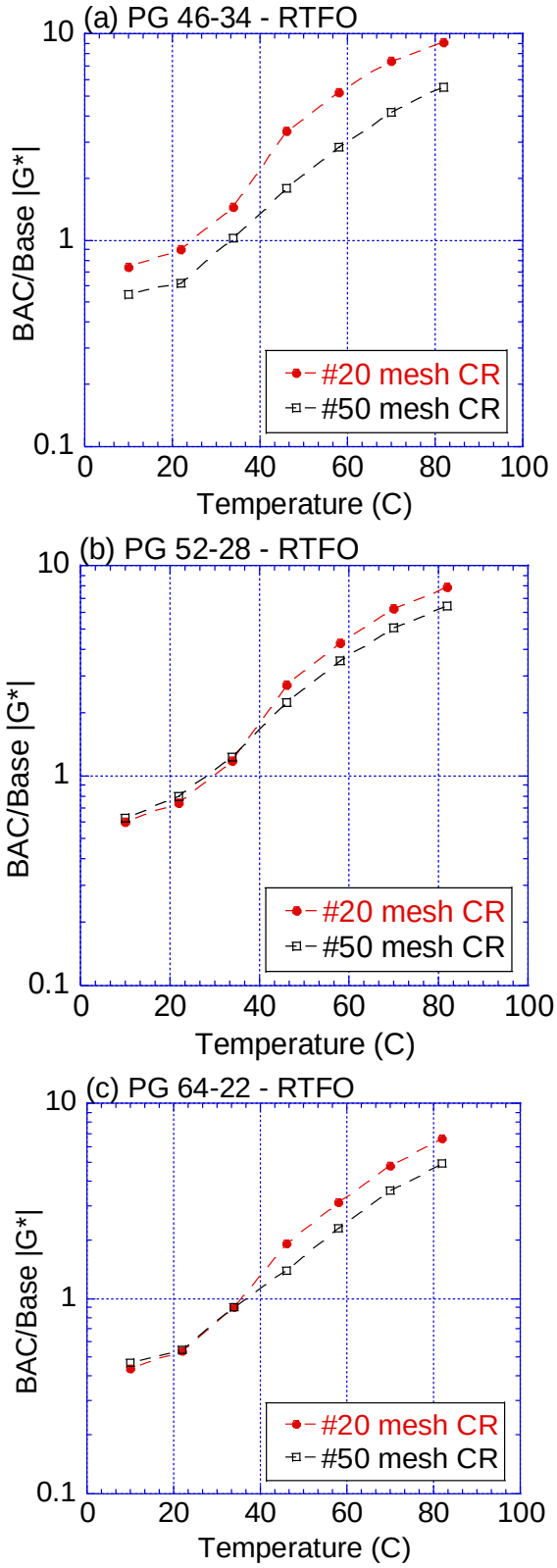

Figure 56. Change in RTFO aged base binder |G*| for (a) PG 46-34, (b) PG 52-28, and (c) PG 64-22.

6.4.3 *Back-Calculated G*$^*_r$*

Shu model described in (Equation 5 to 7) was utilized to back-calculate the moduli of the swollen CR particles G^*_r within the CRM binder composite. Figure 57 shows master curves of back-calculated G^*_r for the different CRM binders. These master curves clearly demonstrate the viscoelastic behavior of CR after interaction with asphalt binder at elevated temperatures (Jamrah et al. 2015). A major observation that can be made from this data is the high similarity between the various Gr master curves. Overall, G^*_r master curves were within 8 to 12% of each other. The wide stiffness variation in base binders used in this study was selected such that a clear variation in G^*_r can be observed. However, to back-calculate G^*_r using the Shu model, the volumetric percentage of CR in each CRM binder is needed (Equation 7). This value was assumed equal in all base binders used in this study at 45% (300% swelling after Dong et al. 2012). This is a major assumption, and may have hindered the reliability of these calculations, which in turn caused the high similarities in back-calculated Gr.

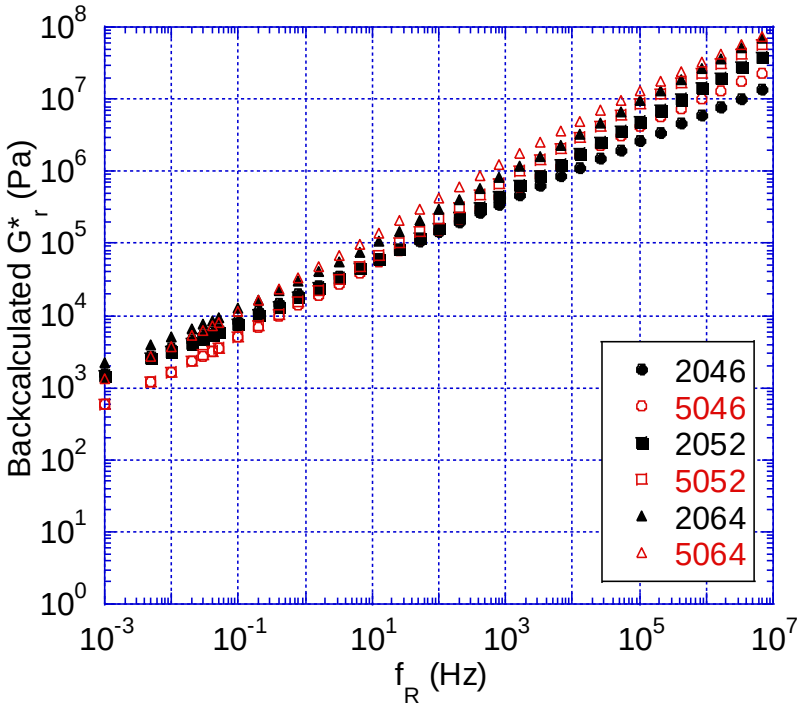

Figure 57. Back-calculated G^*_r master curves for CRM binders.

To further examine back-calculated G^*_r, comparisons were made for the different CR mesh sizes and the different base asphalt binders. Figure 58 shows G^*_r at 63 rad/sec as a function of CR size. While marginal differences were observed between all CRM binders, the influence of base PG binder is more pronounced with small #50 CR mesh size.

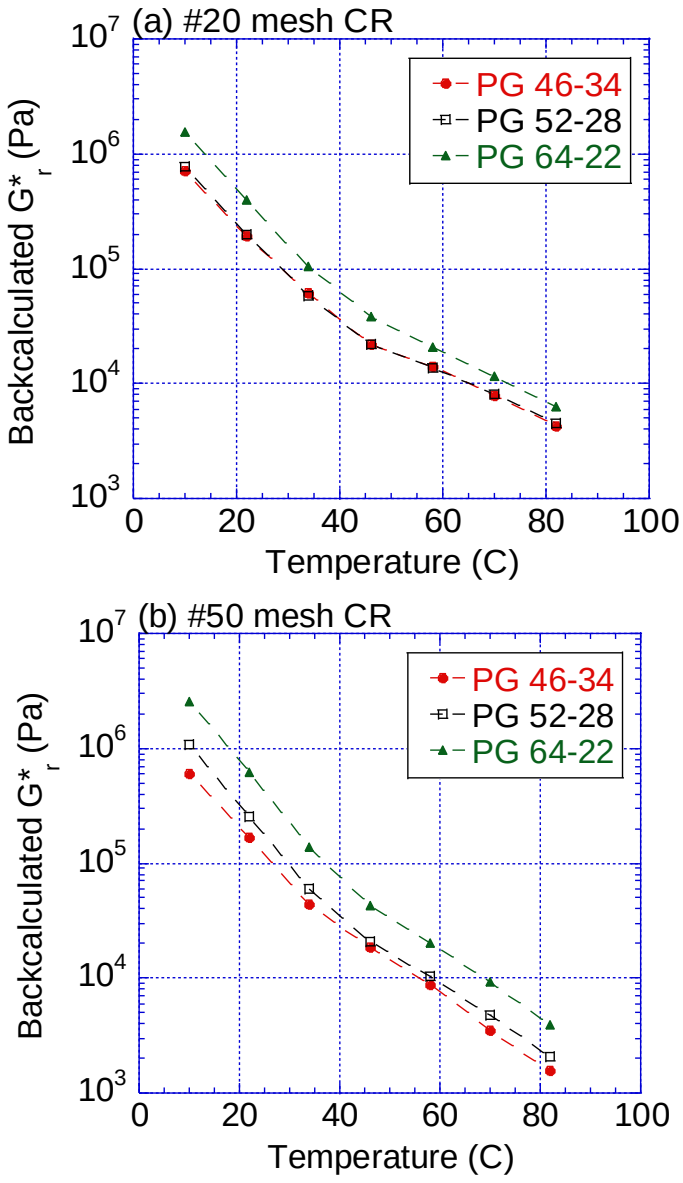

Figure 58. Back-calculated G^*_r for (a) #20 mesh, and (b) #50 mesh CR.

The softer the base asphalt (e.g. PG 46-34 and P 52-28) CRM binders consistently showed lower G^*_r stiffness in Figure 58. This indicates better success in modification, where CR particles

absorbed more light asphalt fractions and caused an overall softening effect on the rubber as indicated by a lower modulus. Figure 59 highlights similar findings as Figure 58. Overall, CR size has minimal impact on back-calculated G^*_r, with #20 mesh resulting in slightly higher values with increasing temperatures. Back-calculated G^*_r for each CRM binder shown in this section at 63 rad/sec will be correlated to performance characteristics in the next sections to identify if a strong correlation between the properties exists.

6.4.4 CRM Binder Fatigue Characteristics

LAS testing was conducted on CRM binders in RTFO aged conditions to simulate aged behavior. Testing was conducted at equi-viscous (RTFO aged) intermediate temperature conditions shown in Table 10.

Table 10: Intermediate equi-viscous test temperatures for RTFO aged binders.

Base Binder	RTFO Aged, Equi-viscous Intermediate Temperature (° C)
PG 46-34	10.0
PG 52-28	18.8
PG 64-22	23.5

Figure 60 shows LAS test results for the different CRM binders characterized in this study at 2.5 and 5.0% strain. The results clearly illustrate the improvement (increase) in fatigue life number of cycles to failure for all base binders, at both strain levels.

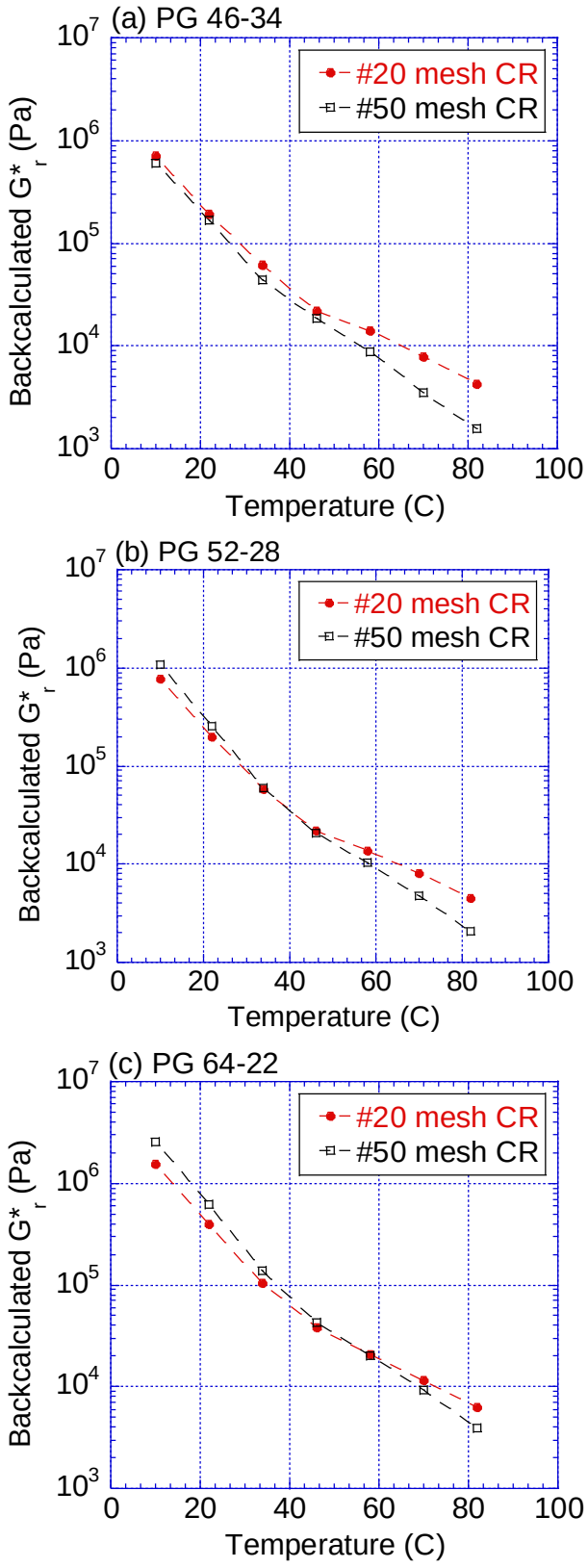

Figure 59. Back-calculated G*$_r$ for (a) PG 46-34, (b) PG 52-28, and (c) PG 64-22.

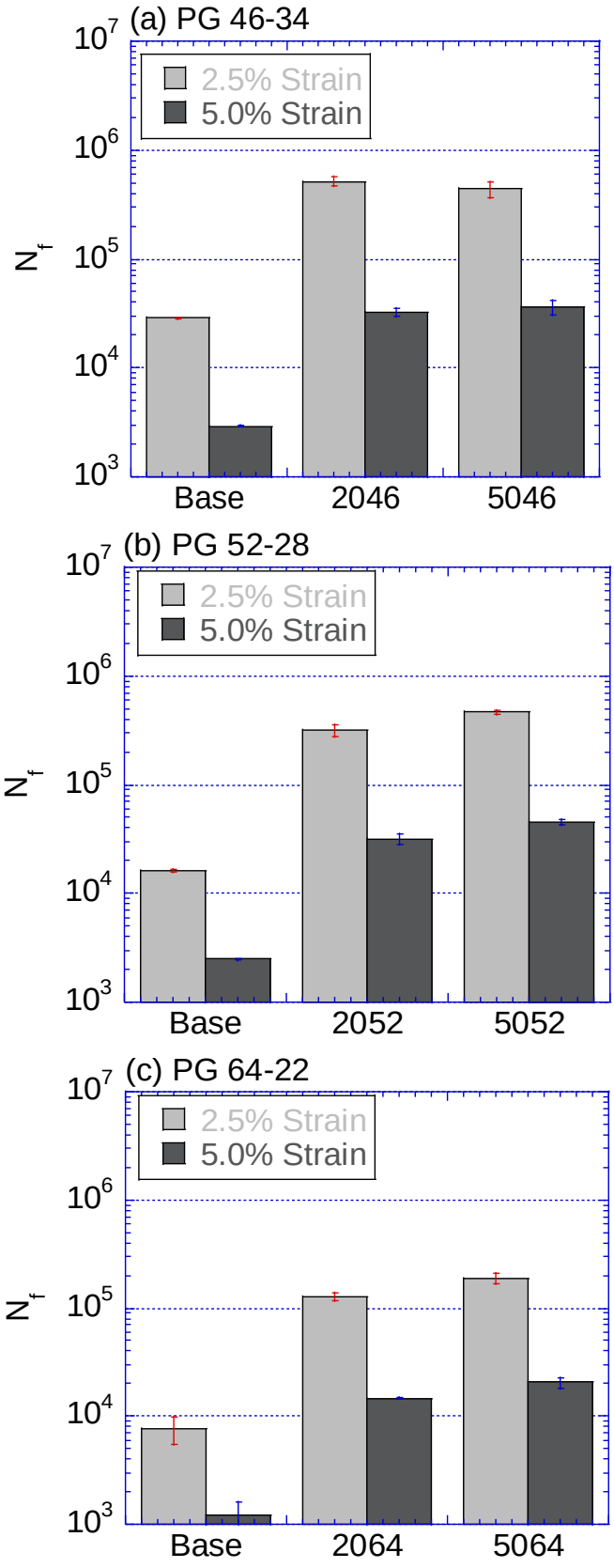

Figure 60. LAS test results grouped for base binder PG grades.

Overall, it is observed from Figure 60 that the best fatigue life is seen in soft base binders (PG 46-34 and PG 52-28). In PG 46-34 CRM, CR mesh size seemed to have a negligible effect on N_f at low strain levels. However, #50 mesh CR showed a slightly better fatigue resistance in all CRM binders. In addition, a more pronounced effect of base binder on fatigue life was observed for #20 CR. Considering that these CRM binders were tested at equi-viscous conditions, the clear differences in fatigue characteristics as the base binder stiffens (e.g. PG 46-34/PG 52-28 vs. PG 64-22) highlights the significance of base material properties on overall CRM binder fatigue behavior.

6.4.5 CRM Binder Rutting Behavior

Similar to LAS testing, MSCR tests were conducted on CRM binders in RTFO aged conditions to simulate aged behavior. Testing was conducted at equi-viscous high temperature (RTFO aged) conditions shown in Table 11.

Table 11: High equi-viscous test temperatures for RTFO aged binders

Base Binder	RTFO Aged, Equi-viscous High Temperature (° C)
PG 46-34	54.7
PG 52-28	58.7
PG 64-22	67.7

Figure 61 and Figure 62 show MSCR Nonrecoverable Creep Compliance (J_{nr}) and %Recovery at 0.1 and 3.2 kPa stress levels respectively. The results clearly illustrate the improvement in rutting characteristics for all base binders, at both stress levels. It is also noted that better rutting resistance was consistently observed in #20 CRM binders. Higher J_{nr} values in #50

CR mesh size is consistent with findings from "EVALUATING CRM BINDER RHEOLOGY IN THE DSR" section where this CR size produced softer CRM binders as compared to #20. In addition, higher J_{nr} values in PG 46-34 CRM binders are also consistent with findings from the same section where both CR sizes were reported as having a more apparent softening effect on this base material. Overall, PG 46-34 produced the highest rutting resistance with #20 CR mesh, while PG 52-28 CRM binder exhibited best characteristics with #50 CR mesh.

6.5 Relationship Between G^*_r and CRM Binder Performance

Figure 63 shows the relationship between back-calculated G^*_r and performance characteristics obtained from LAS and MSCR tests on CRM binders. While relationships seemed to improve with higher strain/stress levels, overall relationships between G^*_r and LAS Nf were found to be poor. On the other hand, significantly better relationships were found with MSCR Jnr and %Recovery. As shown in the earlier section (Figure 57 and Figure 59), this can be explained by the high similarities in back-calculated G^*_r for all CRM binders at low and intermediate temperatures. More variations in G^*_r were observed at high temperatures, leading to better statistical correlations. It is also speculated that the assumption of equal CR volumetric percentage in all CRM binders (Equation 7) in the Shu model has caused these similarities.

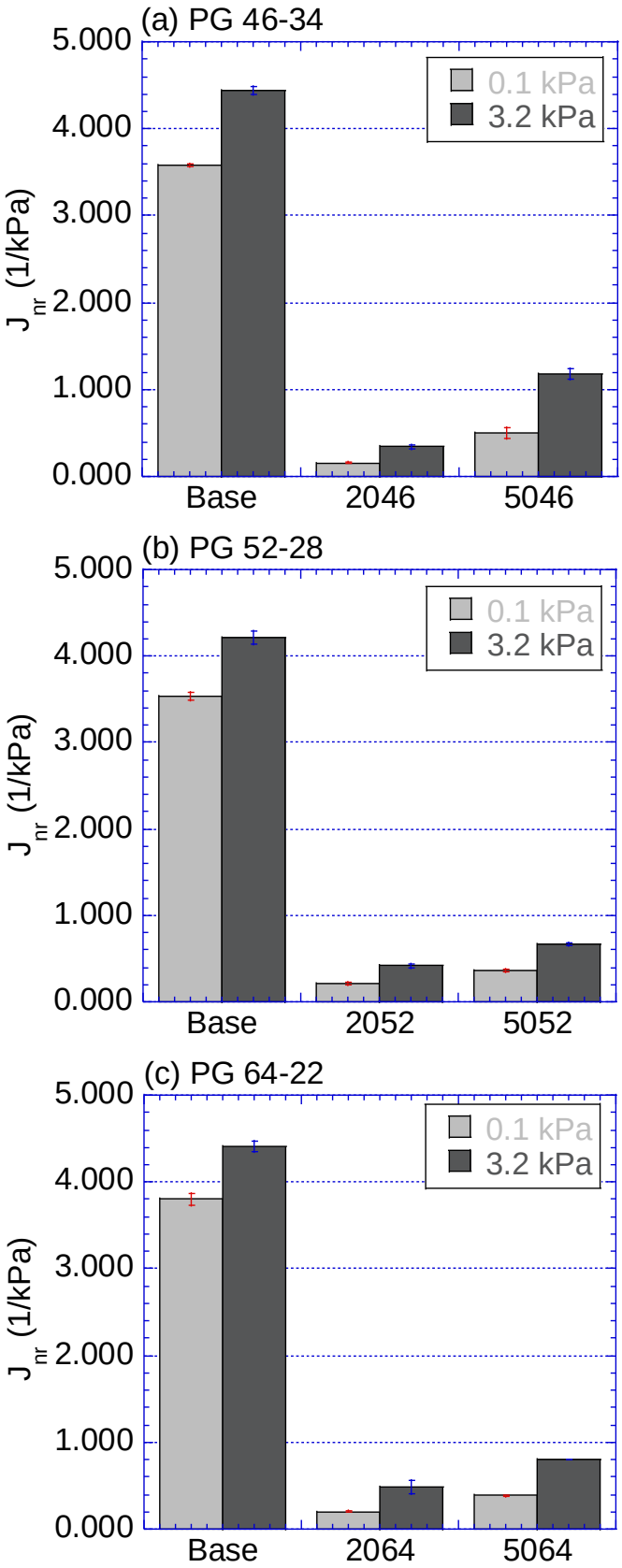

Figure 61. MSCR Nonrecoverable Creep Compliance (Jnr).

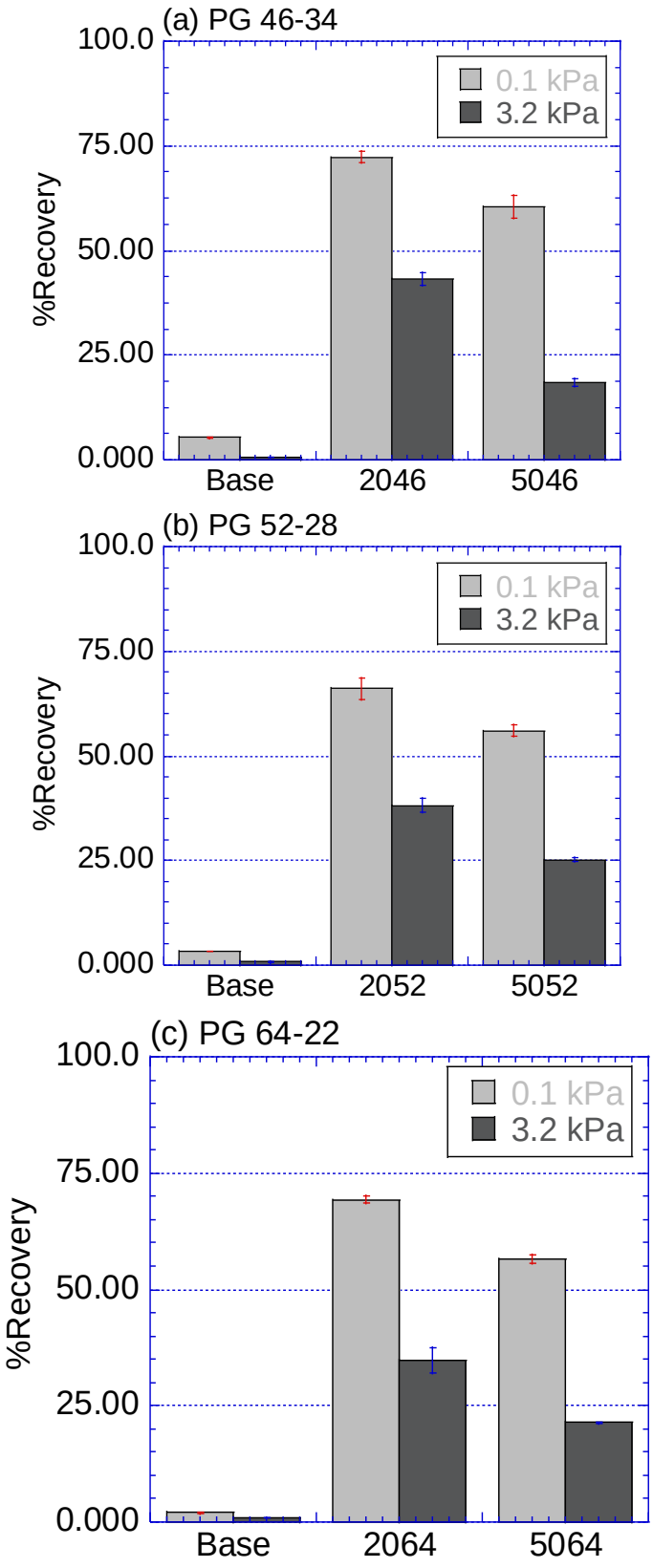

Figure 62. MSCR %Recovery.

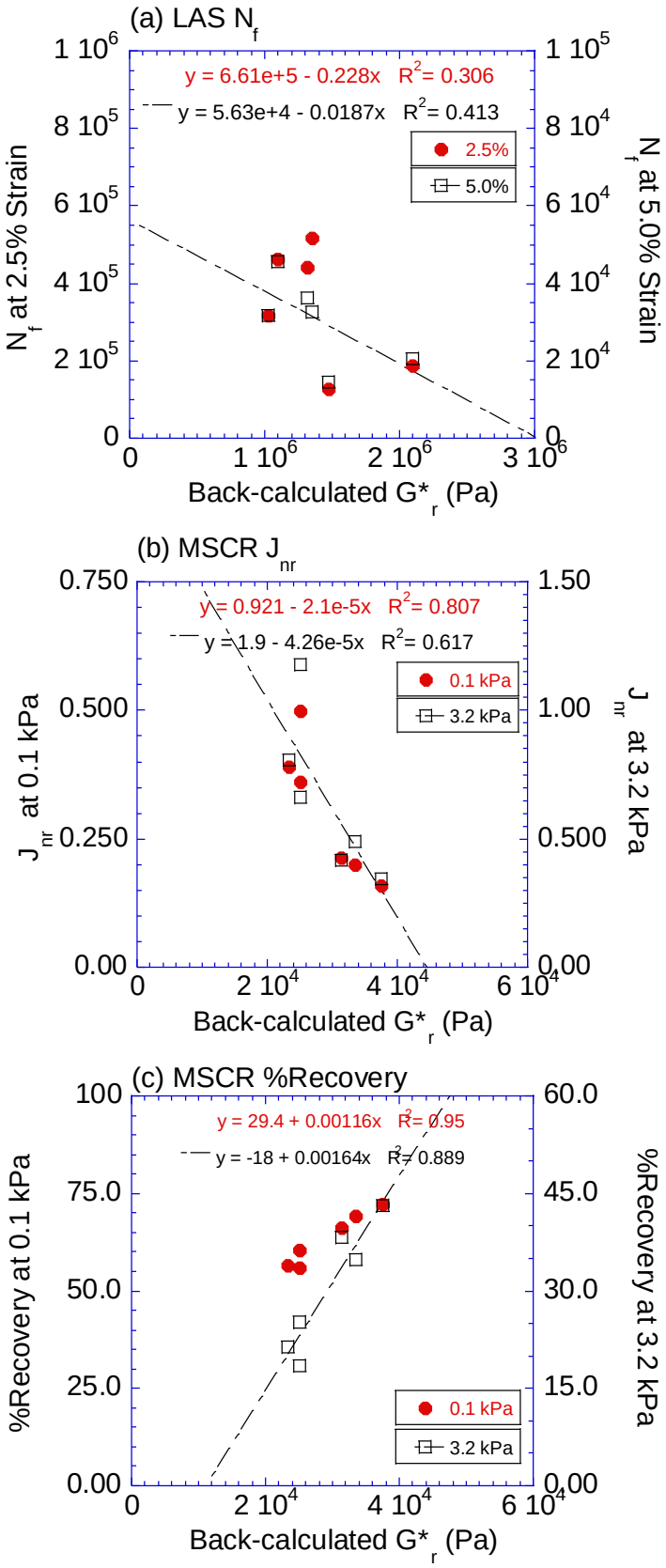

Figure 63. Relationship between G*$_r$ and (a) N$_f$, (b) J$_{nr}$, and (c) %Recovery.

6.6 CRM Binder Crossover Temperature

Due to the weak correlations between G^*_r and performance characteristics at intermediate temperatures, and in an effort to establish reliable relationships between CRM binder performance and rheological parameters derived from DSR testing; the overall behavior of CRM binders was re-evaluated in this portion of the study. An accurate performance indicator derived from rheological testing of CRM binders can be of significant value for Quality Control (QC) purposes in the field. As indicated in earlier sections, the major limitation in utilizing the Shu model was the need for volumetric percent of swollen CR particles. When this parameter was assumed equal; inaccurate and highly similar G^*_r values were derived for all CRM binders. Different techniques can measure CR swelling; with Scanning Electron Microscopy being one of them (Medina and Underwood 2017). However, this adds complexity to a process that is meant to simplify screening CRM binders for performance characteristics. Therefore, to avoid using micromechanical models, and to simplify this process; an attempt was made to evaluate CRM binder data as measured by the DSR. The investigation revealed a clear change in the temperature where the crossover between BAC (binder and CR composite) and BACD (CR filtered out) |G*| occurs. This temperature; defined as the *Crossover Temperature* is the deflection point when |G*| of BAC-CRM equals |G*| of BACD-CRM. This is demonstrated in Figure 64 and Figure 65 for all CRM binders where Crossover T increases with stiffening base asphalt binders. In addition, it is observed that Crossover T is slightly lower in #50 mesh CR size.

Unlike back-calculated G^*_r (Figure 58), Figure 66 shows the variation in Crossover T in the different base asphalt binders as a function of CR mesh size. A clear distinction is shown for each CRM binder.

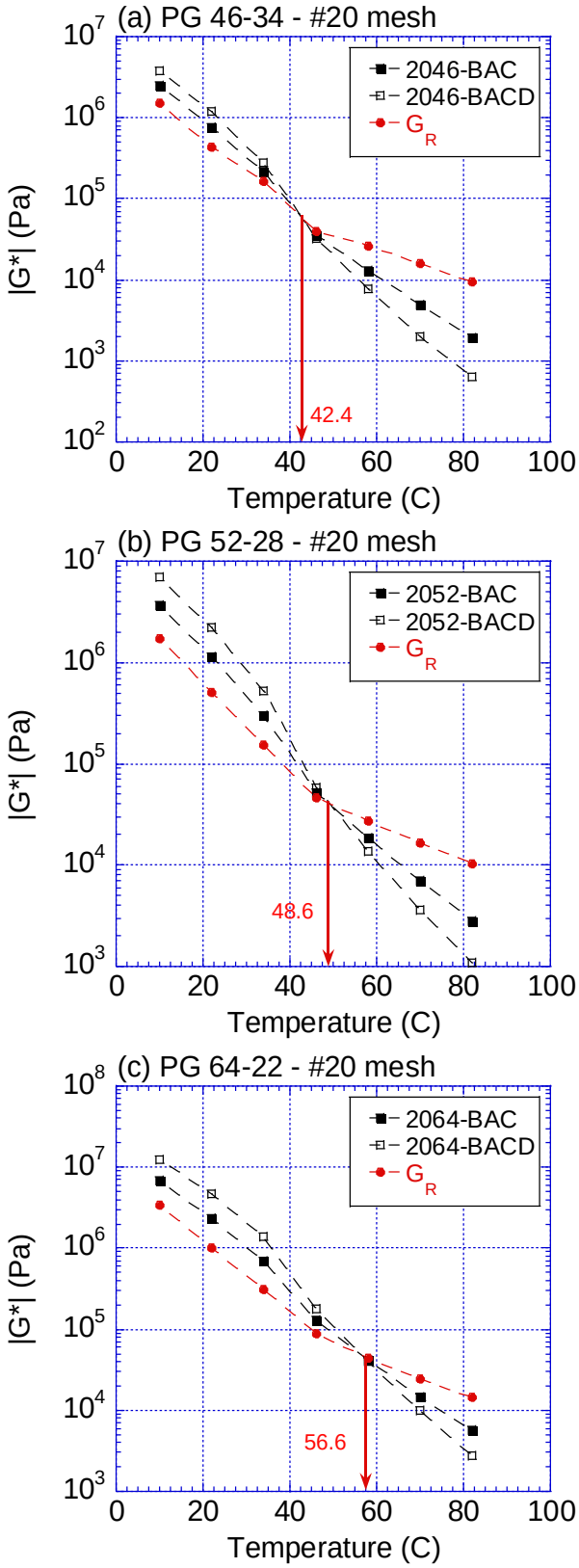

Figure 64. Crossover Temperature for #20 CRM binders.

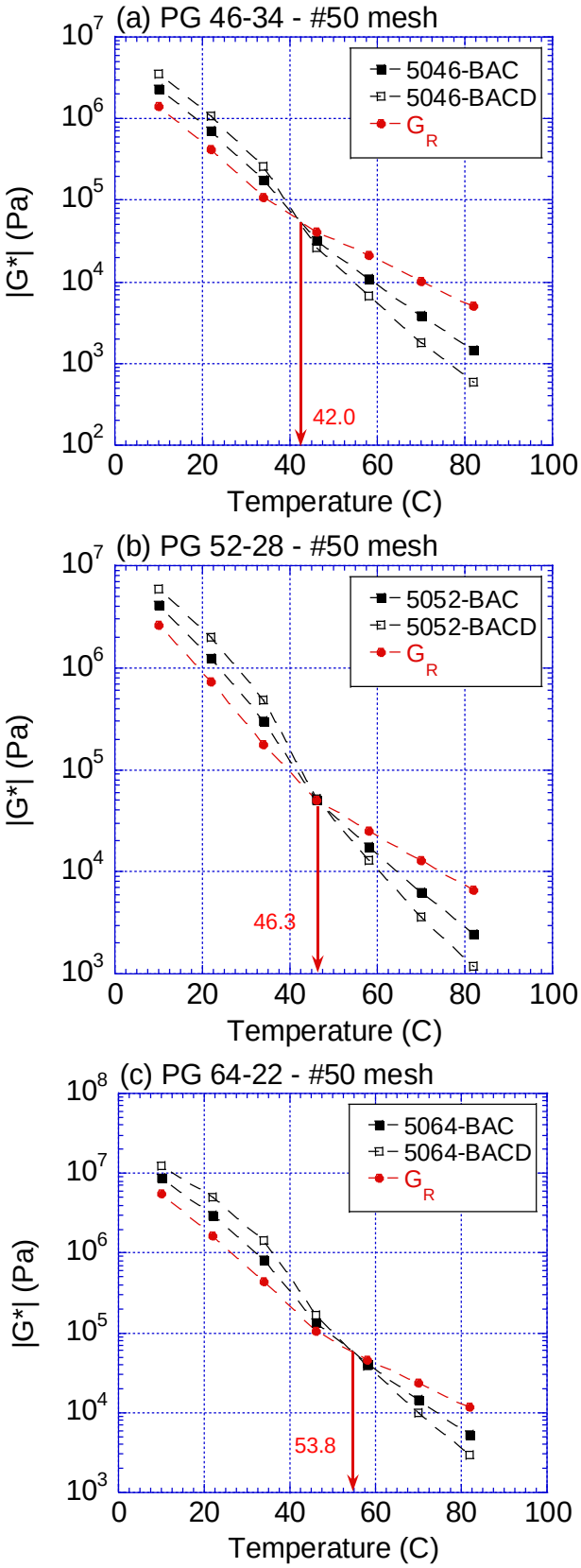

Figure 65: Crossover Temperature for #50 CRM binders.

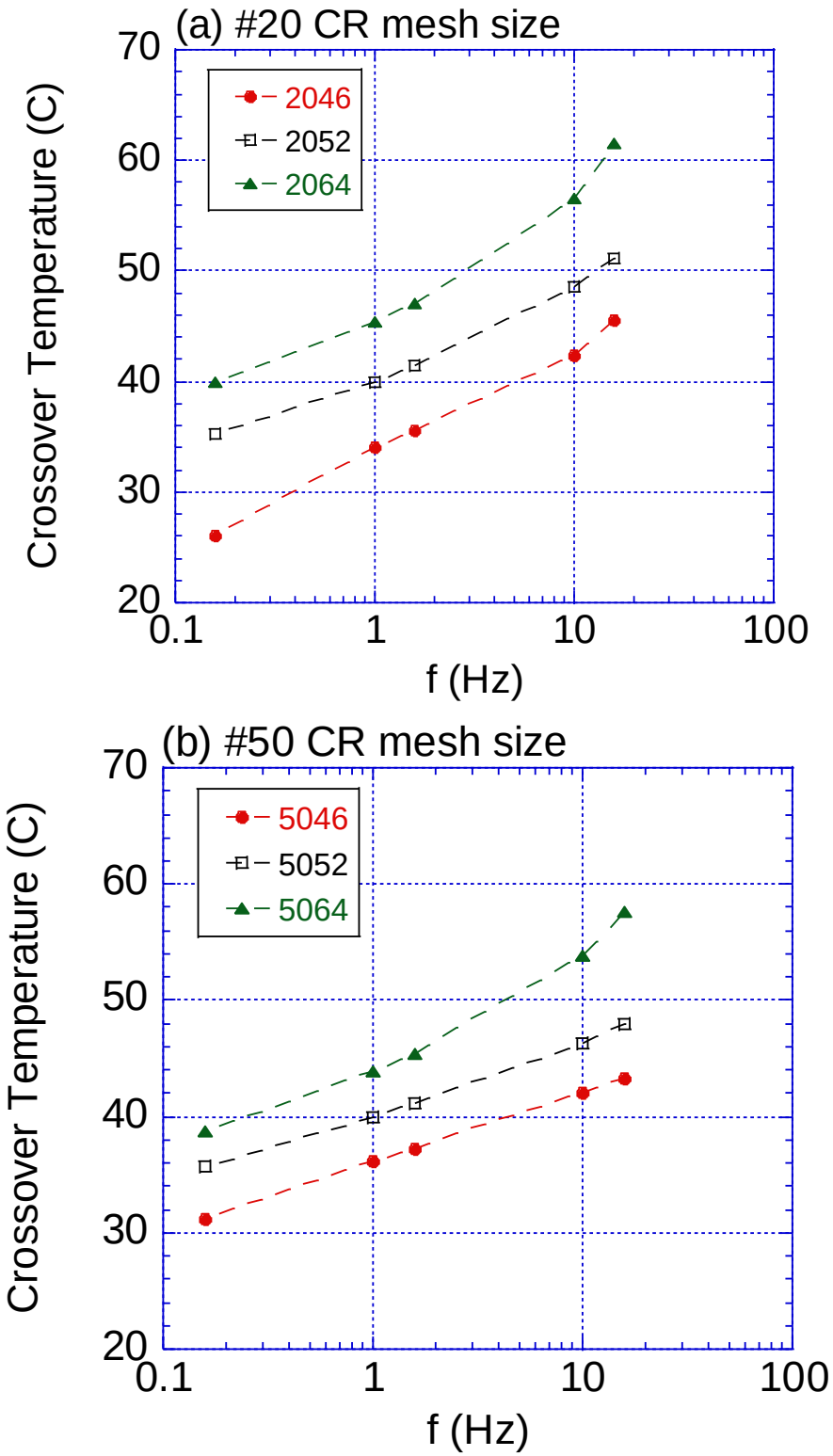

Figure 66. Variation in Crossover Temperature based on CR mesh size.

6.7 Relationship Between Crossover Temperature and Performance

In order to evaluate the best potential use of the newly proposed parameter Crossover T, the corresponding |G*| *"Crossover |G*|"* and phase angle *"Crossover δ"* at this given temperature for each CRM binder were calculated from their respective master curves. This data is shown in Figure 67. Each of these parameters was correlated to CRM binder performance, and the strongest correlations were found between Crossover T and fatigue N_f, as well as between MSCR characteristics and *Crossover δ*. These relationships are presented in Figure 68.

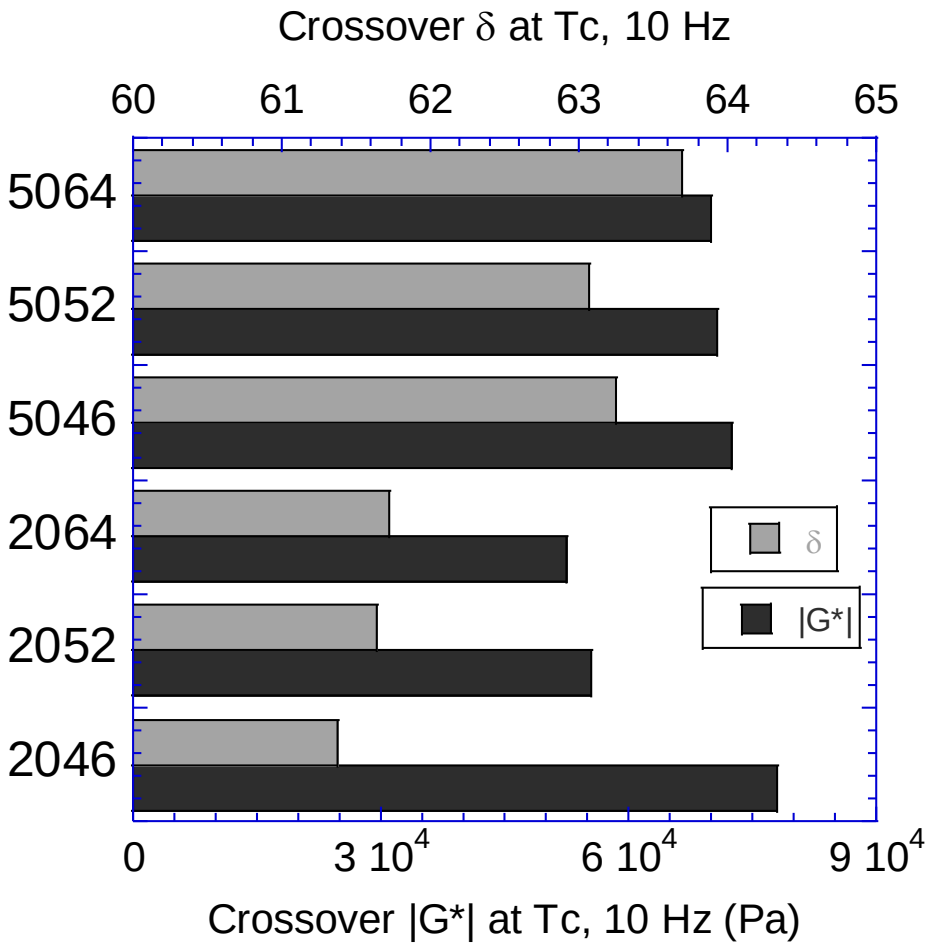

Figure 67. Crossover |G*| and δ for all CRM binders.

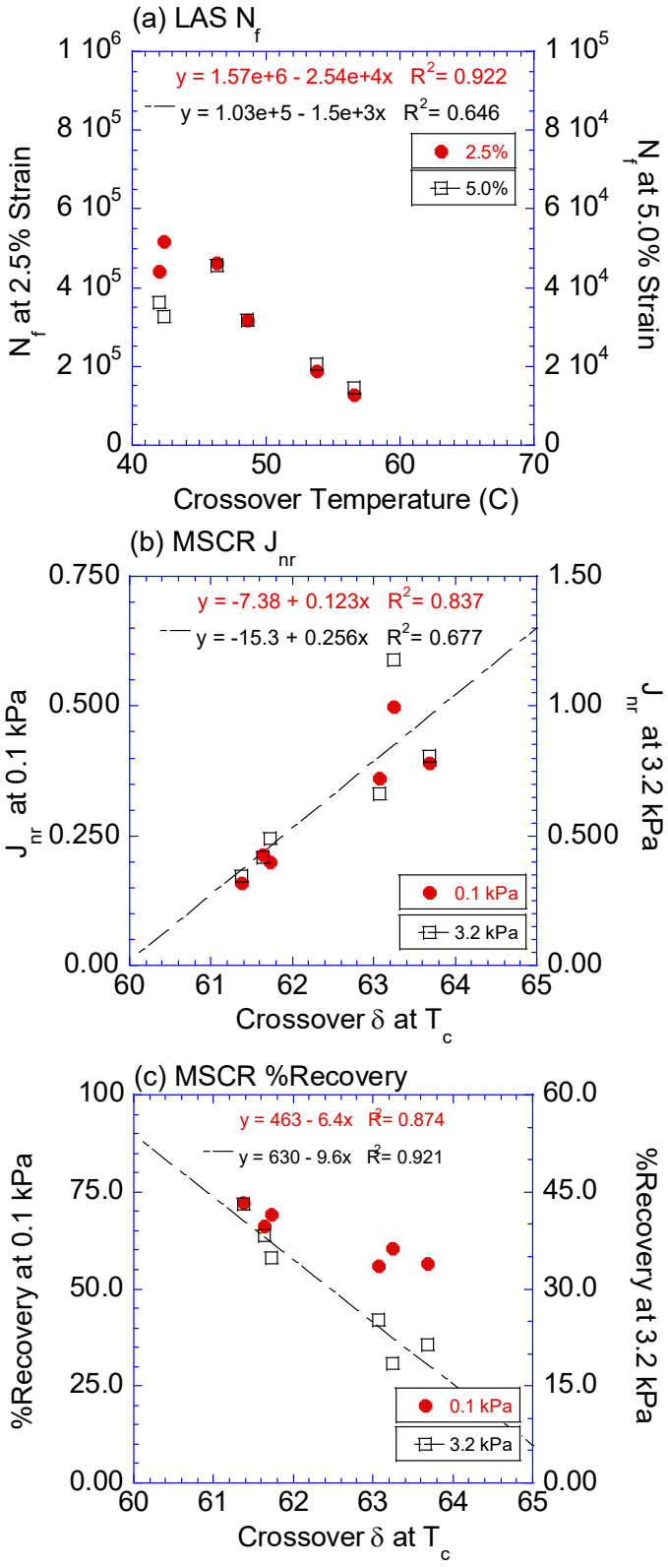

Figure 68. Relationships between (a) Crossover T and LAS N_f, and between Crossover δ and (b) MSCR J_{nr}, and (c) MSCR %Recovery

Significant improvements were observed in correlations to LAS N_f as compared to G^*_r. In addition, correlations equal to, or better than those made with G^*_r were established between rutting MSCR properties and Crossover δ.

6.8 Chapter Conclusions

The objectives of this study were addressed by an experimental approach where the rheological changes in CRM binders from different material variables in both unaged and short-term aged conditions were quantified as a function of CR mesh size and base asphalt binder PG grade. In addition, reliable relationships between linear viscoelastic CRM binder rheology and performance characteristics were established. Based on the analysis presented in this portion of the study, the following specific conclusions can be drawn:

- For unaged CRM binders, rheological changes were observed in all base binders. In addition:
  - The most significant softening/stiffening effects were seen in PG 46-34. This is caused by higher level of light asphalt fractions in this binder, leading to a more successful modification.
  - The influence of base PG binder is more pronounced with larger CR mesh size.
  - The influence of CR size is more pronounced in softer base binders.
- For RTFO aged CRM binders, desired stiffening/softening effects of CR on base asphalt were also observed.
  - Better softening effects were observed in PG 52-28 and PG 64-22, while the best stiffening effect was seen in PG 46-34.
  - The influence of base PG binder is more pronounced with larger CR mesh size.

  - Better softening effects are achieved in softer base binders, while better stiffening effects are achieved with the larger #20 mesh CR.
  - CR size effect is more significant with increasing DSR test temperatures; where larger CR size leads to better stiffening.
  - CR size effect is negligible at low temperature properties in both PG 52-28 and PG 64-22, whereas the smaller CR size caused better softening effect in PG 46-34.
- Back-calculated CR modulus from Shu model demonstrated the viscoelastic nature of this material after interaction with heated asphalt.
- Results of both performance tests (LAS and MSCR) illustrated the positive effect of CR on all base asphalt binders.
  - The best fatigue life is observed in softer base binders (PG 46-34 and PG 52-28).
  - Smaller CR size showed slightly better fatigue resistance in all CRM binders, except for PG 46-34 CRM where CR size had a negligible effect on N_f.
  - Base binder plays a more significant role in CRM binder fatigue performance when larger CR size is used.
  - LAS results highlighted the significance of base material properties on overall CRM binder fatigue behavior as these tests were done at equi-viscous conditions.
  - Better rutting resistance, as indicated by the MSCR test, was consistently observed with larger CR size.
  - Higher MSCR Jnr values in smaller CR size is consistent with lower |G*| in these binders as compared to larger CR size.
  - Overall, PG 46-34 produced the highest rutting resistance with larger CR size, while PG 52-28 exhibited the opposite.

- The relationships between G^*_r and N_f were found to be poor, while significantly better relationships were found with MSCR Jnr and %Recovery.
    - This is explained by the similarities in G*r for all CRM binders at intermediate temperatures, whereas more variations were observed at high temperatures
    - The assumption of equal CR volumetric percentage in all CRM binders is likely to have caused these similarities.
- Crossover Temperature defined as the deflection point when |G*| of BAC-CRM equals |G*| of BACD-CRM was introduced.
    - This parameter shows a clear distinction between CRM binders.
- Significant improvements were observed in correlations to LAS N_f using Crossover T as compared to G^*_r.
- In addition, correlations equal to or better than those made with G^*_r were established between rutting MSCR properties and Crossover δ.

Due to the weak correlations between G^*_r and performance characteristics at intermediate temperatures, and to simplify screening CRM binders for performance characteristics; it is recommended that Crossover T and the corresponding Crossover δ be used in screening CRM binders and estimate performance characteristics for materials produced within base binder and CR size variations included in this study. This can be done without the need to measure or assume CR swelling and does not require the use of micromechanical models.

CHAPTER 7. SUMMARY & RECOMMENDATIONS

This dissertation presents a comprehensive comparative analysis evaluating performance characteristics in CRM binders as influenced by different material variables including a wide range of base asphalt binder Performance Grades and CR sizes. The conclusions drawn herein provide a better understanding of CR modification techniques relative to performance-based specifications on asphalt binders and will encourage the overall adoption of CRM materials in paving applications.

In Chapter 3, an experimental investigation was carried out to evaluate the feasibility of using the parallel plate DSR geometry for characterizing CRM binder rheology with an increased gap of 2.0 mm at high test temperatures. A comparison between asphalt binder rheological properties obtained from the parallel plate and concentric cylinder geometries was made. In addition, hot mix asphalt mixtures were designed, and performance samples were fabricated from six different CRM binders and tested for the dynamic modulus property over a wide range of temperatures and frequencies. Mixture mechanical properties were then used to identify the more suitable DSR testing geometry for characterizing CRM binders in relation to mix properties. In this chapter it was concluded that there were no significant variations in measured CRM binder rheology between parallel plate and concentric cylinder geometries at 10% CR content and sizes tested (i.e., #20, #50 and #30 mesh). However, parallel plate DSR geometry provided slightly better or equal correlations to mixture performance. The analysis also suggested that the use of concentric cylinder may be required if CRM materials larger than #20 mesh are used. It is recommended that this observation be validated in larger CR sizes and a variety of base binders.

The portion of the dissertation recommends using parallel plate DSR geometry for characterizing CRM binders instead of the concentric cylinder geometry for all sizes smaller than

#20 mesh at 10% concentration. While for #20 mesh size at 25% concentration, the PP geometry did not provide identical binder rheological results as the CC geometry; mixture |E*| predictions based on parallel plates measured |G*| and phase angle were closer to those measured in the lab. For the #30 and #50 mesh sizes, the CC and PP geometries produced very similar |G*| values at 25% concentration. Phase angles were also similar, except some differences were observed at low frequencies in #50 mesh size at 20% concentration. It is also recommended that when used, the DSR concentric cylinder geometry should be limited for use at 46° C or higher for characterizing CRM binders using the 14.46 mm cylinder. Future work is recommended to include a different mixture designs (e.g., gap graded mixtures) and binder sources to further investigate the suitability of PP geometry as compared to the CC geometry.

The mechanisms of interaction between asphalt binders and CR were investigated in Chapter 4. An experimental approach was used to quantify the rheological changes in CRM binders using the |G*| test. In addition, the damage tolerance of modified and unmodified binders was investigated using the LAS test. The effect of CR mixing temperature on CRM binder rheology was investigated. It was shown that at 190 ^{o}C the rubber particles have swollen enough to make the overall CRM binder soft and crack resistant at low temperatures. However, insufficient swelling in CRM binders mixed at 130°C and 160°C indicates that the 'softening' effect occurs at a much lower temperature than 15°C. As mixing temperature increased from 130°C to 190°C, better interactions occur, and more light fractions are absorbed by the rubber as demonstrated from black space plots. The Finite Element model presented can be used to back-calculate the swollen CR modulus for the base binder and CR size used in this portion of the dissertation. It is recommended that this model be further developed and validated for a wide range of base binders and CR sizes and concentrations. It was also shown that CR inclusions in a CRM binder clearly

exhibit viscoelastic behavior and that the degree of viscoelasticity/temperature dependency of CR increases with increasing mixing temperatures. It was also observed that better improvement in fatigue life of CRM binders is achieved with increased mixing temperature.

In Chapter 5 the relationship shown in Chapter 4 between swollen CR modulus and the overall properties of the modified material was used to quantify the extent of CR pre-treatment and to identify sufficiently pre-treated CR materials in the laboratory before being incorporated in CRM HMA mixtures. The proposed screening method showed that inadequate pre-treatment of CR materials provides an undesirable viscosity increase in base binder indicating that the oil used in the pre-treatment process was either not suitable, or that low percentages of oil pre-treatment were used. This was also confirmed by the significant differences in |G*| for the rubberized and residual binders. This conclusion should be further validated by testing asphalt mixtures utilizing different pre-treated CR materials.

Chapter 6 quantified the rheological changes in CRM binders from different material variables in both unaged and short-term aged conditions were quantified as a function of CR mesh size and base asphalt binder PG grade. In addition, reliable relationships between linear viscoelastic CRM binder rheology and performance characteristics were established. It was demonstrated that for unaged CRM binders, the most significant softening/stiffening effects were seen in softer base asphalts caused by higher level of light asphalt fractions in this binder, leading to a more successful modification. In addition, the influence of base PG binder was more pronounced with larger CR mesh size, while the influence of CR size was more pronounced in softer base binders. The relationships between back-calculated G^*_r and N_f were found to be poor, while significantly better relationships were found with MSCR Jnr and %Recovery. This is explained by the similarities in G^*_r for all CRM binders at intermediate temperatures, whereas

more variations were observed at high temperatures. The assumption of equal CR volumetric percentage in all CRM binders is likely to have caused these similarities. Results of both performance tests (LAS and MSCR) illustrated the positive effect of CR on all base asphalt binders where the best fatigue life is observed in softer base binders (PG 46-34 and PG 52-28). Smaller CR size showed slightly better fatigue resistance in all CRM binders, except for PG 46-34 CRM where CR size had a negligible effect on Nf. It was also concluded that the base binder plays a more significant role in CRM binder fatigue performance when larger CR size is used. Better rutting resistance, as indicated by the MSCR test was consistently observed with larger CR size. Overall, PG 46-34 produced the highest rutting resistance with larger CR size, while PG 52-28 exhibited the opposite. A new rheological parameter, Crossover Temperature defined as the deflection point when |G*| of BAC-CRM equals |G*| of BACD-CRM was introduced and was found to provide a clear distinction between CRM binders. Significant improvements were observed in correlations to LAS N_f using Crossover T as compared to G^*_r. In addition, correlations equal to or better than those made with G^*_r were established between rutting MSCR properties and Crossover δ.

Due to the weak correlations between G^*_r and performance characteristics at intermediate temperatures, and to simplify screening CRM binders for performance characteristics; it is recommended that Crossover T and the corresponding Crossover δ be used in screening CRM binders and estimate performance characteristics for materials produced within base binder and CR size variations included in this study. This can be done without the need to measure or assume CR swelling and does not require the use of micromechanical models.

APPENDICES

APPENDIX A: |G*| MASTERCURVES FOR 10 AND 25% CR

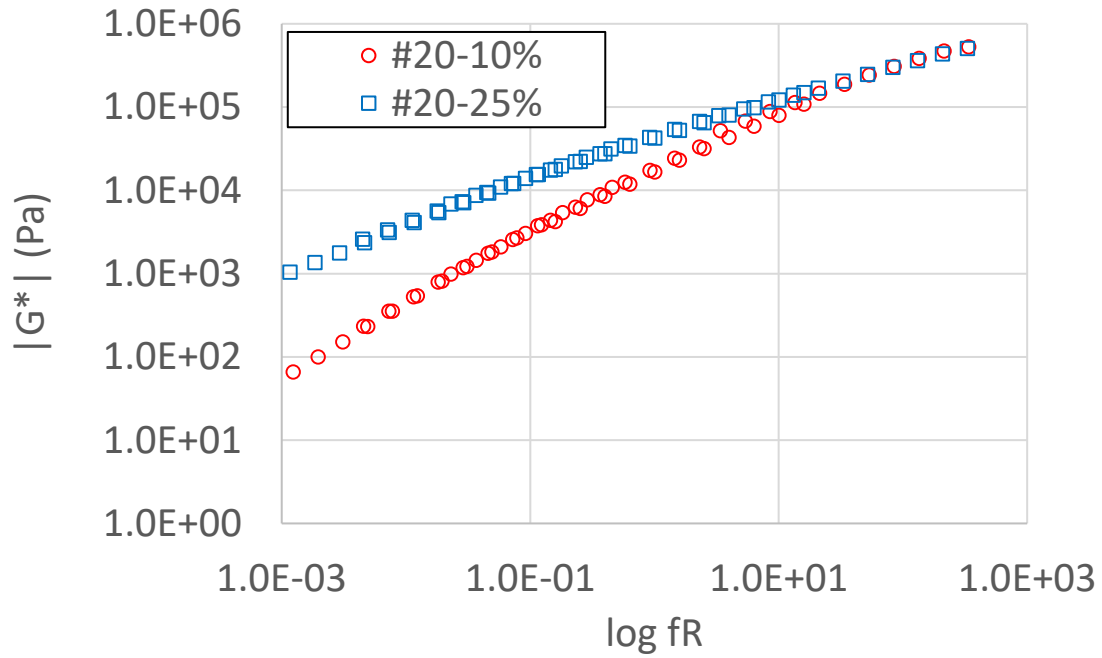

Figure 69: Dynamic shear modulus |G*| mastercurves for #20 CRM binders.

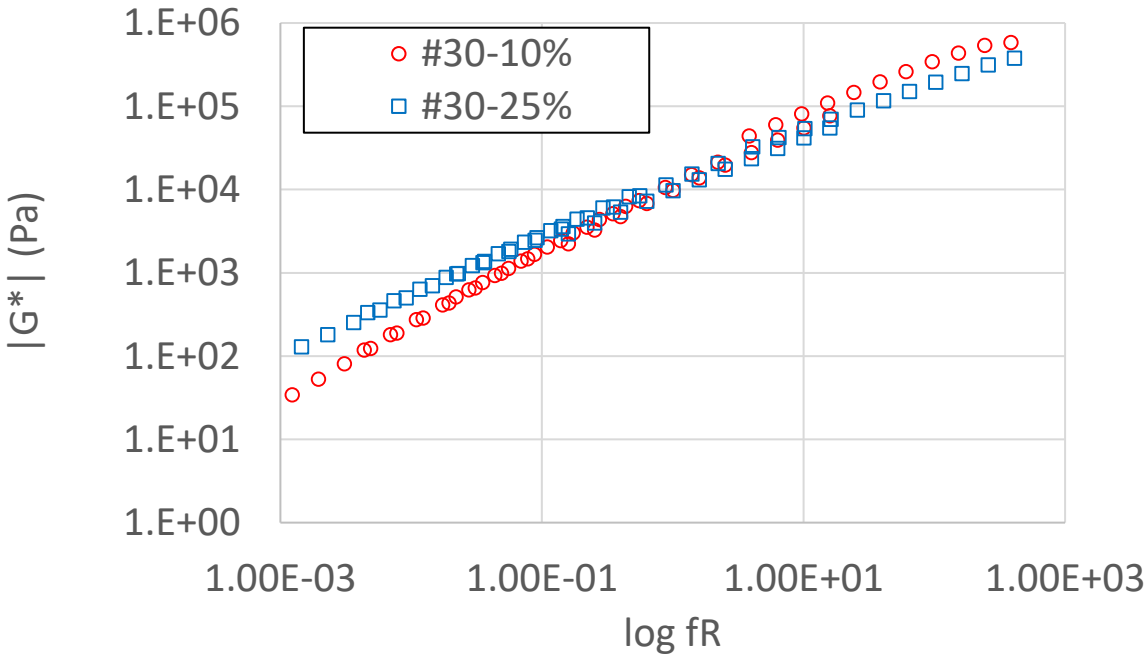

Figure 70: Dynamic shear modulus |G*| mastercurves for #30 CRM binders.

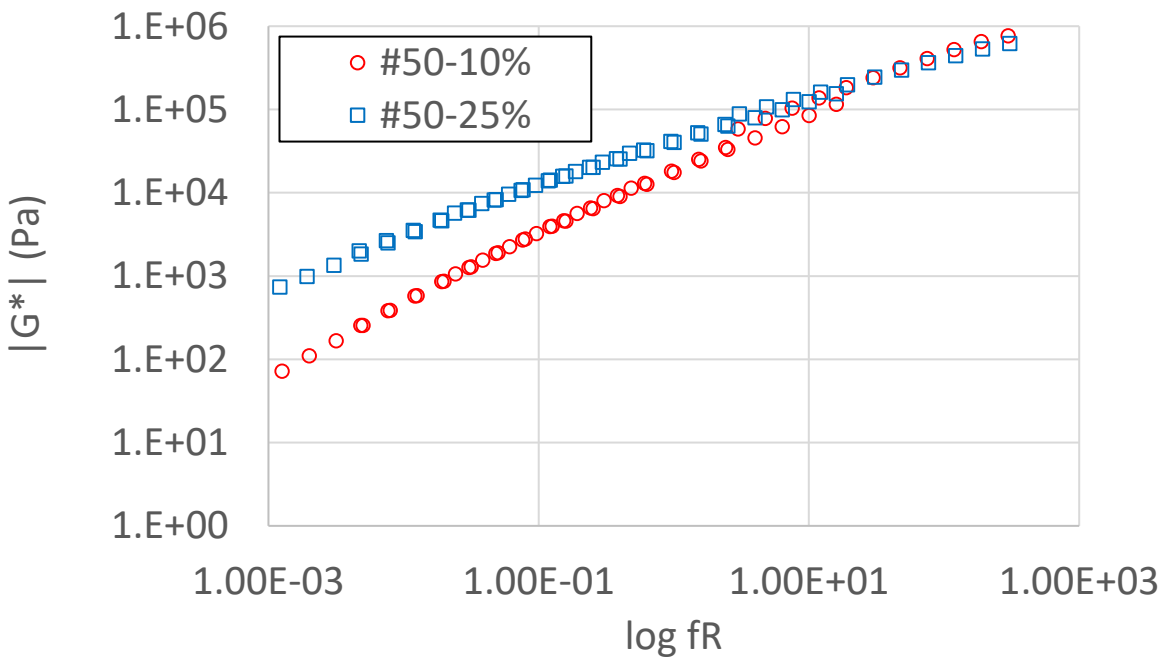

Figure 71: Dynamic shear modulus |G*| mastercurves for #50 CRM binders.

APPENDIX B: EFFECT OF MIXING TEMPERATURE ON VECD CURVES

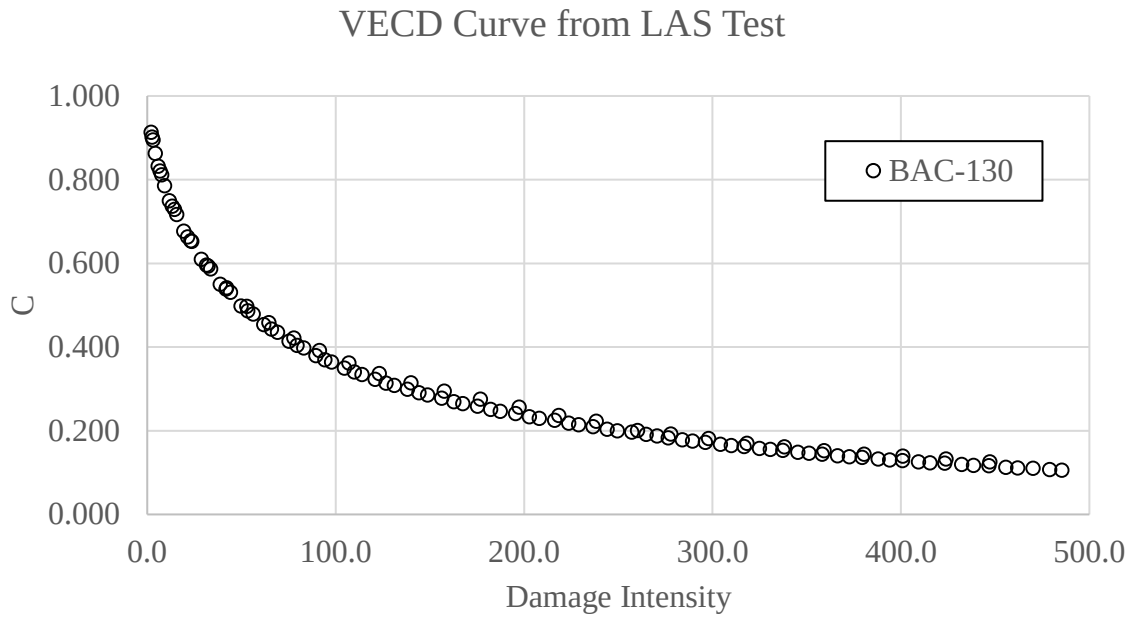

Figure 72: VECD Curve for BAC (with CR particles Composite) binder mixed at 130 °C.

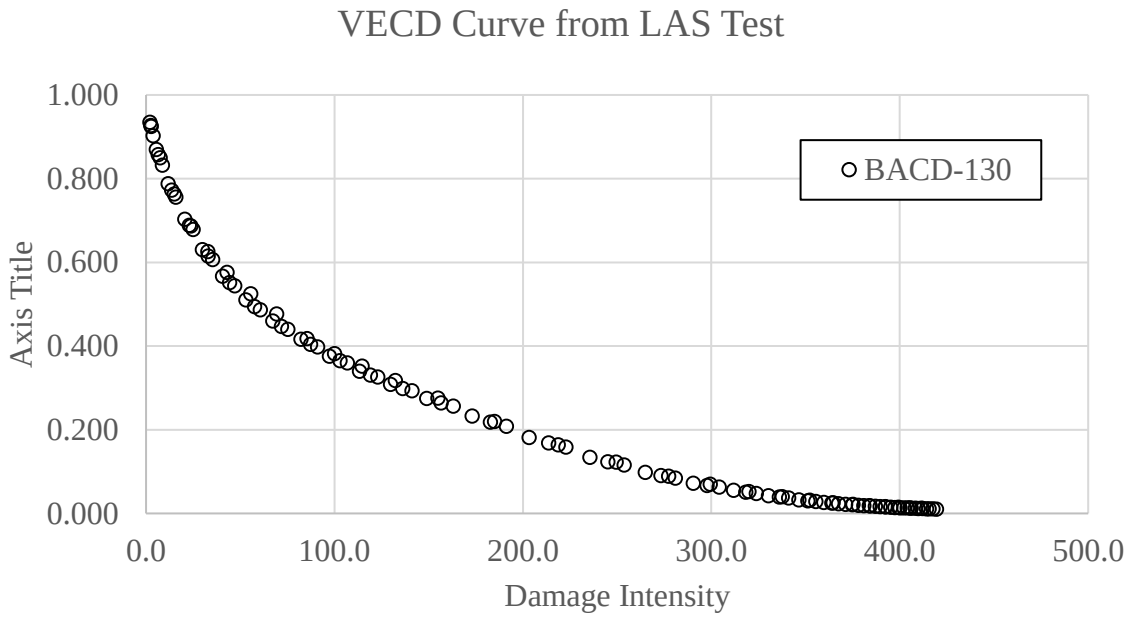

Figure 73: VECD Curve for BACD (CR filtered out) binder mixed at 130 °C.

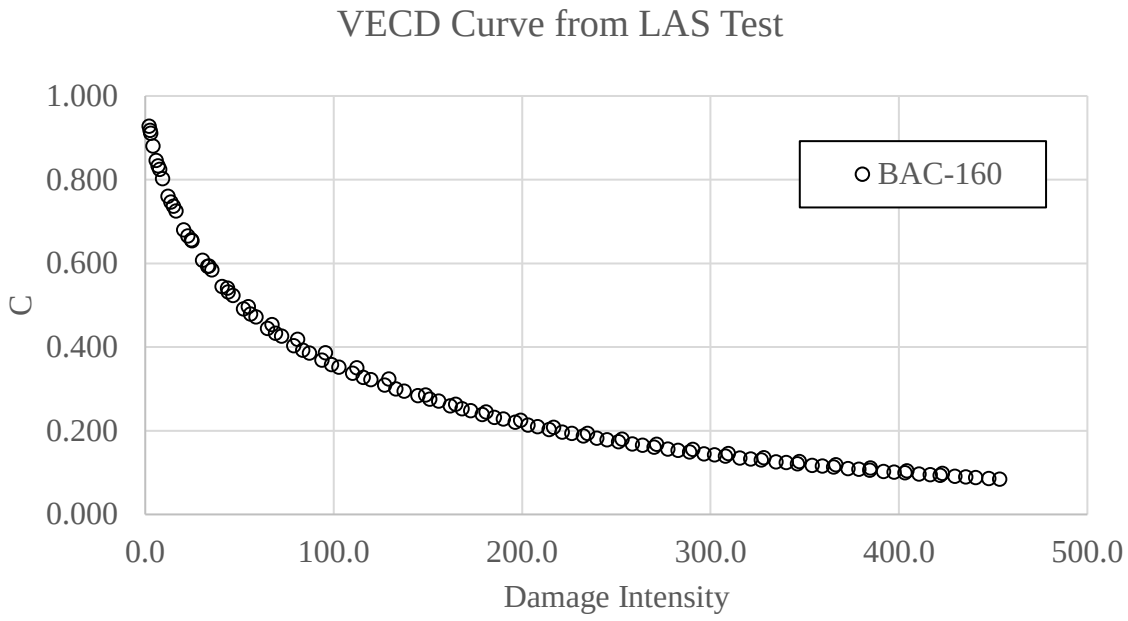

Figure 74: VECD Curve for BAC (with CR particles Composite) binder mixed at 160 °C.

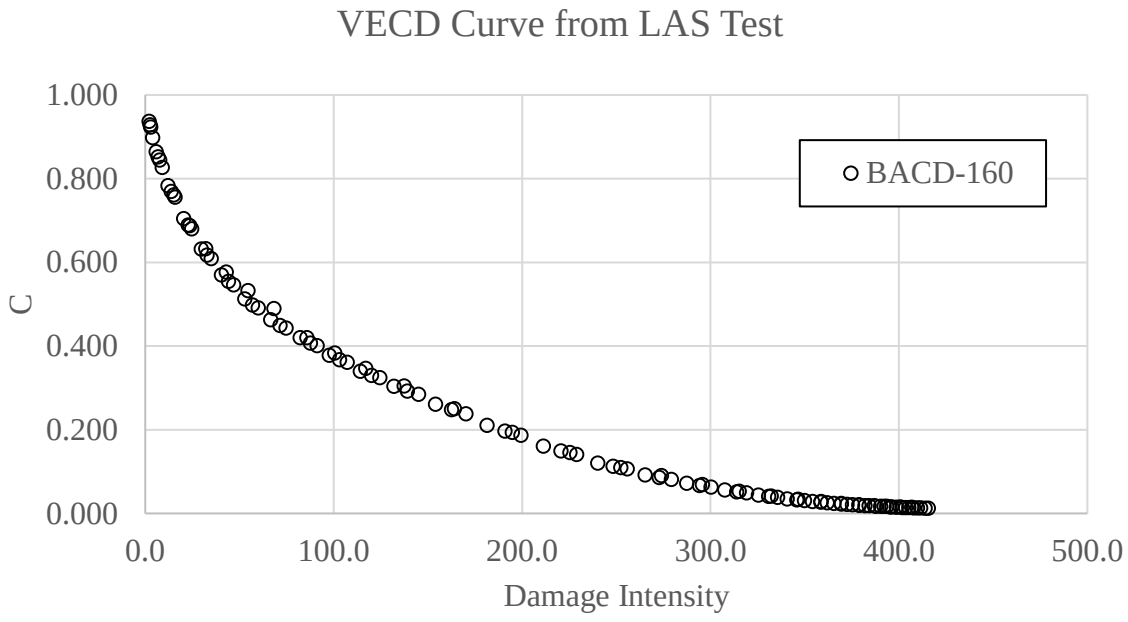

Figure 75: VECD Curve for BACD (CR filtered out) binder mixed at 160 °C.

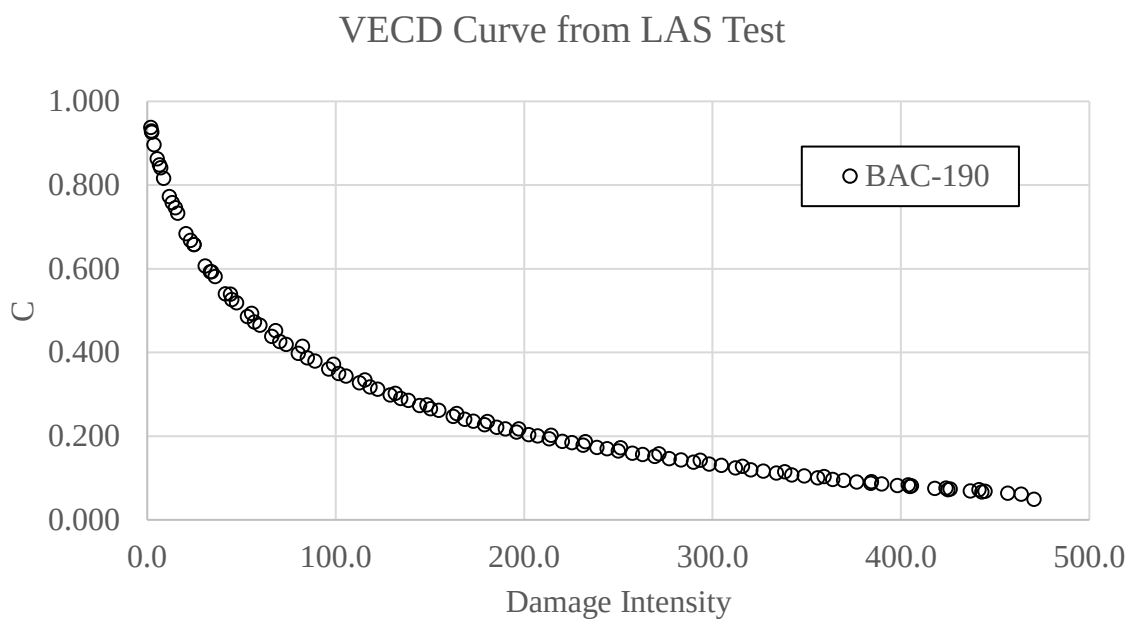

Figure 76: VECD Curve for BAC (with CR particles Composite) binder mixed at 190 °C.

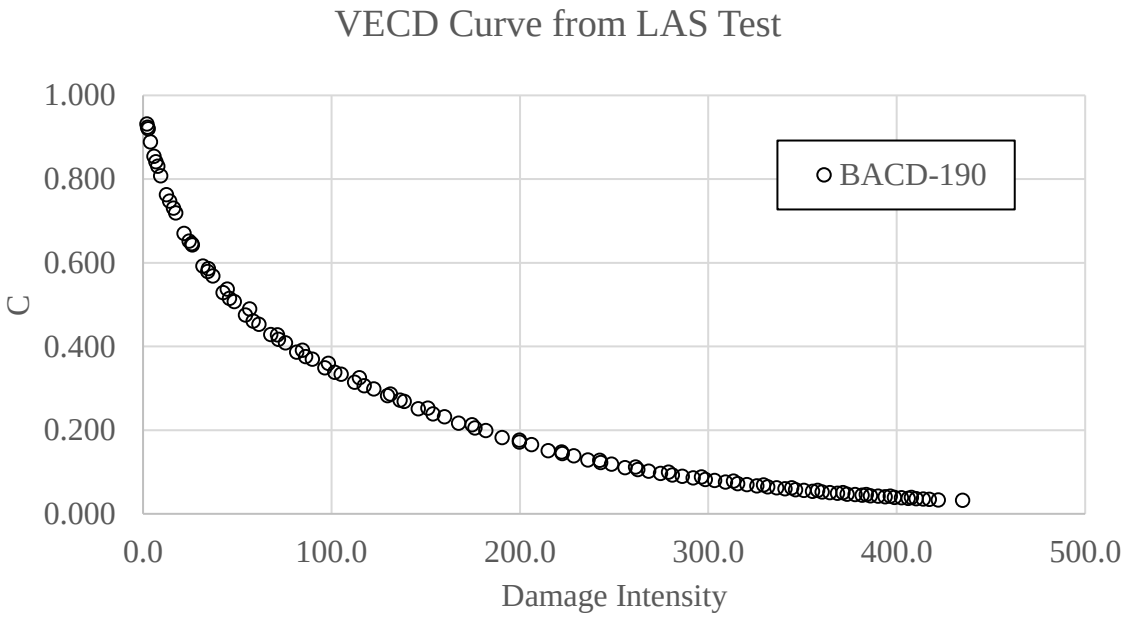

Figure 77: VECD Curve for BACD (CR filtered out) binder mixed at 190 °C.

APPENDIX C: STORAGE AND LOSS MODULI OF CRM BINDERS

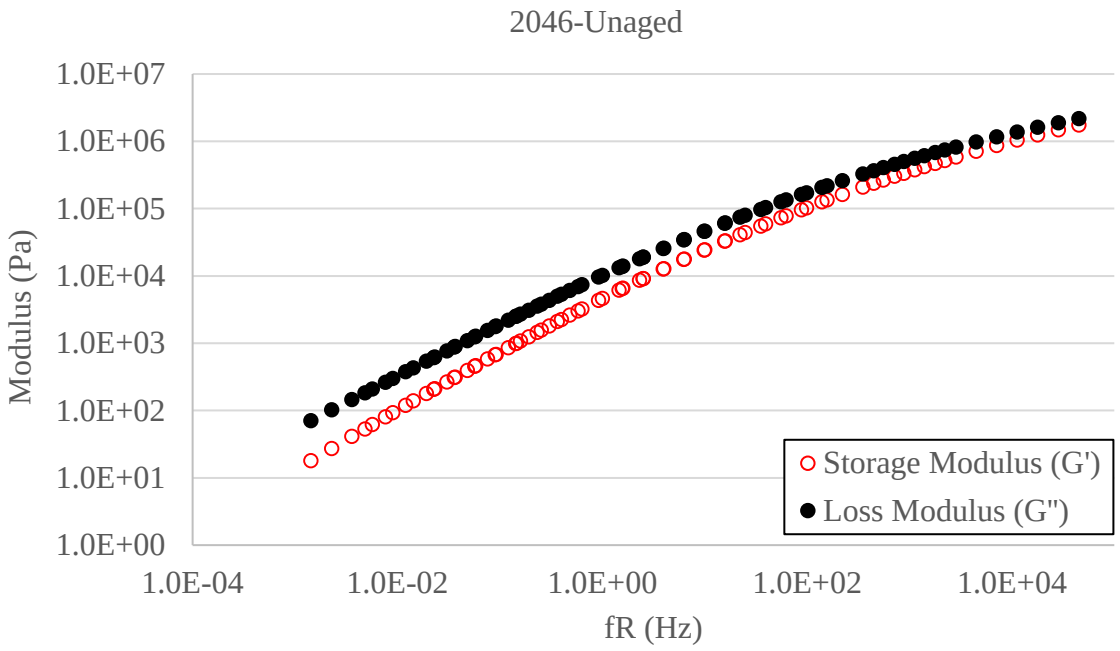

Figure 78: Storage and Loss moduli of unaged 2046 CRM binder.

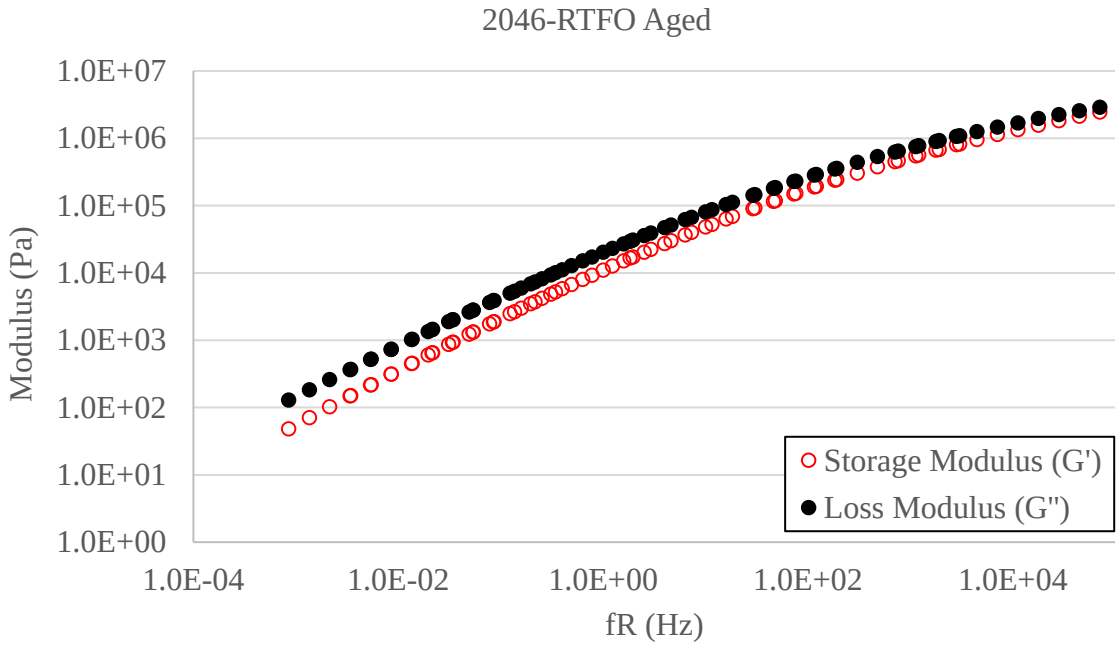

Figure 79: Storage and Loss moduli of RTFO aged 2046 CRM binder.

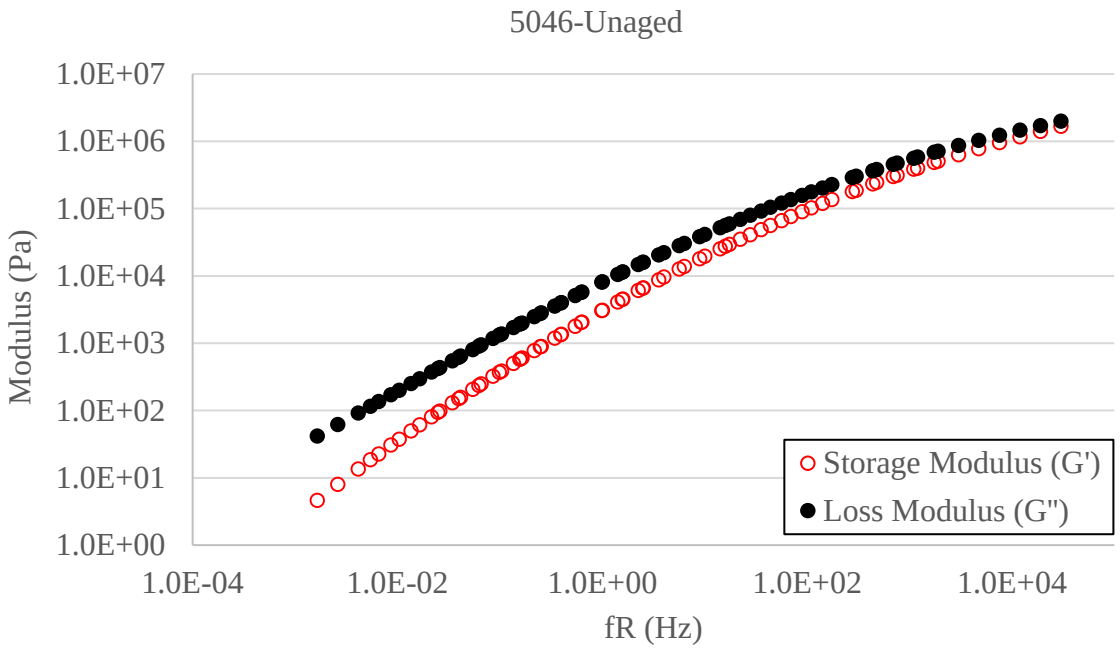

Figure 80: Storage and Loss moduli of unaged 5046 CRM binder.

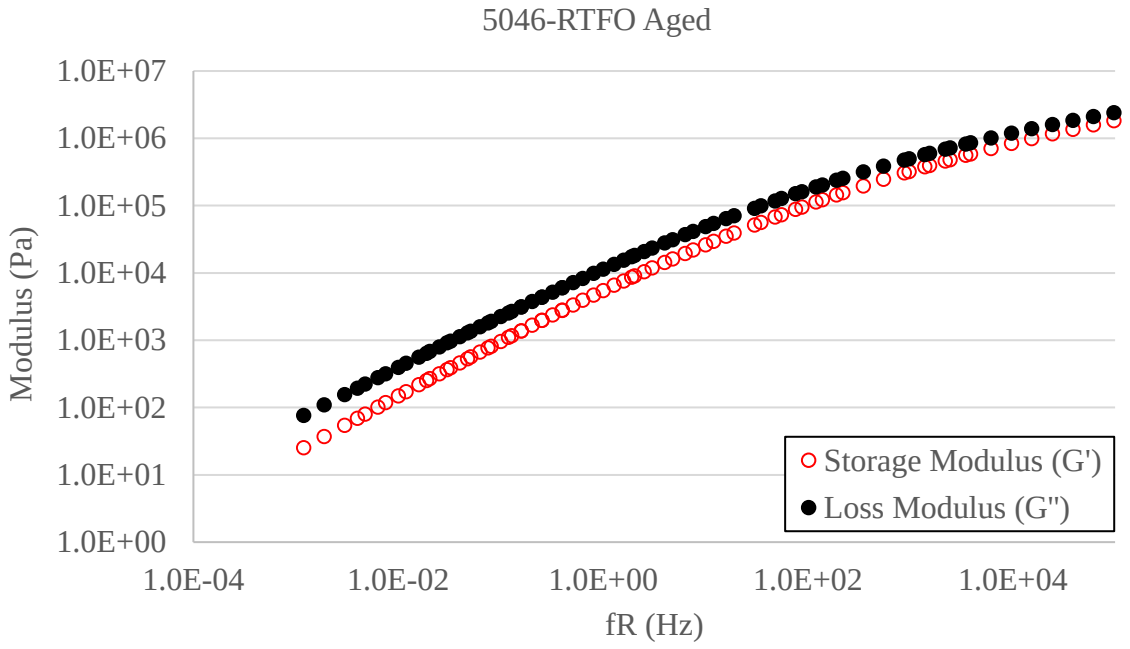

Figure 81: Storage and Loss moduli of RTFO aged 5046 CRM binder.

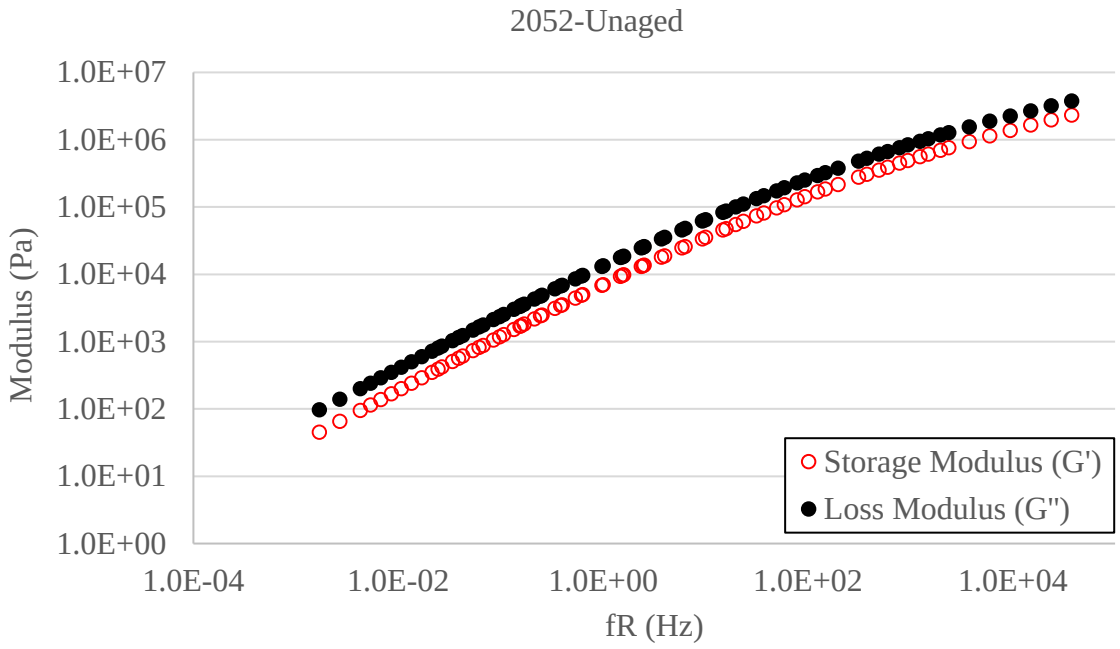

Figure 82: Storage and Loss moduli of unaged 2052 CRM binder.

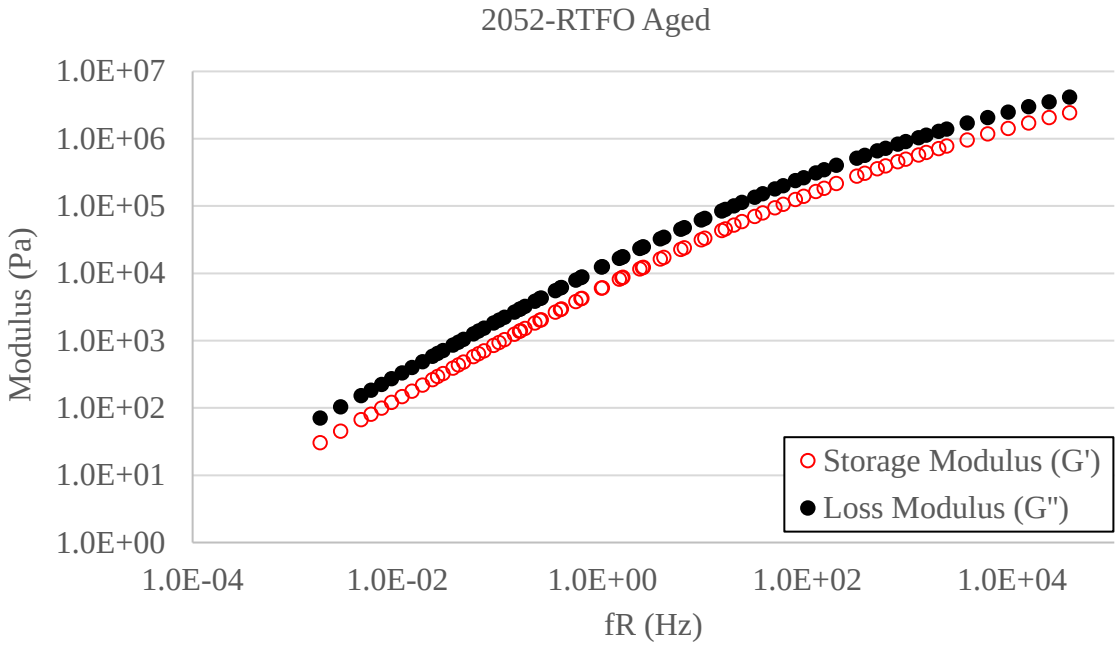

Figure 83: Storage and Loss moduli of RTFO aged 2052 CRM binder.

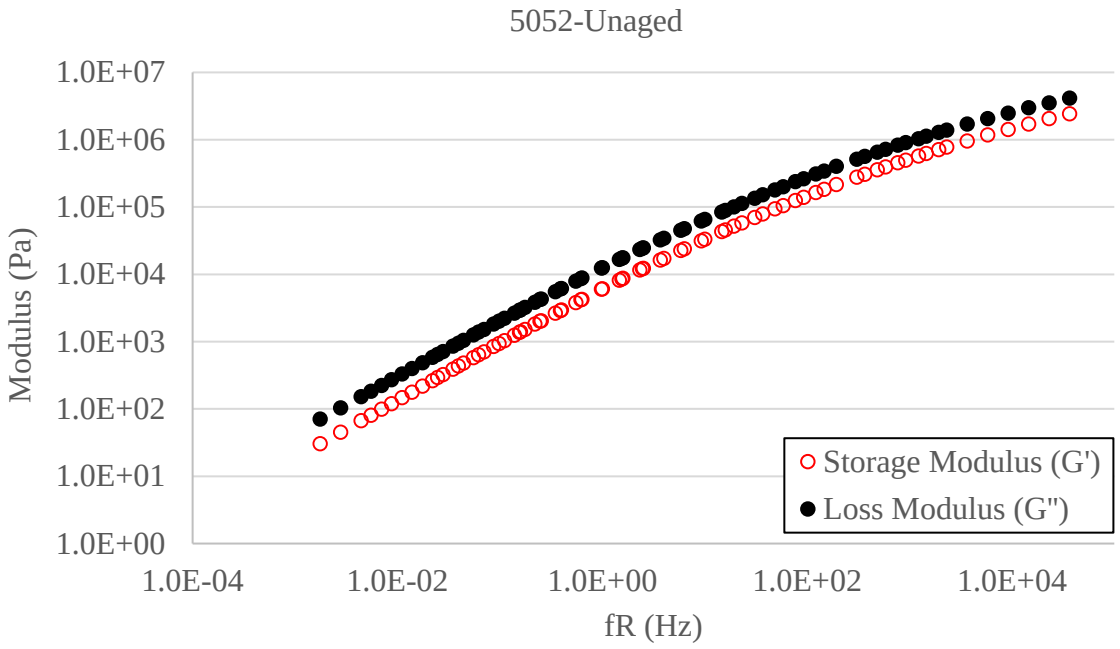

Figure 84: Storage and Loss moduli of unaged 5052 CRM binder.

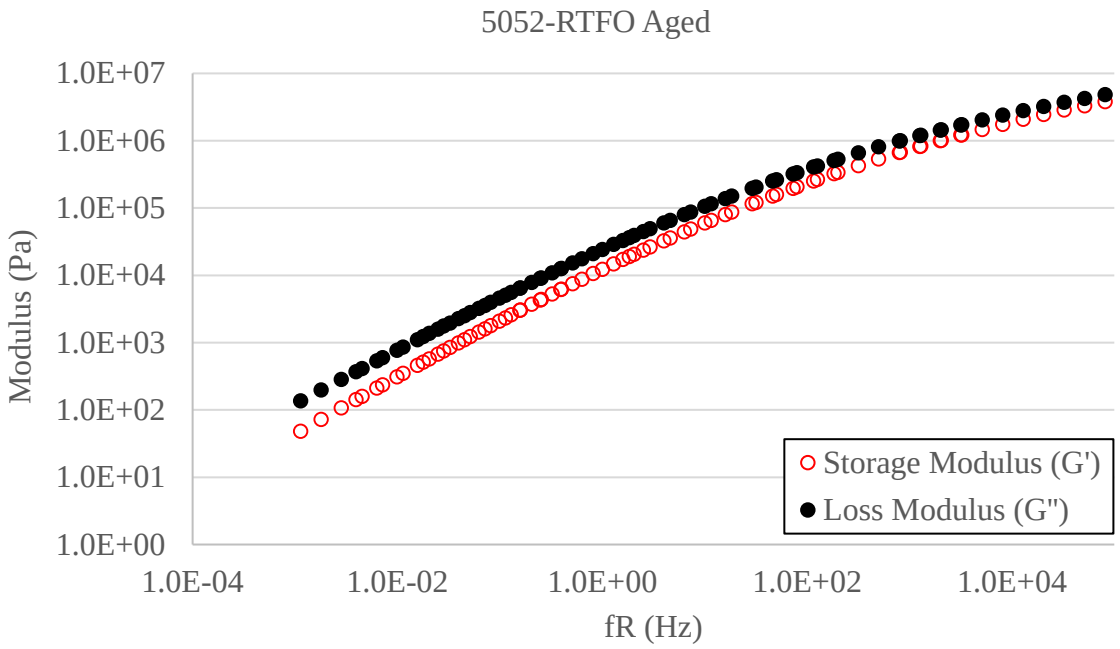

Figure 85: Storage and Loss moduli of RTFO aged 5052 CRM binder.

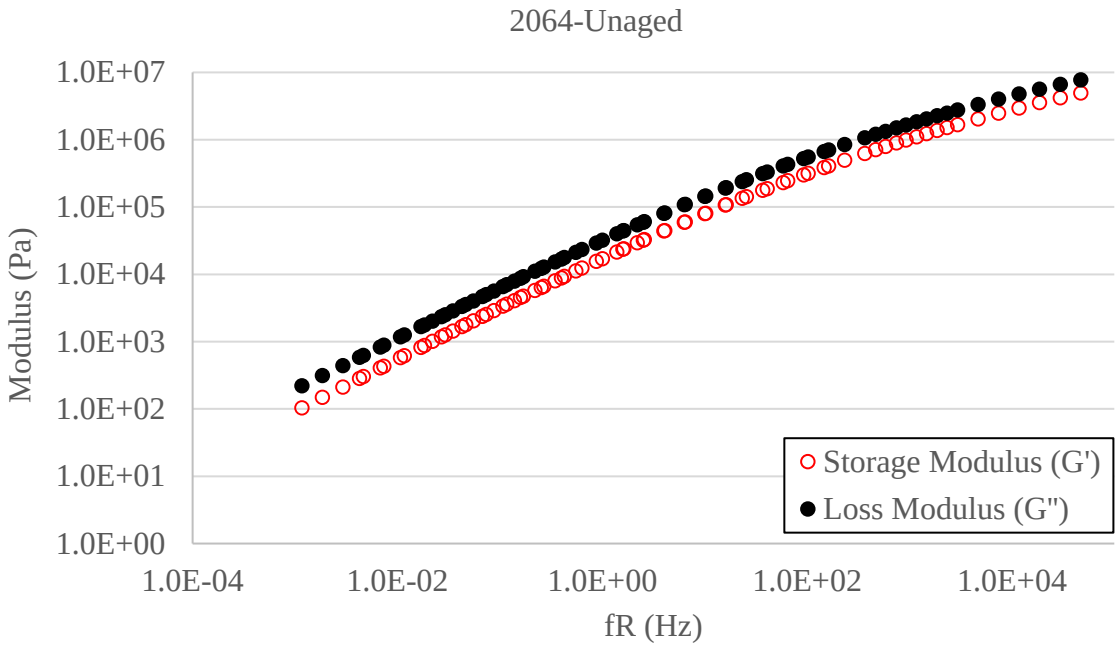

Figure 86: Storage and Loss moduli of unaged 2064 CRM binder.

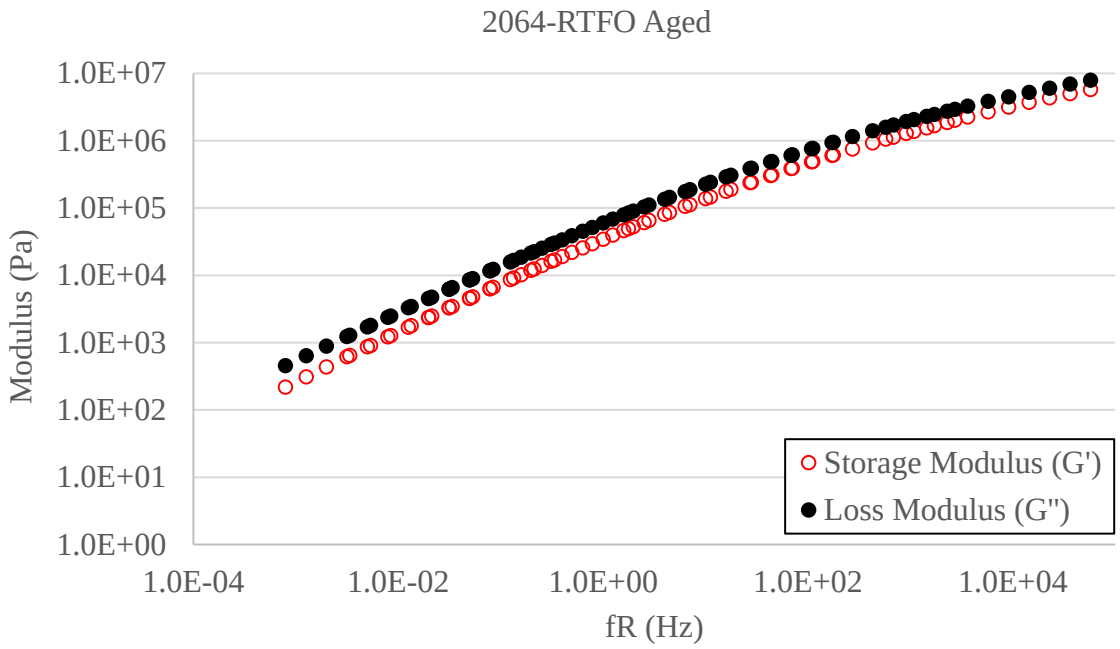

Figure 87: Storage and Loss moduli of RTFO aged 2064 CRM binder.

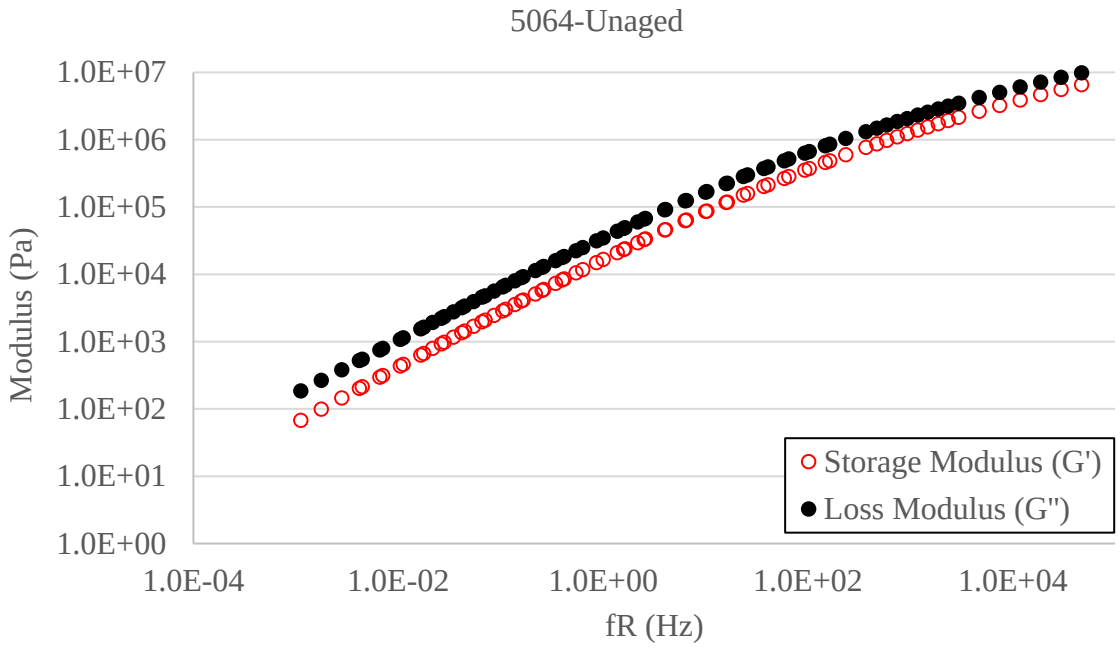

Figure 88: Storage and Loss moduli of unaged 5064 CRM binder.

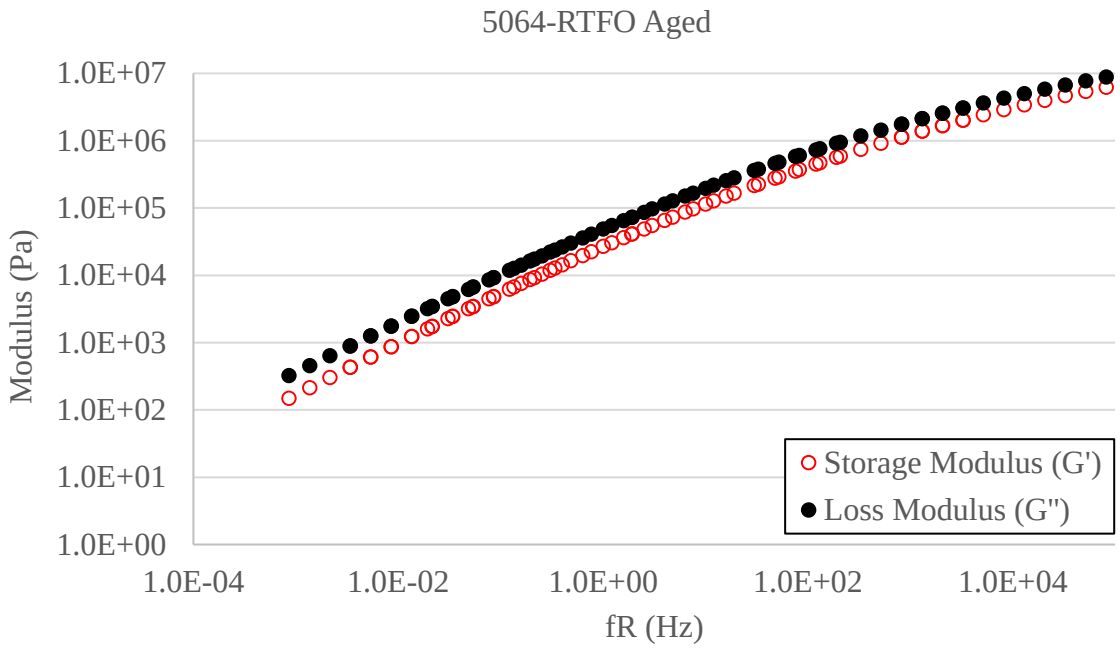

Figure 89: Storage and Loss moduli of RTFO aged 5064 CRM binder.

APPENDIX D: SIGMOID AND SHIFT FACTOR COEFFICIENTS FOR CRM BINDERS

Table 12: Sigmoid and shift factor coefficients for CRM binder master curves in Chapter 6.

BAC Binder ID	Shift Factors		Sigmoid Coefficients			
	a1	a2	b1	b2	b3	b4
2046	5.420E-04	-1.262E-01	-3.208	10.916	0.684	0.290
5046	4.982E-04	-1.189E-01	-3.482	11.151	0.688	0.308
2052	5.411E-04	-1.241E-01	-2.962	10.975	0.622	0.290
5052	5.424E-04	-1.238E-01	-3.255	11.265	0.649	0.299
2064	5.150E-04	-1.252E-01	-2.606	10.948	0.639	0.278
5064	5.084E-04	-1.249E-01	-2.630	11.043	0.634	0.288
BACD Binder ID	**Shift Factors**		**Sigmoid Coefficients**			
	a1	**a2**	**b1**	**b2**	**b3**	**b4**
2046	6.544E-04	-1.422E-01	-4.077	11.659	0.739	0.340
5046	6.187E-04	-1.354E-01	-3.292	10.881	0.603	0.362
2052	5.968E-04	-1.351E-01	-4.053	12.151	0.697	0.322
5052	5.607E-04	-1.278E-01	-3.134	11.236	0.577	0.351
2064	6.970E-04	-1.536E-01	-3.219	10.886	0.919	0.354
5064	6.309E-04	-1.443E-01	-3.039	11.107	0.786	0.342

REFERENCES

REFERENCES

AASHTO PP60-14, (2014). Preparation of Cylindrical Performance Test Specimens Using the Superpave Gyratory Compactor (SGC). American Association of State Highway and Transportation Officials, Washington, D.C.

AASHTO T315-14, (2014). Standard Method of Test for Determining the Rheological Properties of Asphalt Binder Using a Dynamic Shear Rheometer (DSR). American Association of State Highway and Transportation Officials, Washington, D.C.

AASHTO T316-14, (2014). Standard Method of Test for Viscosity Determination of Asphalt Binder Using Rotational Viscometer. American Association of State Highway and Transportation Officials, Washington, D.C.

AASHTO TP 101-14 (2014). Estimating Damage Tolerance of Asphalt Binders Using the Linear Amplitude Sweep. American Association of State Highway and Transportation Officials, Washington, D.C.

AASHTO T 350-14 (2014) "Standard Method of Test for Multiple Stress Creep Recovery (MSCR) Test of Asphalt Binder Using a Dynamic Shear Rheometer (DSR)", American Association of State Highway and Transportation Officials, Washington, D.C.

AASHTO TP 342-14, (2014). Determining Dynamic Modulus Mastercurve of Hot Mix Asphalt (HMA). American Association of State Highway and Transportation Officials, Washington, D.C.

Abdelrahman, M.A., and Carpenter, S.H., (1999). Mechanisms of Interaction of Asphalt Cement with Crumb Rubber Modifier. Transportation Research Record: Journal of the Transportation Research Board, Vol. 1661, p. 106-113.

Airey, G.D., Rahman, M.M., and Collop, A.C., (2003). Absorption of Bitumen into Crumb Rubber Using the Basket Drainage Method. International Journal of Pavement Engineering, 4:2, 105-119, DOI: 10.1080/1029843032000158879

Alavi, M.Z., (2015). Characterization of Rubberized Asphalt Binder with Concentric Cylinder Geometry. Transportation Research Board Annual Meeting, AFK20 Committee Meeting, January 12, 2015, Washington D.C. (also inhttp://pccas.org/uploads/3/3/0/0/3300836/2015-03-25_ar_binder_concentric_cylinder_testing_-_alavi.pdf)

Allen, R. G., Little, D. N., & Bhasin, A. (2012). Structural Characterization of Micromechanical Properties in Asphalt Using Atomic Force Microscopy. Journal of Materials in Civil Engineering, 24(10), 1317-1327. doi:10.1061/(asce)mt.1943-5533.0000510

ASTM D6114, (2009). "Standard Specification for Asphalt-Rubber Binder".

ASTM D8, (2009). “Standard Terminology Relating to Materials for Roads and Pavements”

Attia, M., & Abdelrahman, M. (2009). Enhancing the performance of crumb rubber-modified binders through varying the interaction conditions. International Journal of Pavement Engineering, 10(6), 423-434. doi:10.1080/10298430802343177

Bahia, H. and R. Davies, (1995). Factors Controlling the Effects of Crumb Rubber on Critical Properties of Asphalt Binders. Journal of the Association of Asphalt Paving Technologists, Volume 64, p. 131 – 143.

Bahia, H.U., and Davies, R., (1994). Effect of Crumb Rubber Modifiers (CRM) on Performance-Related Properties of Asphalt Binders. Journal of the Association of Asphalt Paving Technologists, Vol. 63, p. 414-449.

Bari, J. (2005). Development of a New Revised Version of the Witczak E* Predictive Models for Hot Mix Asphalt Mixtures. PhD Dissertation. Arizona State University.

Baumgardner, G., and D’Angelo, J.A., (2012). Evaluation of New DSR Testing Geometry for performance Testing of Crumb Rubber Modified (CRM) Binder. In Transportation Research Record: Journal of the Transportation Research Board, No. 2293, pp. 73-79.

Bennert, T., (2013). Grade Determination of Crumb Rubber-Modified Performance Graded Asphalt Binder. Center for Advanced Infrastructure and Transportation (CAIT), Rutgers University.

Bertollo S.M., (2004). Mechanical properties of asphalt mixtures using recycled tyre rubber produced in Brazil – a laboratory evaluation. Washington, D.C. 83rd Transportation Research Board Annual Meeting.

Caltrans (2009). “Asphalt Rubber Usage Guide”. State of California Department of Transportation, Materials Engineering and Testing Services.

Campillo, J., (2014). Properties of activated crumb rubber modified binders. M.S Thesis. Arizona State University, Phoenix, AZ.

Carlson, D. D., and Zhu H., (1999). Asphalt-Rubber an Anchor to Crumb Rubber Markets. Third Joint 270 UNCTAD/IRSG Workshop on Rubber and the Environment. International Rubber Forum, Veracruz, Mexico, October 1999.

Chesner, W., Collins, R., and MacKay, M., (1988). “User Guidelines for Waste and By-product Materials in Pavement Construction”. Publication Number: FHWA-RD-97-148

D’Angelo, J. “The Relationship of the MSCR Test to Rutting”, Road Materials and Pavement Design Construction and Building Materials, Volume 10, Pages 61-80

Dong, D., Huang, X., Li, X., and Zhang, L., (2012). Swelling process of rubber in asphalt and its effect on the structure and properties of rubber and asphalt. Journal of Construction and Building Materials, 29 (2012) 316–322.

Eaton, P., and West, P. (2010). Atomic force microscopy. Cary, NC, USA: Oxford University Press.

Epps, J. 1994. Uses of Recycled Rubber Tires in Highways. Synthesis of Highway Practice 198, National Cooperative Highway Program, National Academy Press.

Glover C., Davison R., Bullin J., Estakhri C., Williamson S., Billiter T., Chipps J., Chun J., Juristyarini P., Leicht S., and Wattanachai P., (2000). A comprehensive laboratory and field study of high-cure crumb-rubber modified asphalt materials. Report 1460-1. Texas Transportation Institute, USA.

Green, E.L. and Tolonen, W.J. (1977). The Chemical and Physical Properties of Asphalt-Rubber Mixtures. Report ADOT-RS-14 (162), Arizona Department of Transportation.

Heitzman, M.A., (1992). "State of the Practice – Design and Construction of Asphalt Paving Materials with Crumb Rubber Modifier". Publication Number: FHWA-SA-92-022

Hicks, R. G., Lundy, James R., Epps, Jon A., (1999). Life Cycle Costs for Asphalt-Rubber Paving Material. Rubber Pavements Association. Tempe, Arizona.

Hintz, C., Velasquez, R., Johnson, C., and Bahia, H. (2011). "Modification and Validation of Linear Amplitude Sweep Test for Binder Fatigue Specification", Transportation Research Record: Journal of the Transportation Research Board, Vol. 2207, p. 99-106.

Huang, S., & Pauli, A. T. (2008). Particle Size Effect of Crumb Rubber on Rheology and Morphology of Asphalt Binders with Long-term Aging. Road Materials and Pavement Design, 9(1), 73-95. doi:10.3166/rmpd.9.73-95

Hung, S.S., Farshidi, F., Jones, D., Harvey, J.T., (2015). Comparison of Concentric Cylinder and Parallel Plate Geometries for Asphalt Binder Testing using a Dynamic Shear Rheometer.

Jamrah, A., Kutay, M. E., Varma, S. (2015). "Backcalculation of Swollen Crumb Rubber Modulus in Asphalt Rubber Binder and Its Relation to Performance", Transportation Research Record: Journal of the Transportation Research Board, Vol. 2505, p. 99-107.

Jones, D., Liang, Y., & Harvey, J. (2017). Performance Base Specifications: Increasing Crumb Rubber Usage by Using Small Amounts of CRM in HMA. Retrieved from http://www.ucprc.ucdavis.edu/PDF/UCPRC-TM-2017-05.pdf

Proceedings of the Transportation Research Board 94th Annual Conference, January 11-15, 2015.

Jung, J.S., Kaloush, K. E., and Way, G. B., (2002). "Life Cycle Cost Analysis: Conventional Versus Asphalt-Rubber Pavements". Rubber Pavements Association. Tempe, Arizona.

Kaloush K.E., Witczak M.W., Sotil A.C., Way G.B., (2003). Laboratory evaluation of asphalt rubber mixtures using the dynamic modulus (E*) Test. Washington, D.C. 82nd Transportation Research Board Annual Meeting.

Kocevski, S., Yagneswaran, S., Xiao, F., Punith, V.S., Dennis W. Smith Jr., Amirkhanian, S., (2012). Surface modified ground rubber tire by grafting acrylic acid for paving applications. Journal of Construction and Building Materials, 34, 83-90, DOI: 10.1016/j.conbuildmat.2012.02.040.

Leung, F., Macdonald, G., Penton, S., (2006). Noise Reducing Asphalt Pavements: a Canadian Case Study. 10th International Conference on Asphalt Pavements - August 12 to 17, 2006, Quebec City, Canada.

Lougheed, T. J., and Papagiannakis, A. T. "Viscosity characteristics of rubber-modified asphalts." Journal of Materials in Civil Engineering 8.3 (1996): 153-156.APA

Medina, J. R., and Underwood, B. S. (2017) "Micromechanical shear modulus modeling of activated crumb rubber modified asphalt cements", Construction and Building Materials, Volume 150, Pages 56-65

Memon, G. M., & Chollar, B. H. (1997). Glass transition measurements of asphalts by DSC. Journal of Thermal Analysis, 49(2), 601-607. doi:10.1007/bf01996742

Memon, N., (2011). "Characterisation of conventional and chemically dispersed crumb rubber modified bitumen and mixtures". University of Nottingham. Nottingham, UK: PhD thesis.

Navarro, F., Partal, P., Martínez-Boza, F., & Gallegos, C. (2004). Thermo-rheological behaviour and storage stability of ground tire rubber-modified bitumens. Fuel, 83(14-15), 2041-2049. doi:10.1016/j.fuel.2004.04.003

Newcomb, D.E., Stroup-Gardiner, M., Kim, J.R., Allen, B., and Wattenhoffer-Spry, J., (1994). Polymerized Crumb Rubber Modified Mixtures in Minnesota. (Report No. MN/RC-94/08). National Technical Information Services, Springfield, Virginia 22161.

Palit, S. K., Reddy, K. S., and Pandey, B. B. "Laboratory evaluation of crumb rubber modified asphalt mixes." Journal of Materials in Civil Engineering 16.1 (2004): 45-53.

Pampulim, V., (2013). "How the rubber meets more rubber". Asphalt Rubber 2012 Conferenece. Munich, Germany.

Paul, B., (1960). Prediction of Elastic Constants of Multiphase Materials - Technical Report No. 3. Brown University, Providence.

Putman, B., Thompson, J., and Amirkhanian, S., (2005). High Temperature Properties of Crumb Rubber Modified Binders. The Fourth International Conference on Maintenance and Rehabilitation of Pavements and Technological Control.

Rahman, M., (2004). Characterisation of Dry Process Crumb Rubber Modified Asphalt Mixture. University of Nottingham. Nottingham, UK: PhD thesis

Roberts, F.L., Kandhal, P.S., Brown, E.R., and Dunning, R.L. (1989). Investigation and evaluation of ground tyre rubber in hot-mix asphalt. Alabama, USA: NCAT Auburn University.

Rubber Manufacturers Association, (2016). “2015 U.S. Scrap Tire Management Summary”.

Shenoy, A., (1999). Rheology of filled polymer systems. Netherlands: Kluwer Academic Publishers. doi:10.1007/978-94-015-9213-0

Shu, X., (2007). Application of Particulate-Filled Composite (PFC) Theory to Hot-Mix Asphalt (HMA) Mixtures. Ph.D Dissertation. The University of Tennessee, Knoxville

Shulman, V.L. (2000),Tyre Recycling After 2000:Status and Options, European Tyre Recycling Association, Paris, France.

Sousa J.B., (2005). Experiences with use of reclaimed rubber in asphalt within Europe. Birmingham: Rubber in Roads.

Steffe, J. F., (1996). Rheological Methods in Food Process Engineering. Freeman Press 2807 Still Valley Dr. East Lansing, MI , Copyright 1996, pg 158-169.

Stroup-Gardiner, M., Chadbourn, B., and Newcomb, D.E., (1996). Babbitt, Minnesota: Case Study of Pretreated Crumb Rubber Modified Asphalt Concrete. Transportation Research Record: Journal of the Transportation Research Board, Vol. 1530, p. 34-42.

Tarefder, R. & Zaman, A.(2010). “Nanoscale Evaluation of Moisture Damage in Elastomeric Polymer Modified Asphalts”, ASCE Journal of Materials in Civil Engineering, 2010.

Tayebali, A.A., B. Vyas, and G. Malpass, (1997). Effect of Crumb Rubber Particle Size and Concentration on Performance Grading of Rubber Modified Asphalt Binders. Progress of Superpave (Superior Performing Asphalt Pavement): Evaluation and Implementation, ASTM STP 1322, R.N. Jester, Ed., American Society for Testing and Materials, p. 30 – 47.

Thodesen, Carl 2008 “Development of Prediction Models of High Temperature Crumb Rubber Modified Binders”. https://tigerprints.clemson.edu/all_dissertations/196

Way, G.B., (1999). Flagstaff I-40 Asphalt Rubber Overlay Project, Nine Years of Success Arizona Department of Transportation. Paper Presented to the Transportation Research Board, 78th Annual Meeting, August 1999.

Way, G.B., Vilamoura, (2000). OGFC Meets CRM. Where the Rubber meets the Rubber. 12 Years of Durable Success. Asphalt Rubber 2000 Conference.

Junan Shen & Serji Amirkhanian (2005) The influence of crumb rubber modifier (CRM) microstructures on the high temperature properties of CRM binders, International Journal of Pavement Engineering, 6:4, 265-271, DOI: 10.1080/10298430500373336

Stroup-Gardiner, Mary, David E. Newcomb, and Bruce Tanquist. "Asphalt-rubber interactions." Transportation Research Record 1417 (1993): 99.

Xiao, F., Amirkhanian, S., and Juang, C. S. "Rutting resistance of rubberized asphalt concrete pavements containing reclaimed asphalt pavement mixtures." Journal of Materials in Civil Engineering 19.6 (2007): 475-483.